ARTICLE IN PRESS
JID: JMAA [m5+;October 13, 2021;11:10]

Available online at www.sciencedirect.com

ScienceDirect

Journal of Magnesium and Alloys xxx (xxxx) xxx

www.elsevier.com/locate/jma

Review

A comprehensive review on biocompatible Mg-based alloys as temporary orthopaedic implants: Current status, challenges, and future prospects

Darothi Bairagi[a], Sumantra Mandal[a,*]

[a] *Department of Metallurgical and Materials Engineering, Indian Institute of Technology, Kharagpur 721302, India*

Received 29 May 2021; received in revised form 21 August 2021; accepted 5 September 2021
Available online xxx

Abstract

Mg and its alloys are drawing huge attention since the last two decades as a viable option for temporary implants applications. A commendable progress has already been made in the development of these alloys. The biodegradable nature of Mg, appreciable biocompatibility of elemental Mg, and its close resemblance to natural bone in terms of density and elastic modulus make them highly preferable option amongst other available alternatives in this field. This review article presents an overview covering the recent advancements made in the field of Mg-based biodegradable implants for orthopaedic implant applications. The paper focuses on alloy development and fabrication techniques, the state of the art of important Mg-based alloy systems in terms of their mechanical properties, *in-vitro* and *in-vivo* degradation behaviour and cytotoxicity. Further, the paper reviews the current progress achieved in the clinical transition of Mg-based alloys for orthopaedic fixtures. The review also includes the degradation mechanisms of the alloys in physiological environment and highlights the mismatch existing between the rate of bone healing and alloy degradation due to rapid corrosion of the alloys in such environment, which has still restricted their widespread application. Finally, the surface coating techniques available for the alloys as an effective way to reduce the degradation rate are reviewed, followed by a discussion on the future research prospects.

Keywords: Mg-based alloys; Biomaterials; Temporary implants; Biocompatibility; Degradation behaviour; orthopaedic fixtures.

1. Introduction

Biomaterials are substances consisting of natural or synthetic materials, engineered in a predefined manner to obtain a form that alone or as a part of a multi-component complex structure can interact with the biological system of a living being. They serve as a replacement for a lost or disputed body part along with restoring the function of the same. Undoubtedly, biomaterials play a vital role in uplifting the overall lifestyle and longevity of human life, and thus attracting a great deal of attention in today's era. Biomaterials find numerous applications in different parts of a human body such as neural prosthetics, pacemakers and artificial valves for the heart, cardiac stimulators used in the cardiovascular system [1–6], stents for unclogging blood vessels [3,7,8], reconstruction of the urinary tract [9], bone replacements in different parts of the body like wrist, shoulder, knee, ankle, hip, dental, and spine [10–13] etc. Amongst the miscellaneous applications of biomaterials, orthopaedic implants cover a significant share [6,14]. Over the last few decades, concurrent with the enormous improvement in the field of medical sciences, the life expectancy and average life span of an individual have increased globally, leading to an increase in the elderly population throughout the world, especially in the developed countries. In 2019, the US Census Bureau projected that by the year 2034, the aged people population over the age of 65 years (78.0 million) is expected to surpass the number of people under the age 18 (76.7 million) [15–17]. According to a study published by Long and Rack [18], about 90% of the population over 40 year's age are prone to suffer from various kinds of degenerative diseases such as arthritis, osteoporosis,

* Corresponding author.
E-mail address: sumantra.mandal@metal.iitkgp.ac.in (S. Mandal).

https://doi.org/10.1016/j.jma.2021.09.005

Table 1
Different fracture sites in human body requiring various temporary fixation devices [32].

Fracture sites		Internal fixators
Head	Skull fracture	Wires, pins, and plates
	Craniofacial fracture	Wires, screws, and plates
Trunk	Clavicle fracture	Intramedullary nails and plates
	Scapular fracture	Screws and plates
	Pelvic fracture	Screws, plates and external fixators
	Spinal fracture	Fixation device consists of rods, pedicle screws and plates
Upper limb fracture	Humeral fracture	Open reduction with plates and screws; close reduction with intramedullary nail
	Radius, ulnar fracture	Open reduction with plates and screws; close reduction with intramedullary nail
	Metacarpal and phalangeal fracture	Close reduction with external fixators; open reduction with intramedullary nail, screws, and plates
Lower limb fracture	Femoral fracture	Open reduction with plates and screws; close reduction with intramedullary nail
	Tibial and fibular fracture	Open reduction with plates, screws, and intramedullary nail
	Metatarsus fracture	Open reduction with plates, screws, and intramedullary nail
	Calcaneal fracture	Close reduction with screws and wires

and trauma. One of the most prevalent health problems faced by these people is musculoskeletal disorders [19,20], giving rise to a massive demand for orthopaedic implants worldwide. The market for orthopaedic implants, which accounted for 45,901 million dollars in 2017, is predicted to touch 66,636 million dollars by the year 2025, thus recording a compound annual growth rate of 4.7% [21]. Apart from orthopaedics, currently the demand is also soaring for temporary implants like cardiovascular stents [22–24], cardiac stimulators [25], and scaffolds [26,27]. The ever-rising demand for the implants indicates a steep upswing in the implant manufacturing industry in the near future and parallelly necessitates acceleration in research and developmental work concentrated over finding suitable materials for implant manufacturing, especially for orthopaedics.

The permanent implants that act as a replacement of natural bone by restoring its function, should possess enough strength to bear the load along with adequate ductility, biocompatibility, sufficient wear and corrosion resistance in physiological environment [28,29]. Most importantly, the implants should be able to serve their purpose ideally until lifetime, without causing immature failure or any requirement for replacement through revision surgery [2,30]. However, there are many instances that need only temporary support until the tissue heals. The fixtures like screws, plates, micro-clips, stabilizing devices etc. are used to join and fix the complex structure of fractured bones or ligaments. They serve a completely different purpose than that of permanent ones and are ideally meant to stay inside the body only until the fracture heals completely [31–33]. Table 1 highlights different fracture sites in human body requiring some sort of temporary fixation until they heal. Most of the commercially used fixtures have traditionally been made of permanent metallic alloys, including titanium [34–37], stainless steels [38–40], and Co-Cr alloys [41,42]. Despite their high mechanical strength, biocompatibility, and sufficient corrosion-resistant properties, they impart stress shielding effect [43,44] due to a significant mismatch in elastic modulus between natural bone and those implant materials [8,45,46]. Due to this, the bone needs to carry a much lesser load, thus gradually inducing re-fracture and implant loosening, along with significant compromise in bio-efficacy. Moreover, it requires a second surgery to remove the fixture after the fracture gets repaired [30,47,48], causing tremendous pain to the patient. Further, such surgery is extremely expensive. Studies have found that these follow-up operations, carried out to remove the permanent implants, contribute to around 30% of all orthopaedic surgical procedures combined [49]. Failing to timely removal of these permanent fixtures may give rise to severe allergic problems due to the accumulation of ions surrounding the fractured site causing osteolysis, impeding the formation of new bone [47,48]. Biodegradable polymers like polyglycolic acid (PGA), poly L-lactic acid (PLLA), and their copolymers have been approved as potential candidates in applications related to soft bone and tissue engineering, where a high degree of formability is essential to form complex shapes along with alterable surface properties [50–54]. However, their use is mostly limited to low load-bearing fracture sites and carries a high risk of untimely failure due to their insufficient load-bearing capacity [51,53]. Furthermore, the by-products of polymers are prone to cause an inflammatory response for the long term and do not accommodate for osseointegration [51]. All these limitations of biodegradable polymers have compelled the researchers to explore some alternative biodegradable options.

Extensive research is being carried out since the last two decades on biodegradable Mg and Zn based alloys [55–58], which possess enormous potential to completely replace the permanent metallic fixtures and revolutionize the implant industry. In this context, Mg-based alloys are gaining remarkable attention over other alternatives due to their several desirable properties. Although Mg and Zn both come under the list of essential elements required for a healthy body, Mg is a much preferable option over Zn since the recommended daily consumption of Mg for an adult (240–420 mg/day) is 52.5

times higher than that of Zn (8–11 mg/day) [59,60]. Furthermore, the elastic modulus (E) and density (ρ) of Mg and its alloys (E = 41–45 GPa, ρ = 1.74–1.84 g/cc) are much closer to that of a natural bone (E = 15–25 GPa, ρ = 1.8–2.1 g/cc), compared to any other biocompatible metallic materials including Zn ($E\sim$ 90 GPa, $\rho\sim$ 7.13 g/cc) [61–64]. Mg, being an active element with low standard electrode potential (−2.372 V vs. SHE) [65], has a high tendency to corrode in aqueous solution and more aggressively in bodily fluid, in the presence of chloride ions. The intermediate products that are formed due to its degradation are bioabsorbable, and the excess can be excreted through kidneys, unlike that of the permanent metallic implants which show a tendency to accumulate inside the body. Additionally, magnesium-based implants have shown to stimulate new bone formation in the physiological environment when they are implanted as bone fixtures [66–68]. The unique combinations of biodegradability, excellent biocompatibility, and adequate mechanical properties of Mg-based alloys make them one of the most suitable candidates for temporary fixation devices.

An extensive *in-vitro* and *in-vivo* investigations have been carried out on some Mg-Al and Mg-RE (rare-earth elements) based alloys, including AZ31 [69-71], AZ61 [72-74], AZ91 [75,76], WE43 [77], WE54 [78], LAE442 [79,80], JDBM [81,82], and ZM21 [83,84] to figure out their potential in terms of bio-implants. It has been observed that these alloys exhibit good mechanical strength and adequate corrosion resistance required for temporary orthopaedic implant applications. However, several studies have revealed the elemental toxicity of Al, which might adversely affect the neurons and osteoblast cells in body, leading to dementia or Alzheimer's disease [85,86]. It has also been reported that some of the rare earth elements *viz*. Ce, Ho, Pr etc. have a tendency to cause severe hepatoxicity in body [87–90]. Therefore, Mg-based implants containing Al and some of these rare earth elements carry a risk to induce moderate to severe toxic effects in body and the toxic effect become prominent when the concentration of these alloying elements in body cross a certain limit [85,88]. However, it is also important to mention here that one of the Mg-RE based alloy system (MgYREZr) has fulfilled the requirements of temporary implants and has gained the CE (Conformite Europeene) approval for commercial use in 2013 [91]. Therefore, the prospects of these alloy systems in temporary implant applications cannot be overlooked. Alongside those alloy systems, the incorporation of some body nutrient elements like Zn, Ca, Mn, Sr etc. in Mg has recently become quite popular for the fabrication of biocompatible temporary implants. It is due to the reason that these alloying elements are considered as essential trace elements for body and therefore, regarded as non-toxic upto a considerable amount. In this regard, Mg-Zn, Mg-Ca, Mg-Zn-Ca alloys [92,93] and bulk metallic glasses [94,95], Mg-Sr, Mg-Zn-Mn [96], Mg-Zn-Ca-Mn [97–99], and Mg-Nd-Zn-Zr [81] alloys are gaining attention as potential biocompatible implant materials.

Despite possessing several desirable properties, the commercialization of Mg-based devices as temporary implants is still limited due to their uncontrollable degradation rate in the physiological environment. The presence of a high concentration of chloride ions (∼96–106 mEq/L) in bodily fluid [100] and a pH of around 7.4–7.6 [101], makes the Mg-based implants to degrade much more aggressively compared to the typical aqueous solution. Moreover, the rapid rate of formation of gas bubbles has a negative impact on the patient's health. In this degradation process, the implants lose adequate mechanical integrity to bear the load and become highly prone to sudden untimely failure. Therefore, the development of Mg-based implants with a controlled degradation rate to sustain the required period of the bone healing process (∼24–32 weeks) still stands as a challenge, and it compels the researchers and scientists to put more efforts in modifying bio-corrosion properties of Mg alloys by suitable means [101,102].

This review paper presents several aspects of Mg-based alloys, which make them an ideal choice for temporary implant fixtures. The article comprehensively discusses the properties of some important Mg-based alloy systems emphasizing on the alloys possessing favourable biocompatibility, the degradation process of the alloys, the current progress of their clinical translation, the importance of bioactive surface coatings to overcome rapid degradation problem, and the future prospects these alloys.

2. Suitability of Mg alloys as temporary implants

There are some key attributes that a temporary implant must serve. Mg-based alloys comply with most of these requirements. Based on the intended application, the requirement of properties definitely varies. However, when we are mainly focusing on temporary orthopaedic fixtures, the most desirable properties include biocompatibility, adequate mechanical properties, natural degradability, and osteogenesis. Fig. 1 schematically represents the property requirements of temporary implants and their correlation with alloy designing, processing and surface modification techniques. These alloy designing coupled with material processing and surface modification techniques employed to improve the alloy properties have been reviewed elaborately in the subsequent sections.

2.1. Biocompatibility

Biocompatibility and nontoxicity stand as the first and foremost requirement of any implant material. As soon as a foreign material is implanted in human body, a set of reactions take place between the implant material and the host tissues which decide the acceptability of the implant by the body [103]. In case of permanent implants, biocompatibility depends on how strongly the newly generated tissue integrates with implant surface. However, temporary implants are intended to work as support for fractured bone until it heals, and then it is supposed to degrade within the body at a controlled rate [5,104]. It is of great concern if the degradation product starts interacting with any physiological element in a negative manner. Therefore, the temporary implant ma-

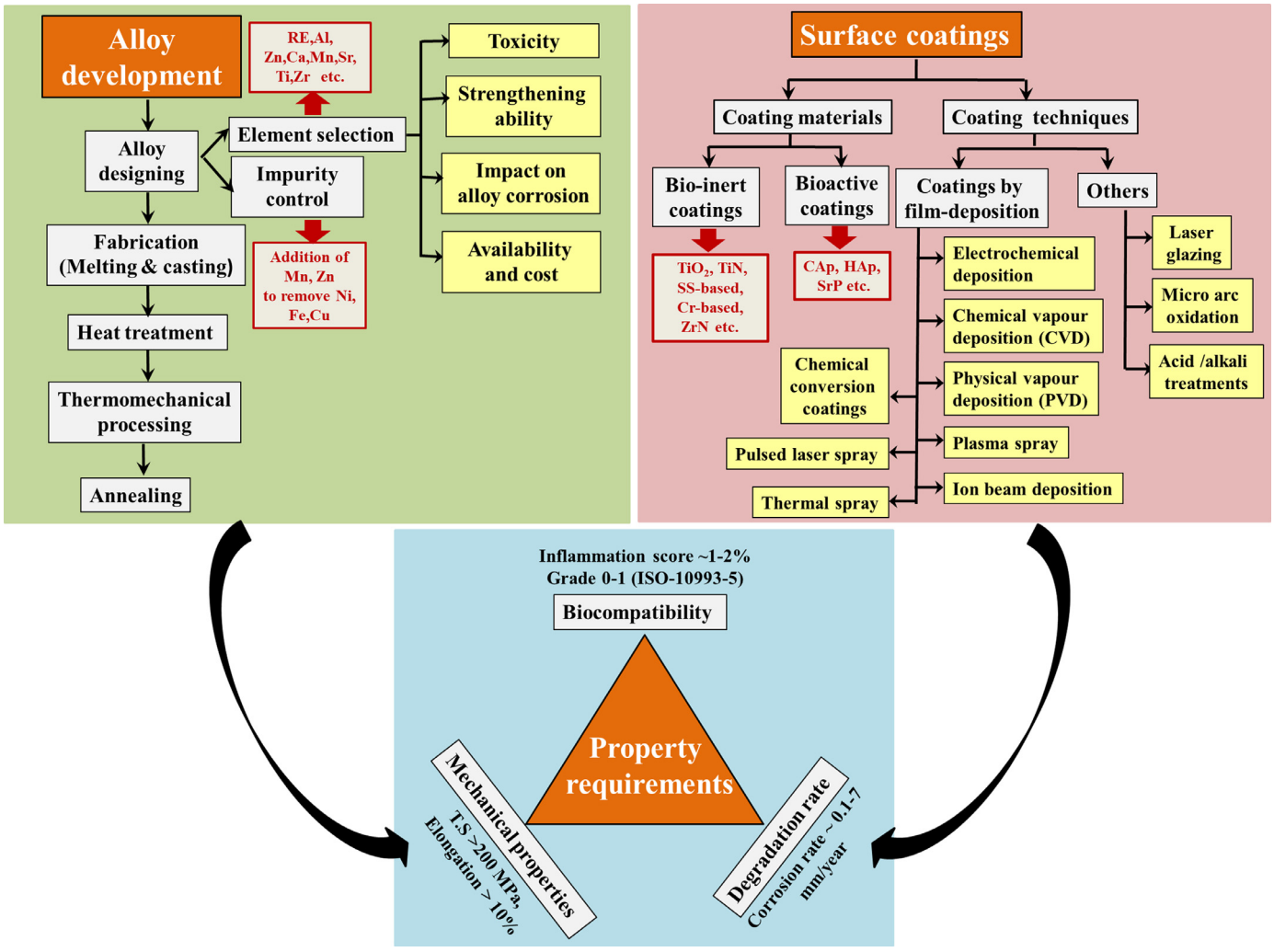

Fig. 1. Correlation amongst the property requirements of temporary implants and the alloy designing techniques in terms of alloy development and surface modifications for Mg-based alloys required for orthopaedic applications.

terials should be non-toxic in nature and must not cause any inflammatory or allergic reactions within body.

Mg being an integral part of bone structure and the fourth most ample cation available in the human body, possesses high biocompatibility which makes it as one of the most suitable choices for temporary implants. It is estimated that approximately 21 to 35 g of Mg is stored in one healthy adult of 70 kg body weight [105,106]. Around 20% of the total available Mg is stored within bones, whereas 35–40% of it is found in tissues and ligaments [107], leaving around 1% mixed in body fluid [107,108]. Apart from this, around 300 enzyme related reactions depend either directly or indirectly of Mg availability [109,110]. The daily allowable limit of Mg intake is second highest (~420 mg) amongst all essential nutritional elements [107]. Moreover, the products generated due to degradation of Mg and its alloys can be absorbed by macrophages and excreted safely through urine without causing any harm to physiological activity [109,111].

Several studies have been carried out to investigate the effect of Mg-ions, generated through degradation process, on cell viability. When we are considering Mg-based alloys for bone implant applications, it is crucial to understand the impact of Mg ions on stem cells. Stem cells are building blocks for different type of cells within human body, including natural bones. The proliferation and differentiation of stem cells form osteoblasts, which act as structural units to form new bones [112,113]. A study conducted by Abed *et al.* [114] has indicated that the presence of Mg ions in extracellular matrix can help in stimulating the gene expression of melastatin-type transient receptor potential 7 (TRPM7) channels in MG-63 type osteoblast cells of human. Later, He *et al.* [115] have carried out a systematic investigation to understand the influence of Mg-ion concentration on human bone cells. They examined the effect of Mg-ions on gap junction intercellular communication (GJIC) within human osteoblast. It has been found out that Mg-ion concentration of 3 mM can induce significant increase in cell viability ($P < 0.05$, where P indicates proliferation index) along with improving the activity of alkaline phosphates and osteocalcin levels. All these factors were observed to be simultaneously increased with in-

Table 2
Comparison of mechanical properties of common implant materials [8,45,46,120,129].

Materials / Alloys		Density (g/cc)	Elastic modulus (GPa)	YS (MPa)	TS (MPa)	Elongation (%)
Natural bone		1.7–2.0	3–20	60–90	80–150	1–6
Permanent implant materials	SS-alloys	7.9–8.1	190–205	180–250	350–620	30–40
	Ti-alloys	4.4–4.5	110–117	270–400	460–900	8–15
	Co-Cr alloys	8.3–9.2	210–230	290–410	530–950	30–40
Potential temporary implant materials	Mg-based alloys	1.74–2.0	41–45	120–180	140–290	1–11
	Zn-based alloys	7.14–7.3	90–100	115–205	160–390	3–15
	Fe-based alloys	7.8–8.1	200–205	140–260	210–360	30–45
	DL-PLA	_	1.9	_	27–41	3–10

crease in Mg-ion concentration and exposure time. They concluded that Mg-ions can significantly enhance the GJIC between bone cells. Since, the gap junctions play a crucial role in signal transmission, it can promote bone generation and remodelling. The osseous growth of Mg implants has been proven in many experimental trials on other animals with the aid of computer tomography and fluorescent imaging. It is reported that the use of Mg implants can significantly enhance the formation of new bone around the implanted bone of mice. According to a report published by Zhang *et al.* [116], an intramedullary implantation of a pure Mg pin into the distal femur of rats resulted in formation of new bones at the peripheral sites of cortical bones. It is evident from their study that the Mg ions can help in mediating the Mg transporter 1 (MagT1) and TRPM7, which promote a substantial increase in calcitonin gene-related polypeptide α (CGRP) in the peripheral cortex of the Mg-pin implanted bone. The released CGRP is proven to trigger the binding process of cyclic adenosine monophosphate to its protein molecule. Thus, it leads to significant enhancement of osterix and consequently results in abundant osteogenesis. A recent study conducted by Nie *et al.* [117] has shown that Mg^{2+} ions (concentration of 10 mM) with collagen-1 coating can regulate the activity of MC3T3-E1 cells via different protein-coupled receptor pathways. More detailed information regarding the effect of Mg-ions on cell viability can be obtained from several other studies reported in literature [118,119].

2.2. Mechanical integrity

Mechanical properties are vital in deciding the suitability of a material to be used as an orthopaedic implant for an intended application. The properties which get prime importance include elastic modulus, tensile strength, fatigue strength, hardness, and elongation. Ideally, the biomedical implants should have an elastic modulus value as close as possible to that of natural bone to avoid 'stress shielding effect' [43,44]. The data provided in the **Table 2** compares the elastic modulus values of several bio-implant materials. These data imply that Mg implants have the closest elastic modulus to that of natural bone, and one of the most vital reasons behind replacing commercial permanent implant materials by Mg-based alloys lies here. It has been reported in several literatures that the combination of tensile strength and ductility necessary for a temporary implant should be >200 MPa and >10%, respectively [120–122]. The fatigue strength of the implant material is a crucial factor since they are bound to bear repetitive loadings due to our regular activities. The cyclic loading combined with corrosive body fluid may also cause corrosion fatigue. The amount of repetitive loading, however, depends on type of implant and its function, the skeletal position, and daily human activities.

2.3. Natural degradability

In the case of temporary implants, the implant material is desired to be biodegradable in nature which means the material should degrade by itself when in contact with corrosive body fluid. The whole idea of placing a temporary implant is to fix the fractured bone in place and provide necessary support until the regenerative process related to bone healing is completed. The course of regenerative process can be roughly divided into 3 major phases namely, inflammatory phase (duration: 3–7 days; represents the response of the body towards the foreign implanted device and proliferation of bone cells should lead to osseointegration), reparative phase (duration: 3–4 months; in this phase integration of implanted device with the associated bone initiates and bone regeneration starts), and remodelling phase (duration: several months; in this phase the implant should ideally start degrading gradually in a uniform and progressive manner, whereas osteogenesis should promote structural modelling to fix the fracture eventually) [32,123–125]. However, the type of bone and its location highly influence the duration of the phases and associated processes. Therefore, the requirement is to curb the rate of degradation significantly until the initiation of remodelling phase and this duration is minimum 24–32 weeks [123,126]. But, the degradation rate of Mg and its alloys is much higher in body than that of bone healing rate. Therefore, most of the research works are now orientated towards improving the *in-vivo* corrosion properties of the implants.

2.4. Osteogenesis

Osteogenesis is a process of developing new tissues to repair a fractured bone. It is an essential requirement for temporary implants as the fractured bone should join with the aid of newly generated tissues and cells prior to implant

degradation [127,128]. This physiological process is highly influenced by various cellular, biochemical and pathological factors. Some bio-active materials (e.g., hydroxyapatite, Ca-phosphates, phosphate derivatives etc.) increase the probability of osteogenesis due to their close resemblance with human bone composition [128–131]. This group of materials are preferred for temporary implants. Osteogenesis is an inherent property of Mg and its alloys, which make them highly preferable compared to any other bio-inert material. The osseous growth of Mg implants has been proven in many experimental trials on animals with the aid of computer tomography and fluorescent imaging [128,132].

3. Fabrication techniques adopted for Mg-based implants

The processing history of the alloys directly influence their structure and hence dictate their properties and performance. The basis of producing a pre-determined set of desirable properties lies in engineering the structure of the material through appropriate processing steps. The progressive advancement in the field of materials engineering has enabled the fabrication of Mg-based alloy systems through several conventional processes such as casting, heat treatment of alloys, wrought techniques (thermomechanical processing), powder metallurgy route etc. Alongside these conventional techniques, laser additive manufacturing has emerged as an advanced technique for manufacturing Mg-based alloys. This section provides a brief overview on the different processing techniques commonly adopted for attaining desirable properties in Mg-based alloys.

3.1. Casting

Amongst the conventional processing techniques available for fabricating Mg-bone implants, casting is considered as the most convenient process which is widely employed. This is due to the fact that it is comparatively simpler and cost-effective process which provides additional scope for further improvement of properties through heat treatment and hot deformation. Moreover, the melting-casting route provides a more convenient way to regulate the concentration of alloying elements to be added to Mg and hence, imparts an easier control on the overall alloy composition [133,134]. It can be observed from literature survey that majority of the Mg-based alloys are fabricated through casing route only. Sand casting, squeeze casting, stir casting, high pressure gravity casting etc. are some of the variations commonly used for processing Mg-based alloys. However, it is challenging to achieve sound cast product due to high affinity of magnesium towards oxygen [135]. Protective flux-cover (20% KCl+50% $MgCl_2$+15%MgO+15% CaF_2 in wt%) or inert gas mixture is used during melting to reduce tendency of oxidation [136]. Moreover, the presence of unavoidable segregation and inhomogeneities in cast structure almost always necessitates a follow-up processing through suitable heat treatment and/or hot deformation.

3.2. Heat-treatment and thermomechanical processing

Mg-based alloys in as cast condition have been extensively investigated by researchers. Most of the binary and ternary alloys in cast form consist of α-Mg matrix and one or more second phase precipitates depending on alloying addition. In as-cast alloys, the second phase precipitates are preferentially distributed along the grain boundaries, which is not much useful in strengthening the alloys; rather it deteriorates the ductility and corrosion properties of the alloys [121].

Heat treatment is considered as an effective method through which the microstructure of the alloy can be altered desirably without changing the shape or chemical composition of the cast alloy [137–140]. T4 (solid solutionizing followed by natural ageing), T5 (artificial ageing), and T6 (solid solutionizing + artificial ageing) are the most commonly adopted heat treatments for Mg-based alloys and the treatment temperature depends on the change in solubility of the element with temperature. In general solution heat treatment (between 613 and 838 K) followed by ageing (between 423 and 533 K) has shown remarkable improvement in strength as well as degradation resistance of the alloys by altering the distribution, volume fraction, shape, size, type and coherency of the second phase precipitates [139,141,142]. Moreover, multi-stage solutionization treatment has been adopted for some Mg-based alloys instead of using conventional solutionization process, in order to avoid incipient melting of the alloys and to ensure maximum solubility of the alloying elements during solutionization [143,144].

As mentioned above, an inherent problem associated with most of the as-cast Mg-based alloys is their insufficient ductility due to formation of secondary intermetallic phases during solidification along grain boundaries in an interconnected network like manner. In this regard, appropriate thermomechanical processing, alone or often in combination with proper heat treatment schedule, has shown remarkable improvement in mechanical as well as in bio-corrosion properties of the alloys. Partial dissolution of interconnected network of secondary phases and their redistribution [138,141], increase in dislocation density [145], and grain refinement [146–149] are regarded as some of the major reasons behind improved alloy properties achieved through thermomechanical processing. Hot deformation techniques are essentially used for Mg-alloys to improve its formability by activating additional slip systems [150,151]. Extrusion [152–154] and rolling [155,156] are the most widely investigated techniques for deforming Mg-based alloys. Recently, hot forging techniques like hard plate hot forging (HPHF) [146] and impression die forging are also gaining popularity. Severe plastic deformation (SPD) techniques [121,157,158] like equal channel angular processing (ECAP) [99], high pressure torsion (HPT) [159,160], cyclic extrusion and compression (CEC) [161,162], and multi directional forging (MDF) [163,164] have also been used to significantly refine the grains (1–5 μm), much lower than that is achieved through conventional hot deformations. Since thermomechanical processing is useful in breaking down the interconnected second phase to much smaller and evenly dis-

tributed ones, they can significantly improve the strength and ductility of the alloy, making them appropriate for implant applications. During thermomechanical processing, formation of new coherent precipitates take place at the interface of the matrix and already existing secondary phases which has been observed to contribute towards further strengthening of the alloy [146]. Therefore, thermomechanical processing can be considered as an essential step in achieving a desired combination of strength and ductility for the alloys. However, the usefulness of thermomechanical techniques invariably depends on choosing appropriate hot deformation parameters for a particular alloy system. Table 3 summarizes the commonly used processing techniques, related deformation parameters, and their role in improving mechanical properties of some important Mg-based alloys. The implications of the heat-treatment and plastic deformation techniques on mechanical properties for the different alloy systems are mentioned elaborately later in Section 4.1 of this article.

3.3. Powder metallurgy route

Powder metallurgy route allows to fabricate Mg-based alloys or composites of high precision with generation of minimum wastage. The process ensures production of near-net shape implant with complex geometries and thus eliminate the additional machining steps. The accuracy of design, calculated control over porosities, ability of mass production, and uniformity of products achieved through powder metallurgy route is hardly attainable through casting [165,166]. All these advantages make this fabrication route a popular one for manufacturing Mg-based bone implants.

Powder metallurgy is extensively utilized in manufacturing Mg-based bio-composites for implant applications. The dispersion of nanometric reinforcing agents in Mg matrix can significantly improve the strength and overall mechanical properties of an Mg-based bio-composite. Phosphate based bio-ceramics namely, hydroxyapatite and tricalcium phosphates have gained huge attraction as reinforcements for Mg-based bio-composites since they are biocompatible in nature. On the other hand, bio-inert reinforcements like alumina (Al_2O_3), zirconia (ZrO_2), and carbon nanotubes are also extensively used in fabricating these composites. Khalajabadi *et al.* [167] have studied the effect of incorporating MgO in Mg-HAp nanocomposites formed through powder metallurgy. They have reported that with incorporation of 10 wt% MgO, the corrosion resistance of the composite increased from 0.25 kΩ cm^2 to 1.23 kΩ cm^2 due to development of a complex surface layer over the substrate. The film was composed of several components like $Mg(OH)_2$, HAp, $Ca_3(PO4)_2$, and amorphous Ca-phosphate. Torabi *et al.* [168] have investigated the properties of Mg-HAp bio-nanocomposites (the concentration of HAp was varied between 2 and 10 wt%) fabricated through powder metallurgy route. They have reported that the highest value of UTS was associated with the Mg-5HAp composite and the mechanical properties deteriorated with increasing the concentration of reinforcement above 5 wt%. Dubey *et al.* [169] fabricated Mg-Zn-HAp composites through powder metallurgy route. They have concluded that an apatite layer can readily deposit on the bio-composite surface which aids in restricting further corrosion. Kumar *et al.* [170] have recently published a comprehensive review covering the latest developments achieved in the field of Mg-implants developed through powder metallurgy route.

Spark plasma sintering (SPS) is a comparatively advanced technique in powder metallurgy which utilizes Joule heating to generate heat internally for densifying the powder compacts [171,172]. Therefore, SPS can achieve a near theoretical density even at a lower sintering temperature compared to conventional sintering process [172]. Thus, the process is very effective in limiting the grain growth during sintering. A limited number of studies have been carried out which particularly concentrate on fabricating Mg-based alloys/composites through SPS. Knapek *et al.* [173] have utilized this technique to fabricate a novel Mg-4Y-3Nd (wt%) alloy. It was observed that both the mechanical and degradation properties were improved by sintering at ∼ 823 K and the microstructure of the alloy was also refined. Dutta *et al.* [174] have reported that they have successfully fabricated Mg composite with bioglass reinforcements using SPS technique. The cell viability tests also showed positive results in terms of interaction with MG63 cells in this composite.

3.4. Laser based additive manufacturing technology

Laser additive manufacturing (LAM) technology has evolved as an advanced fabrication technique since the last three decades. Although LAM has been widely utilized in fabricating Ti and Fe based bio-implants for clinical use, the application of LAM in manufacturing Mg-implant is still at its early stage of development.

The fabrication process through LAM combines three different aspects, viz. computer aided design (CAD), laser processing unit, and a computerized control system. In this fabrication method, the 3D model of the desired product is first converted into a digital STL (Standard Tessellation Language) file and then laser processor is utilized to build the product layer-by-layer with the help of computer aided tomography. Since it is a fully automated technique, it has the capability to produce near net shaped complex structures with high precision. The rapid melting and solidification associated with laser technology can effectively restrict the grain growth and hence result in a refined microstructure [175,176]. The process also ensures high product yield and significantly reduces the material wastage. Besides, LAM can be utilized for processing a wide range of materials (including polymers, metals, composites, and even ceramics) by properly tuning two important parameters related to laser viz., power density and interaction time [177–179]. Most importantly, the technique can produce customized implants with specific need based on defect site and size of the defect [104]. Such customized patient specific implants can enhance the efficiency of the bone healing process significantly.

Li *et al.* [180] have successfully fabricated a Mg scaffold with interconnected pores employing additive manufacturing.

Table 3
Influence of alloy composition (wt%) and processing history on mechanical properties of the Mg-based alloys.

Mg and its alloys	Processing history	Grain size	Mechanical properties				Ref.
Alloy composition (wt%)			YS (MPa)	TS (MPa)	Elongation (%)	Hardness	
AZ31 (Mg-3Al-1Zn-0.13Mn)	As-cast	63 μm	_	163	4.3	_	[190]
	Homogenization at 673 K for 6 h + Extrusion at 573 K, extrusion ratio 9:1, speed 20 mm/s	3.78 μm	198	259	15.6	_	[138]
AZ31 + 1 Ca	Homogenization at 673 K for 6 h + Extrusion at 573 K, extrusion ratio 9:1, speed 20 mm/s	2.98 μm	274 ± 4	311 ± 5	20.8 ± 0.9	_	[138]
AZ61 (Mg-5.84Al-1.2Zn-0.17Mn)	Repetitive upsetting extrusion (RUE) at 613 K, 2 passes	7 μm	130	240	14	_	[191]
AZ91D (Mg-23Al-2 Zn)	As-cast	_	145	275	6	65 Hv	[192]
	Equal channel angular pressing (ECAP), 1 pass	_	198	259	15.6	57 Hv	[192]
EW10 (Mg-1.2Nd-0.5Y-0.5Zr)	As-cast	43.7 ± 0.2 μm	77 ± 4	175 ± 11	12 ± 3	_	[201]
EW10 + 0.4Ca	As-cast	37.6 ± 0.1 μm	74 ± 5	135 ± 11	5 ± 1	_	[201]
ZK60 (Mg-8Zn-1.5Y)	As-cast and then twin rolled at 573 K (84% deformation)	_	390	445	8.3	69 Hv	[202]
	Solution treated at 648 K for 3 h	_	278	342	18	64 Hv	[202]
	T6 treatment (Solution treated at 648 K for 3 h + ageing at 448 K for 10 h)	6.8 μm	334	420	16.1	61 Hv	[202]
Mg-4.71Y-4.58Gd-0.31Zr	T6 treated (Solutionizing at 783 K for 4 h, quenching+ ageing at 473 K for 16 h)	50 μm	255	330	15	1200 Hv (microhardness)	[205]
	High pressure torsion (HPT) at 473 K	20–90 nm	450	475	2.5	1340 Hv (microhardness)	[205]
LAE442 (Mg-4Li-3.6Al-2.4RE)	As-cast	1 mm	220	280	0.4	_	[206]
	Extruded at 623 K, extrusion ratio 23, speed 1 mm/s	21 μm	200 ± 3	250 ± 2	6 ± 0.1	_	[206]
	ECAP (12 passes, strain in each pass is 1.15%)	1.9 μm (after 9 passes)	192 ± 4	221 ± 4	9 ± 0.2	_	[206]
WE43 (Mg-4.38Y-2.72Nd-1.10Gd-0.56Zr)	As cast and heat treated (solution treatment at 798 K for 8 h, quenching + ageing at 473 K for 100 h)	184 μm	145 ± 16	204 ± 6	6.9 ± 0.5	85 Hv	[207]
	Cold impact forging (CIF), total strain 15%, T3-predeformed condition	23 μm	208± 35	259 ± 40	3.3 ± 0.5	74 Hv	[207]
JDBM (Mg-3.13Nd-0.16Zn-0.41Zr)	Homogenised at 813 K for 10 h + Extruded at 523 K, extrusion ratio 25 + ageing at 473 K for 10 h in oil bath	4 μm	189 ± 2	243 ± 3	21 ± 0.9	_	[208]
Mg-5 Zn	As-cast	_	68 ± 1.5	185 ± 5	9.2 ± 0.5	_	[210]
	Homogenised at 623 K for 12 h + Extruded at 573 K, extrusion ratio 12:1, speed 5 mm/s	_	125 ± 5	276 ± 5	29.7 ± 0.5	_	[210]
Mg-4Zn-0.2 Ca	As-cast	90 μm	58.1 ± 1.0	225 ± 5	17.5 ± 1.0	_	[216]
Mg-6Zn-0.82 Ca	Homogenised at 623 K for 12 h + Extruded at 573 K, extrusion ratio 12:1, speed 5 mm/s	32 μm	230 ± 8	304 ± 1.0	15.3 ± 1.6	_	[216]
Mg-Zn-Mn	As-cast	_	78 ± 2	175 ± 3	12	68 Hv	[218]
	Extruded at 573 K, extrusion ratio 10:1, speed 22 mm/s, bar diameter 15 mm	_	210 ± 4	233 ± 2	20	43 Hv	[218]
Mg-4Zn-0.5Ca-0.16Mn	As-cast	79 μm	175	180	0.2	70 Hv	[141]
	Homogenised at 633 K for 24 h	82 μm	110	185	8	63 Hv	[141]
	Hard plate hot forging (HPHF) at 573 K (78% deformation) and then annealed at 623 K for 5 min	14 ± 2 μm	142 ± 8	241 ± 6	19 ± 1	_	[146]
Mg-2Zr-2Sr	As-cast	36 μm	80 (Compressive)	290 (Compressive)	15	_	[260]
Mg-3Sn-2Sr-0.3Ti	As-cast	_	100	160	6.5	68Hv	[223]

Achieving such intricate design is quite impossible by using other conventional techniques. Moreover, the scaffold exhibited only around 20% of volume loss after 4 weeks of immersion in the simulated body fluid (SBF) solution. It has been reported in some literatures that the size and distribution of the pores can affect the rate of hydrogen evolution in Mg-implants. Since, additive manufacturing can effectively control the pore size, it can be employed in fabrication of such porous implants to achieve improved properties. Yang *et al.* **[181]** have reported that the volumetric energy density of laser has an important role in controlling the pore size in Mg implants. They have reported that an optimized volumetric energy density (∼185.19 J/mm^3) can provide sufficient densification without forming any open pores or discontinuities on surface structure. In this study, a bioglass (BG) reinforced ZK60 (Mg-5.6Zn-0.5Zr) composite has been developed by the authors through LAM. The introduction of BG is reported to not only improve the corrosion resistance but also promote enhanced cell proliferation. Also, the fine columnar grains developed in the microstructure resulted in improved mechanical properties (compressive strength ∼153 MPa, Young's modulus∼ 35.5 GPa). A different study conducted on mesoporous bioglass (MBG) reinforced Mg composite, fabricated through LAM, have indicated a deposition of dense apatite layer on the substrate **[182]**. They have concluded that the apatite layer could significantly improve the corrosion resistance (degradation rate ∼0.31 mm/year) of the composite. Moreover, additive manufacturing is reported to induce homogeneous dispersion of alloying elements within the Mg matrix. Most of the elements are dissolved in the matrix due to fast advancement of solid-liquid interface and high temperature gradient achieved through laser processing. This is called as 'solute capture effect' **[183]**. Due to homogeneous distribution of alloying elements and reduced second phase precipitates, the galvanic corrosion is decreased remarkably in LAM fabricated products. Telang *et al.* **[184]** have recently conducted a review that focuses on advancements and future prospects of Mg bio-implants fabricated through LAM.

Although LAM is regarded as a highly promising technique for production of customized Mg-based bone implants, there are several challenges associated with it. Due to low boiling point and high vapour pressure of Mg **[104]**, it is prone to get burnt during laser processing. Also, Mg has the tendency to get oxidized very easily in presence of air since it is very active in nature. Therefore, a high vacuum chamber or protective environment is necessary for producing Mg-implants using LAM. These are the reasons why the manufacturing of Mg-implants using LAM is still at its early stage and requires more attention in future to overcome the constraints.

4. Current status of some common Mg-based alloy systems in terms of their performance

In this section, the mechanical properties, bio-degradation behaviour, and cytotoxic nature of some important Mg-based alloy systems have been reviewed in order to understand their current status as well as the future requirements in terms of alloy development, to realize their clinical transition potential in near future. Although Al and some RE elements have reportedly shown elemental cytotoxicity in body **[**85–90**]**, the alloys bear immense potential for temporary implant applications since they exhibit good mechanical properties and sufficient corrosion resistance. Therefore, the properties of Mg-Al and Mg-RE based alloy systems are included in this section. Besides, the section also focuses on the properties of some potential alloy systems, which have gained huge popularity in recent time, as they contain nontoxic and body-essential nutrient elements as primary alloying components.

4.1. Mechanical properties of Mg-based alloys

Pure Mg in as-cast condition exhibits insufficient tensile strength (∼80–90 MPa) and very limited tensile elongation (∼0.1–0.3%) **[**185-188**]**. This as-cast pure Mg when exposed to thermomechanical processing, results in reduced grain size (as shown in **Fig. 2(a)**), leading to only marginal improvement in mechanical properties **[189]**. Since the mechanical properties exhibited by pure Mg in either as-cast or thermomechanically processed conditions are not adequate to meet the requirements of implant materials, the Mg-based alloys made by incorporation of different alloying elements in appropriate concentration carry major importance in this aspect **[120]**. Suitably adding the alloying elements can facilitate formation of different precipitate phases in the alloy. Evidently, the mechanical properties of an alloy is directly influenced by its microstructural features like the evolution of different second phase precipitates, their distribution, precipitate morphology, average grain size **[121]** etc. In **Fig. 2(b)-(g)** of this article, the representative microstructures of some important Mg-based alloys are shown, marking the important intermetallic phases that form in them both under as-cast and different deformed conditions. The mechanical properties of those alloys have been reviewed in details below.

4.1.1. Mg-Al based alloys

Mg-Al based alloys are one of the most studied alloy systems since the early stage of biodegradable orthopaedic implant development, due to their excellent castability, good mechanical properties, and adequate corrosion resistance **[138,**190–195**]**. The maximum solubility limit of Al in Mg is much higher (≈12.7 wt%) compared to most other alloying elements, resulting in sufficient solid solution strengthening **[120]**. Also, adequate precipitation strengthening is attained by formation of γ-$Mg_{17}Al_{12}$ along grain boundaries (as shown in **Fig. 2(b)**) in these alloys **[192,**196–198**]**. Zn, Mn, Sr or some RE elements (Ce, Ca, Y, Nd) have often been added in Mg in combination with Al in order to enhance the alloy properties. Several literatures have reported that subsequent heat treatment and deformation processes like extrusion, repetitive upsetting-forging are quite successful in improving the alloy properties further by grain refinement through recrystallization (as shown in **Fig. 2(b)**) **[191]**. The typical values of yield strength, tensile strength, and ductility are re-

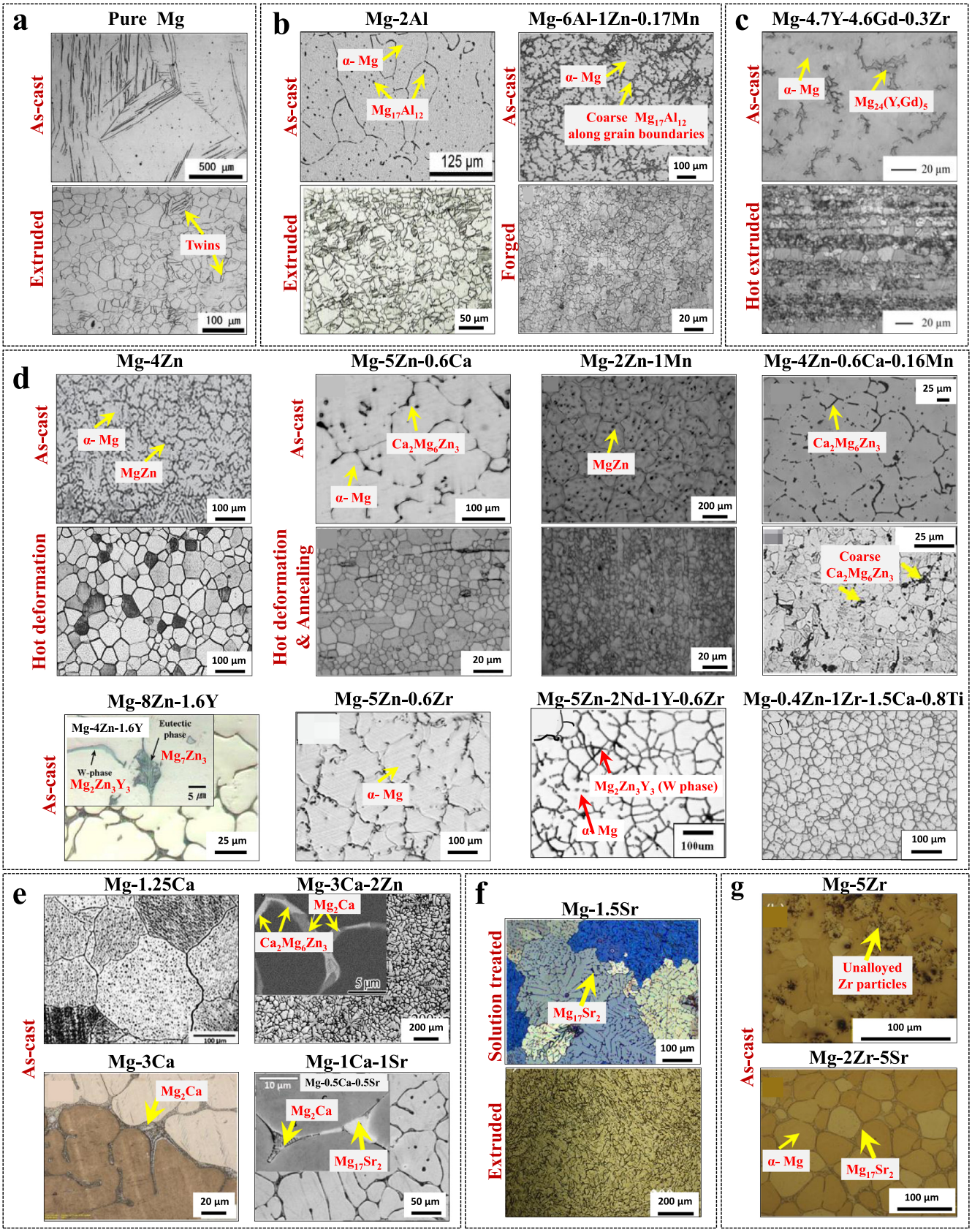

Fig. 2. Representative microstructures of some important Mg-based alloy systems in both as-cast and thermo-mechanically processed conditions: (a) pure Mg [189], (b) Mg-Al based alloys [191,196,197], (c) Mg-RE based alloys [205], (d) Mg-Zn based alloys [141,146,211,212,218,221,224,226,243], (e) Mg-Ca based alloys [246,247,251,254], (f) Mg-Sr based alloys [256,257], and (g) Mg-Zr based alloys [260]. The compositions of the alloys shown in this figure are in wt%.

ported as 145 MPa, 275 MPa and 6% respectively for an as cast AZ91 alloy [192,199]. Moreover, the properties were significantly improved to 290 MPa, 417 MPa and 8.75%, respectively through subsequent deformation by ECAP [199]. However, Al is a well-known neurotoxic element that causes Alzheimer's disease or dementia in patients if the daily intake crosses the maximum allowable limit [85]. Alloys containing Al content more than 4 wt% like AZ91, AM61 have shown harmful effects on neurons and osteoblast cells [28,85]. The potential toxicity that arises from Mg-Al alloys has limited its use as a biocompatible implant and the focus is now shifting more towards addition of essential nutritional elements.

4.1.2. Mg-RE based alloys

Alloying of rare earth elements in Mg has resulted in the highest mechanical strength amongst all the Mg-based alloy systems [200–202]. These alloys can also provide substantial improvement in corrosion resistance (discussed later in this article in **Section 4.2.1**) in combination with tensile strength. Moreover, these alloys are very popular for their high temperature creep resistance property [203,204]. This is indeed not an intended property for implants but it is utilized extensively in automotive powertrain components and aerospace engine components. Y, Gd, Nd, and Ce are some of the most extensively studied alloying elements for Mg-based biomaterials [205–208]. Addition of some other alloying elements in Mg (like Zn and Zr) along with RE elements, have shown remarkable improvement in mechanical properties. MgYREZr alloy (commercially known as WE43) has been reported to possess tensile strength and elongation of 275 MPa and 10% respectively [77,207], and gained an approval for commercial application in human by CE in 2013 [91]. Very high maximum solid solubility limit of some of the RE elements have led to formation of a good fraction of intermetallic phase in the cast and extruded Mg-RE based alloys [200,209], leading to excellent mechanical properties. The Mg-4.7Y-4.6Gd-0.3Zr (all in wt%) alloy in as-cast condition shows the presence of α-Mg matrix and $Mg_{24}(Y,Gd)_5$ precipitates (refer **Fig. 2(c)**) [205]. In the hot extruded condition, the microstructure consisted of fine recrystallized grains and coarse deformed elongated grains elongated in the extrusion direction (**Fig. 2(c)**) [205]. Further execution of high pressure torsion (HPT) at 573 K followed by annealing treatment have resulted in very good mechanical properties (UTS∼375 MPa, YS∼ 335 MPa, elongation∼5.5%) [205]. However, cytotoxicity tests have indicated moderate to high risks associated with some of the RE containing Mg alloys and the level of toxicity increases as a function of RE element concentration in the alloy [87,88]. Despite showing excellent properties, the Mg-RE based alloys always carry certain health risks to be used as a biodegradable temporary implant, as favourable cytotoxicity is considered to be the first and foremost requirement for such implants.

4.1.3. Mg-Zn based alloys

Binary Mg-Zn based alloys typically consist of α-Mg matrix and MgZn as second phase precipitates (**Fig. 2(d)**) [210–212]. Mg-4wt% Zn alloy is reported to show a UTS value of 219 MPa and elongation of ∼16% in as-cast condition [210]. Increase in Zn content upto 5 wt% shows a linear increase in the mechanical strength of the alloy. However, beyond 5 wt%, Zn is reported to deteriorate the alloy properties drastically [210]. An effective way to improve mechanical properties of as-cast Mg-Zn alloys is through heat treatment, which utilizes high maximum solubility of Zn in Mg (6.2 wt%) [120,213]. Lotfabadi *et al.* [214] have reported that T4 treatment at 633 K for a duration of 6 h increases the strength as well as elongation of Mg-1.5 Zn alloy slightly. In contrast, a significant improvement in mechanical properties were obtained with the same treatment for Mg-9 Zn alloy due to presence of residual second phases like $Mg_{51}Zn_{20}$ and $Mg_{12}Zn_{13}$ at grain boundaries [214,215]. Ca, Mn, Zr, Sr, Ti, Mn and Y are some of the alloying elements which have shown promising results when added to Mg-Zn alloys to form ternary or quaternary alloy systems like Mg-Zn-Ca [92,93,216,217], Mg-Zn-Mn [218], Mg-Zn-Ca-Mn [97,99,146,219-221], Mg-Zn-Ti [222,223], Mg-Zn-Zr [224], Mg-Zn-Y [225,226] etc. The microstructures of some of these alloys in both as-cast and hot deformed conditions are shown in **Fig. 2(d)**, marking some of the important intermetallic phases formed in these alloys.

4.1.3.1. Mg-Zn-Ca alloy system. The ternary system of Mg-Zn-Ca alloys is attracting attentions amongst the researchers since optimum addition of Zn and Ca to Mg are effective for improvement of properties as Zn induces strength by solid solution and precipitation strengthening mechanisms whereas Ca improves the corrosion resistance [227]. Additionally, Ca acts as an effective grain refining element in Mg-Zn-Ca alloys [228]. Zhang *et al.* [210] have reported that addition of Ca of concentration greater than 0.2 wt% in Mg-4.0 Zn alloys deteriorate the mechanical properties. The UTS and elongation values of a Mg-4.0Zn-0.2Ca were reported as 225±5 MPa and 17.5 ± 1.0% respectively, whereas for the Mg-4.0Zn-0.5Ca alloy the UTS and elongation have declined to 180±5 MPa and 12.3 ± 1.5%, respectively [86]. It has been identified that change in morphology of second phase is the reason behind exhibition of such characteristics. The polygonal shaped second phase in Mg-4 Zn changed to spherical shape in Mg-4Zn-0.2Ca alloy and consequently, improved the precipitation hardening. However, increase in Ca concentration beyond 0.2% resulted in lamellar second phases, consequently deteriorating the tensile properties. It has been reported that both as-cast and extruded Mg-5Zn-0.6Ca alloy shows presence of α-Mg matrix and $Ca_2Mg_6Zn_3$ phase in microstructure (**Fig. 2(d)**) [86,87]. The average grain size of the as-cast alloy was reported as 100–200 μm with presence of spherical second phases of diameter 1–2 μm, distributed within the grains. However, after extrusion (at 543 K with extrusion ratio 16:1 and extrusion speed 2 mm/s), the average grain size of the alloy significantly decreased to 3–7 μm. The YS, UTS and elongation after extrusion are reported to be 240 MPa, 297 MPa and 21.3% respectively [229].

4.1.3.2. Mg-Zn-Ca-Mn alloy system. After extensive investigation on Mg-Zn-Ca based alloys, it has been reasonably

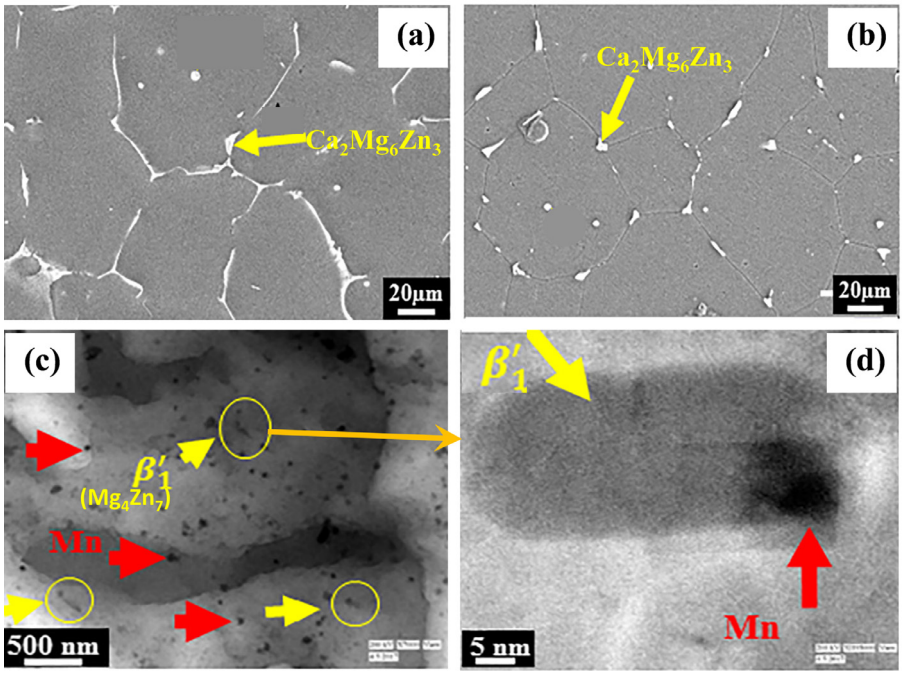

Fig. 3. (a) SEM micrograph of as-cast Mg-4Zn-0.5Ca-0.16Mn alloy, (b) SEM micrograph of homogenized specimen at 633 K for 24 h (AH24) showing partial dissolution of continuous network of eutectic $Ca_2Mg_6Zn_3$ phase, (c) the presence of fine precipitates observed under TEM in the AH24 specimen, (d) enlarged portion from (d) showing the image of β_1' precipitates formed at the interface of Mg matrix and Mn particles [141].

speculated that judicious addition of some non-toxic micro-alloying element, like Mn, can further improve the mechanical as well as the corrosion properties. The microstructure of as-cast Mg-2Zn-1Mn alloy reveals the presence of intermetallic MgZn precipitate phases (Fig. 2(d)) [230]. Increasing the Zn content above 2 wt% is reported to induce higher fraction of Mg_7Zn_3 phase in the alloy [218,230]. Although the as-cast alloy cannot provide sufficient ductility, the hot deformation treatment can significantly refine the grains and improve the mechanical properties appreciably. Addition of Mn in ternary Mg-Zn-Ca alloys does not form any additional intermetallic phase due to extremely limited solubility of Mn in Mg (max solubility ~2 wt%) [120]. However, the volume fraction of $Ca_2Mg_6Zn_3$ phase continuously increases with increasing Mn content upto 0.8 wt% [97]. Experimental results have shown that addition of Mn increases the amount of constitutional supercooling in the alloy, consequently resulting in a decrease in critical size of nucleus during solidification, which ultimately results in grain refining [97]. Addition of 0.8 wt% Mn in Mg-4.0Zn-0.5Ca alloy has resulted in decrease in grain size from 124 μm to 46 μm in as-cast condition of the alloy. Duley *et al.* [141] have reported that homogenization treatment (at 633 K for 24 h) in Mg-4Zn-0.5Ca-0.16Mn alloy can partially dissolve the interconnected crack-initiating network of $Ca_2Mg_6Zn_3$ phase observed in the as-cast condition. The microstructures of the as-cast and the homogenized alloy are shown in Fig. 3(a) and 3(b), respectively [141]. The evolution of different phases through homogenization treatment of this particular alloy obtained through XRD analysis showed that the homogenization treatment induces the formation of additional β' (Mg_4Zn_7) phase, which was not present in the as-cast structure. They have also observed through TEM that the β' phase forms at the interface of Mg-matrix and Mn particles during homogenization treatment (as shown in Fig. 3(c)-(d)). They have reported an appreciable improvement in the ductility of the alloy (e_f~ 8%) compared to the as-cast condition (e_f~ 1%) with marginal decrease in mechanical strength through this homogenization treatment. The improved ductility following homogenization treatment was attributed to the dissolution of interconnected eutectic network of $Ca_2Mg_6Zn_3$. The authors further employed hard plate hot forging (HPHF) on the homogenized alloy of the similar composition [146]. They have concluded that a forging temperature of 573 K promotes significant particle stimulated nucleation (PSN) effect due to presence of higher $Ca_2Mg_6Zn_3$ phase fraction, which leads in a higher fraction of DRX grains and thus resulted in improved mechanical properties (UTS ~ 304 MPa, elongation ~ 6.5%). The ductility is reported to be further improved (elongation ~ 19%) by employing a short annealing treatment for 5 min at 623 K (microstructure is shown in Fig. 2(d)), with a decrease in strength (UTS ~ 241 MPa) [231]. Several works have also been reported on this similar alloy system with varying concentration of the alloying elements. Zhang *et al.* [220] have reported that Mg-2Zn-1.1Ca-0.3 Mn alloy shows optimum combination of strength, elongation and hardness (198 MPa, 5.6%, and 78 HV) when solution treated at 693 K for 24h According to Yandong *et al.* [219], T4 heat treatment (solution treatment at 738 K for 12 h followed by ageing at 448 K and WQ) of Mg-2Zn-0.5Ca-1.0 Mn alloy provide the best combination of UTS and elonga-

tion (180 MPa, 7.5%). Tong *et al.* [99] have reported that 4 consecutive passes of ECAP refines the microstructure of the as-cast Mg-5Zn-0.5Ca-0.3Mn alloy significantly, resulting in grain size of <1 μm. It restricts the basal dislocation movement and improve the mechanical properties of the alloy considerably. The UTS, elongation, and hardness of the alloy after 4 passes of ECAP are reported as 252 MPa, 18.5%, and 91 HV, respectively. It is important to mention here that addition of Mn beyond 0.8 wt% in quaternary Mg-Zn-Ca-Mn alloy system has been identified to deteriorate alloy ductility in as-cast condition due to formation of network-like coarse and brittle Mg-Zn phase along grain boundaries in higher fraction [97,232].

4.1.3.3. Mg-Zn-RE alloy system. Since the inclusion of RE elements as a primary alloying component (in concentration greater than 5 wt%) in Mg-based alloys has been observed to induce severe toxicity in human body, researchers have considered their addition in trace amounts as a secondary or tertiary alloy constituent in developing Mg alloys for implant applications to utilize the strengthening potential of RE elements [233–235]. **Fig. 2(d)** shows the optical microstructure of Mg-8Zn-1.6Y in as-cast condition [225,226]. The inset of this figure reveals the presence of Mg_7Zn_3 and $Mg_2Zn_3Y_3$ (W-phase) in Mg-4Zn-1.6Y alloy, which is known to induce high mechanical strength to these alloys. $Mg_{97}Zn_1Y_2$ (at%) alloy is one of the strongest known Mg-based alloys so far with YS 610 MPa and elongation 5% [236], which is preferentially processed through powder metallurgy route. The strength of these alloys is even higher than commercial Ti based permanent orthopaedic implant alloys like Ti-6Al-4 V. The extremely high strength of these alloys essentially originates from very fine grain size with widely dispersed hard lamellar phase and Long-Period Stacking-Ordered (LPSO) structure [139,154,158]. However, this much of high strength is not required for common temporary implant applications.

4.1.3.4. Mg-Zn-Zr alloy system. Zr acts as dominant grain refiner in Mg-based alloys that contain Zn as a primary alloying element [237,238]. The addition of about 0.4–0.6 wt% of Zr in Mg-3 Zn and Mg-6 Zn alloys has shown promising results. The Mg-3Zn-0.6Zr (ZK30) [239] and Mg-6Zn-0.6Zr (ZK60) [224,239] alloys showed significant improvement in mechanical properties (ZK30: YS-215 MPa, UTS-300 MPa, elongation-9%; ZK60: YS-235 MPa, UTS-315 MPa, elongation- 8%) which are comparable to that of RE element containing WE type Mg alloys (Mg-Y-RE-Zr). The optical microstructure of Mg-5Zn-0.6Zr alloy in as-cast condition is shown in **Fig. 2(d)** [224]. TEM analysis has further revealed that Zn_2Zr_3 and Mg_4Zn_7 are the main intergranular phases present in this system [224]. Moreover, inclusion of Nd and Y in this alloy results in formation of an additional W-phase ($Mg_2Zn_3Y_3$) (**Fig. 2(d)**) [224], which is responsible for further improving the mechanical properties of the alloy significantly. The excellent biocompatibility and osseointegration properties of Zr observed in both *in-vitro* and *in-vivo* conditions are capable of outperforming Ti, thus making it as a suitable alloying element for Mg based bio-implants.

4.1.3.5. Mg-Zn-Ti alloy system. Ti based alloys are considered as an ultimate choice for permanent implants due to its favourable biocompatibility and osteogenesis properties [2,240]. Therefore, addition of Ti as a micro-alloying element in Mg has been considered by many researchers for Mg-based temporary implant applications. As the solubility of Ti in Mg matrix is very low ($\sim$0.02 wt% at 923 K) [241], Ti shows a strong tendency of segregation, which results in PSN [222,242]. Thus, Ti acts as an effective grain refining element for Mg-Zn-Ti alloys. Buha [222] has reported that in presence of Zn as the major alloying element, the solubility of Ti in Mg increases by an order of magnitude. Addition of 0.8 wt% Ti in Mg-0.4 Zn alloy did not show the formation of a new Ti containing precipitate; rather addition of Ti increased the volume fraction of already existing precipitates in the alloy and made them finer, thus improving the mechanical properties of Mg-4.0Zn-0.8Ti alloys [222]. Heat treatment (T6 treatment, 433 K) of this alloy led to homogeneous distribution of precipitates resulting in an increase in hardness (100 HV). Chen *et al.* [243] have reported that Mg-0.4Zn-1.0Zr-1.5Ca-0.8Ti alloy in as-cast condition (microstructure shown in **Fig. 2(d)**) exhibited the best set of mechanical properties (UTS: 145 MPa, elongation: 3.5%, and hardness: 58 HV). Extensive studies of these alloys are yet to be carried out due to extremely challenging alloy processing through melting casting route because of very high melting point of elemental Ti.

4.1.4. Mg-Ca based alloys

Ca, the element with maximum daily intake limit for human-body ($\sim$1400 mg/day) [244,245], is a primary element in forming teeth and bone and plays a crucial role in maintaining the structural as well as functional state of skeletal tissue and in cell signalling. Presence of Ca ion has shown positive effect in bone healing. Promising biocompatible characteristics of Ca has led to the development of Mg-Ca based binary alloys for temporary implant applications. The binary alloys are primarily composed of α-Mg matrix and Mg_2Ca second phases (**Fig. 2(e)**) [246]. The second phases essentially distribute along grain boundaries, thus improving the strength of the alloy by grain boundary pinning and grain refining. However, due to limited solubility of Ca in Mg ($\sim$1.34 wt%) [120], addition of Ca in amount more than 1% has resulted in formation of coarser interconnected Mg_2Ca precipitates along grain boundaries, which deteriorates the ductility of the alloy [247,248]. Therefore, the concentration of Ca is limited to 0.5–1% in most of the Mg-Ca based alloys. The mechanical properties shown by as-cast Mg-1Ca alloy (UTS: $\sim$71 MPa and elongation $\sim$1.9%) [249], are not satisfactory. However, it has sufficiently been improved through hot rolling (UTS: 167 MPa, elongation: 3%) [249,250] and hot extrusion (UTS: $\sim$240 MPa and elongation: $\sim$11%) [249] due to refinement of microstructure. Introduction of Zn in Mg-Ca based alloys resulted in further grain refining leading to more desirable

mechanical properties [251]. Levi *et al.* [252] have reported that solution treatment and age hardening of Mg-Ca-Zn alloy has resulted in dissolution of coarse deleterious Mg_2Ca phase and led to the formation of $Ca_2Mg_6Zn_3$ (Fig. 2(e)). In 2015, Korean government approved an alloy made of Mg-Ca-Zn for clinical use [253]. Recently, addition of Sr in Mg-Ca alloys has shown improved mechanical properties as well as positive effects on osteogenesis [254]. Fig. 2(e) shows the microstructure of Mg-1Ca-1Sr alloy in as-cast condition [254]. The inset of the figure shows the presence of Mg_2Ca and $Mg_{17}Sr_2$ as primary intermetallic phases for Mg-0.5Ca-0.5Sr alloy [254]. Both these phases are helpful in improving the mechanical strength of the alloy. However, higher fraction of Mg_2Ca is known to deteriorate the degradation property of the alloy by inducing significant galvanic effect.

4.1.5. Mg-Sr based alloys

Inclusion of Sr as an alloying element for Mg-based alloys has shown positive impact over osteoblast cell growth and new bone generation along with decreasing tendency of bone resorption. In osteoporosis treatment, strontium ranelate (SR) is used to improve bone strength and bone mineral density [255]. The binary alloys of Mg-Sr in as-cast condition typically form dendritic structure and consist of α-Mg matrix and $Mg_{17}Sr_2$ intermetallic phase which primarily precipitate along the dendritic arms [256,257]. With increasing the concentration of Sr, the mechanical properties improved due to dispersion strengthening by second phase precipitates. Sr is also known for its grain refining ability. However, addition of Sr beyond 3 wt.% leads to deterioration of mechanical properties due to formation of coarser interconnected $Mg_{17}Sr_2$ precipitates along grain boundaries in as-cast alloys [257]. Fig. 2(f) shows the solution treated (homogenised and quenched) microstructure of Mg-1.5Sr alloy [257]. Thermomechanical processing has resulted in improvement of both mechanical properties and corrosion resistance of this alloy by breaking down the interconnected network of eutectic phases and by refining the grains considerably (Fig. 2(f)) [256]. Mg-2Sr alloy in as-rolled condition displayed the best set of mechanical properties (UTS-213 MPa, elongation-3.2%) [256].

4.1.6. Mg-Zr based alloys

Zr is known for its low ionic cytotoxicity and excellent biocompatibility [120]. Zr shows osteogenesis properties equivalent to Ti [258]. The maximum solubility of Zr in Mg is limited to 3.8 wt% [6,120,209]. Addition of Zr in Mg leads to significant grain refinement. The processing of Mg-Zr based alloys are difficult through conventional melting casting route as Zr has a very high melting point (2128 K) [259]. Fig. 2(g) shows the microstructure of Mg-5Zr alloy, which reveals the presence of some Zr particles [260]. It has been found out that the Mg-xZr-ySr alloy with the concentration of x and $y \leq 5\%$ provides an excellent combination of properties in terms of both mechanical integrity and bio-corrosion resistance. The optical microstructure of this alloy is shown in Fig. 2(g) [260]. The Mg-1Zr-2Sr alloy has exhibited nearly 230 MPa of ultimate compressive strength and 31% compressive strain. The addition of 3 wt% of RE element holmium (Ho) to the Mg-1Zr-2Sr alloy has shown to improve the ultimate compressive strength and compressive strain (250 MPa and 32% respectively) [261]. The addition of Ho in the system led to formation of several intermetallic phases like $MgHo_3$ and Mg_2Ho, in addition to $Mg_{17}Sr_2$. These phases are responsible for enhanced mechanical properties of the aforementioned alloy. Another Mg-Zr based system that has been explored by researchers is Mg-Zr-Ca based alloys. Mg-1Zr-1Ca alloy in as-cast condition has exhibited around 175 MPa of ultimate compressive strength, whereas after hot rolling the strength is approximately doubled ($\sim$ 300 MPa) [262].

4.2. Degradation behaviour of Mg-based alloys

High rate of degradation is considered as the main obstacle behind commercialization of Mg-based alloys for orthopaedic implant applications. Therefore, significant attention is required in understanding the influence of different factors on degradation behaviour of the alloys. It has been reported in literature that the desired degradation rate should be $\sim$ 0.1–7 mm per year [28]. In this regard, the alloy designing strategy is considered as an important aspect which can alter the degradation properties of Mg-based alloys. Incorporation of different alloying elements in Mg can significantly modify the microstructure by changing the precipitates type, volume fraction of precipitates, their shape, size, and distribution within the alloy. All these factors can highly influence the mechanical properties as well as the corrosion behaviour of the alloy. Moreover, the presence of any impurity in the alloy is known to induce accelerated galvanic corrosion. Therefore, the effect of alloy designing strategy and purification on degradation behaviour has been discussed in this section.

4.2.1. Effect of alloy design on degradation properties

Incorporation of alloying elements into Mg can form different intermetallic phases within the Mg matrix. The corrosion potential of intermetallic phases that form due to alloying generally differs from that of Mg matrix, thus induces galvanic corrosion in the alloy. The severity of galvanic corrosion depends on the difference in corrosion potential existing between the matrix and the respective phase. The tendency of galvanic corrosion also increases with increasing the volume fraction of second phase precipitates in alloy. Fig. 4 presents a compilation of polarization curves obtained in 0.1 M NaCl solution, revealing the corrosion behaviour of some important intermetallic phases generally form in binary Mg-based alloys and compare them with pure Mg [263]. It can be observed from the figure that the intermetallic phases can be either anodic or cathodic in nature with respect to pure magnesium and thus form a micro-galvanic couple, leading to galvanic corrosion of the alloy. However, adoption of proper alloy designing strategy can tune the microstructure desirably to control the alloy degradation. An appreciable improvement in corrosion properties of pure Mg has been observed through addition

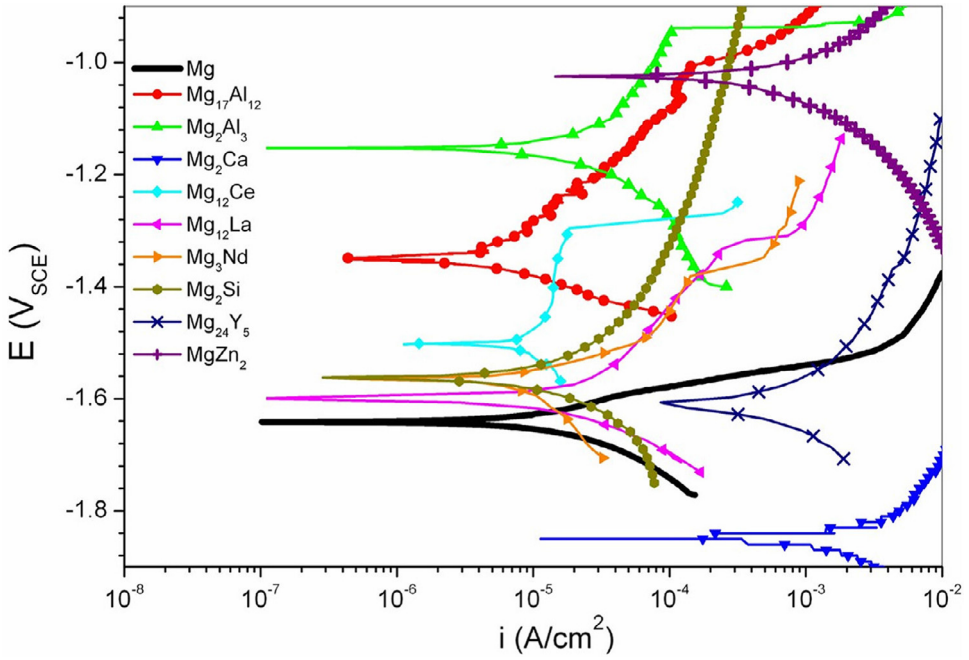

Fig. 4. Representative potentiodynamic polarization curves obtained for some commonly formed intermetallic phases in Mg-based alloys in comparison to pure Mg [263].

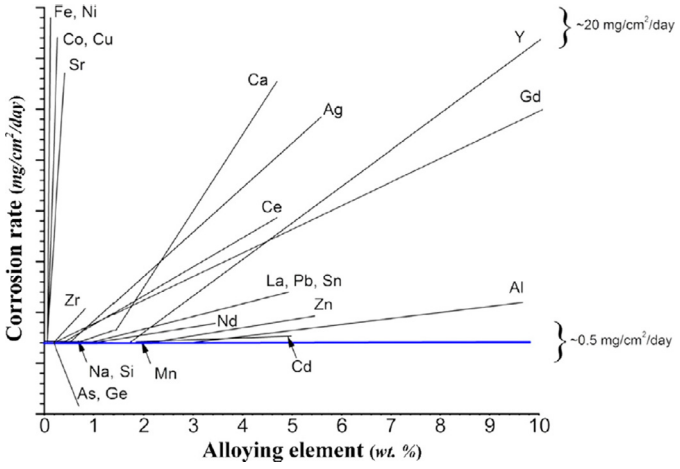

Fig. 5. The influence of different alloying element concentrations on respective binary Mg alloys in NaCl solution [264].

of alloying elements in proper concentration. It has been reported that most of the alloying elements should be added upto a critical limit for improving corrosion resistance of the alloy, which is decided based on the solubility level of the alloying element in Mg [120]. Addition of any alloying element beyond their critical limit often results in deterioration of corrosion properties [187]. Fig. 5 shows the influence of different alloying element concentration on the corrosion rate of the alloy [264]. Appropriate solid solution heat treatment followed by ageing and plastic deformation techniques have been able to significantly improve the corrosion resistance of the alloys by refining the microstructure with fine and well distributed precipitates.

Most of the Mg-based alloys that contain RE elements as the primary alloying element, have shown much better corrosion resistance compared to alloys containing nontoxic and essential alloying elements like Zn and Ca as the major component. This is due to the fact that the second phases those form in Mg-RE based alloys possess corrosion potential almost similar to that of α-Mg matrix, thus reducing galvanic corrosion significantly [200]. Liu *et al.* [200] have summarized the degradation behaviour of as-cast and thermo-mechanically processed Mg-RE based alloys in 0.9% NaCl, SBF, and Hank's solution as well as under *in-vivo* conditions. The as-extruded Mg-3Nd-0.2Zn-0.4Zr (JDBM) alloy [208,265] showed lowest corrosion rate in SBF solution while LAE442 [266] and WE43 [267] exhibited best corrosion properties under *in-vivo* condition. Even after 3 months of implantation, only ~22% reduction in mechanical integrity was observed for WE43. Wang *et al.* [268] have reported that the degradation rate of AZ31 could be significantly reduced by hot rolling and hot extrusion process compared to the as-cast condition. The degradation behaviour of Mg-Al based alloys have been discussed elaborately in several literatures [192, 269], and thereby not emphasized here.

Mg-Zn-Ca based alloys have recently been evolving as superior biocompatible alloys. However, extensive investigation is still going on to achieve an acceptable degradation rate. Addition of Zn in Mg-Ca based alloys is reported to synchronize the corrosion potential of constituting phases. Several literatures have mentioned that Mg-4Zn-0.5Ca alloy provides the best corrosion properties under both *in-vitro* and *in-vivo* conditions [270–272]. Incorporation of Zn and Ca judicially in Mg (Zn=4 wt%, Ca=0.5 wt%) forms α-Mg and ternary $Ca_2Mg_6Zn_3$ phase [210]. However, the addition of

Ca in concentration more than 0.5 wt% is reported to form coarse Mg_2Ca phase preferentially along the grain boundaries within α-Mg matrix. The standard electrode potential of the above three constituent phases can be arranged in a sequence as $Ca_2Mg_6Zn_3 > \alpha$-Mg$> Mg_2Ca$ [273,274]. The alloys with Ca$>$ 0.5 wt%, containing Mg_2Ca as the major phase distributed in α-Mg matrix, are observed to be highly prone to galvanic corrosion. It is due to the reason that the Mg_2Ca precipitates act as anodes in the galvanic coupling formed between these precipitates and α-Mg phase, as per their standard potential. Since the precipitate area fraction is always much lower than the matrix, it leads to unfavourable anode to cathode area ratio. However, in Mg-4Zn-0.5Ca alloys, where Ca content is confined within 0.5 wt%, α-Mg matrix acts as an anode between α-Mg and $Ca_2Mg_6Zn_3$ phase. As the anode to cathode ratio in this case is much higher, it suppresses the galvanic corrosion effectively. The corrosion rates of as-cast and as-extruded Mg-4Zn-0.2Ca alloy in c-SBF solution has been reported as 2.67×10^{-4} A/cm^2 and 2.43×10^{-4} A/cm^2 respectively [275], which are much lower compared to pure Mg (3.715×10^{-4} A/cm^2) [185]. The *in-vivo* and *in-vitro* degradation of Mg-4.0Zn-0.2Ca alloys has been conducted by several researchers [276–278]. After 3 months of implantation, the implant changed its shape from rod to some irregular shape indicating *in-vivo* degradation of implant in presence of body fluid. Approximately 35–38% degradation took place in 3 months [276]. A corrosion product consisting of $Mg(OH)_2$, phosphates and hydroxiapatite (HAp) formed over the implant in presence of corrosive body fluid which covered the implant and served as a protective layer against further corrosion. Superior osteoconductivity and biocompatibility of the Mg-Zn-Ca based alloys under *in-vivo* condition have been attributed to formation of protective HAp layer as a corrosion product. Cho *et al.* [279] have investigated the effect of adding Mn as a 4th element in Mg-Zn-Ca alloy system. The authors have compared the electrochemical properties of Mg-4Zn-0.5Ca alloy with and without addition of Mn. Potentiodynamic polarization test has revealed that the corrosion resistance of Mg-4Zn-0.5Ca alloys significantly improved through the addition of 0.8 wt% Mn. The results obtained through electrochemical impedance spectroscopy (EIS) in Hank's solution (**Fig. 6(a)**) revealed that the Mg-4Zn-0.5Ca-0.8Mn alloy shows the highest corrosion resistance. The mass spectrums of different ions present in Mg-4Zn-0.5Ca-xMn alloys obtained through time-of-flight secondary ion mass spectroscopy (ToF-SIMS) are shown in **Fig. 6(b)-(d)**. It has been concluded that with addition of Mn in concentration ~0.8%, a stable and protective layer of MnO and MnO_2 forms over the specimens (**Fig. 6(e)**), which essentially inhibit the penetration of chloride ions and thus improve corrosion resistance. The corrosion rate of as-cast Mg-4Zn-0.5Ca-0.8Mn alloy is reported as 2.85 μA/cm^2, which is much lower than ternary Mg-Zn-Ca based alloys [279]. Heat treatment followed by hot deformation has shown improved corrosion properties due to redistribution of finer precipitates within the grains homogeneously. Mg-4Zn-0.5Ca-0.75 Mn alloy exhibited a corrosion current density of 0.12 mm/year in SBF solution when extruded at 673 K [98].

Gu *et al.* [280] have studied the *in-vivo* degradation behaviour of Mg-Zn-Zr based ZK60 alloys (Zn ~ 4.8–6.0 wt% and Zr ~ 0.5 wt%) in several biologically equivalent fluids like Dulbecco Modified Eagle's Minimum Essential Medium (DHEM), fetal Bovine Serum (FBS), and Hank's solution. The highest rate of corrosion in this study was observed in DHEM+FBS (0.53 mm/y) and the least in Hank's solution. The authors observed that the corrosion rate of as-extruded ZK60 alloy (0.006 mg/cm^2/h) was comparable to that of commercial Mg-based alloys like as-cast AZ91D, extruded AZ31, and even extruded WE43 alloy. The as-cast and as-extruded ZK60 alloy exhibited almost similar rate of corrosion till 24 h after initiation of corrosion test. However, the corrosion rate of the as-extruded alloy dropped to a much lower value after prolonged immersion time while the alloy in as-cast condition continued to degrade at same pace. This is due to the formation of a stable HAp layer over the extruded alloy which reduced the corrosion attack significantly [280]. Incorporation of Sr in Mg-1Zn-1Mn alloy system is effective in reducing the maximum depth of attack which essentially leads to a more homogeneous corrosion rate [281]. Increase in Sr content upto 1 wt% improves the stability of protective film, beyond which degradation rate increases due to dominance of galvanic corrosion between matrix and second phase $Mg_{17}Sr_2$. Addition of Sr and Sn as micro-alloying elements in Mg-Zr-Ca alloy have resulted significant improvement in the corrosion resistance of Mg-Zr-Ca-Sr-Sn alloy ($i_{corr} = 4.26 \times 10^{-5}$A/cm^2) compared to ternary Mg-Zr-Ca alloy system ($i_{corr} = 5.08 \times 10^{-4}$A/cm^2) in SBF solution [282]. Simultaneous addition of Sr and Sn in Mg-Zr-Ca alloy is capable to replace deleterious Mg_2Ca phase at grain boundaries with Mg_2Sn. The standard electrode potential of Mg_2Sn is much closer to α-Mg matrix than that of Mg_2Ca, thus reducing galvanic corrosion significantly [283].

Clearly, the alloy designing and fabrication technique can highly influence the degradation property of the alloy. The progress in alloy degradation, in turn, can impair the mechanical integrity of the alloys and lead to an early implant failure [284–287]. Therefore, the information regarding the deterioration of the mechanical properties of the Mg-based implants after a certain period of implantation is crucial to decide their applicability in practice. **Table 4** enlists some data regarding the loss in mechanical integrity of the alloys after a certain period of implantation or immersion.

4.2.2. Effect of impurity on degradation behaviour

Along with the adoption of proper alloy design and processing technique, it is necessary to take strict control of the commonly found impurity elements in Mg like Be (tolerance limit: 2–4 ppm), Fe (tolerance limit: 30–50 ppm), Ni (tolerance limit: 20–50 ppm), and Cu (tolerance limit: 100–300 ppm) [263,288–291]. These elements act as active cathodic sites and increase the tendency of galvanic corrosion [263]. Moreover, Ni and Cu have shown toxic effects in body

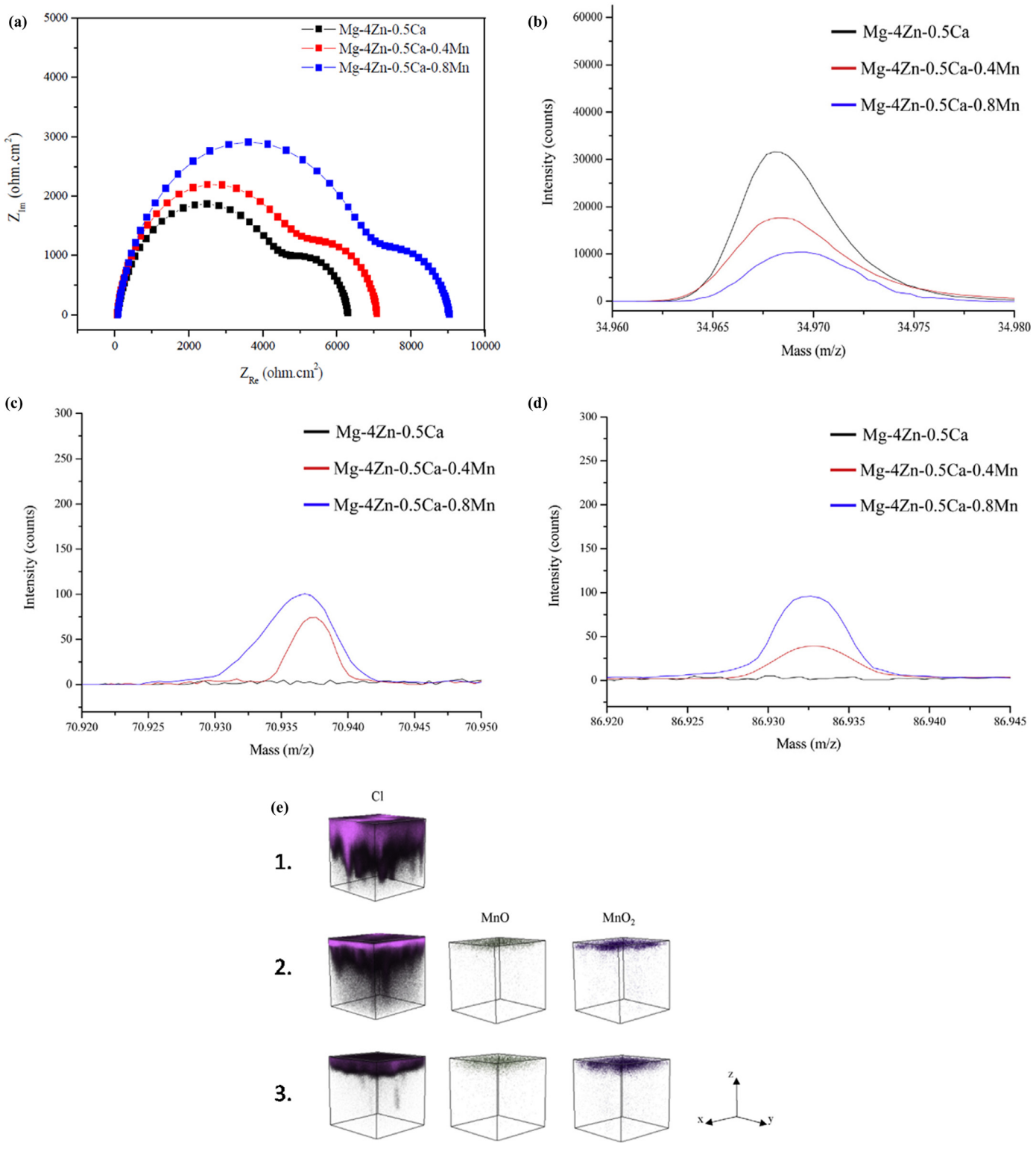

Fig. 6. (a) Nyquist plots obtained for as-cast Mg-4Zn-0.5Ca-xMn alloys in Hank's solution; time-of-flight secondary ion mass spectroscopy (ToF-SIMS) mass spectrums for different ions present in case of as-cast Mg-4Zn-0.5Ca-xMn alloys in Hank's solution after 2 h immersion: (b) Cl^-, (c) MnO^-, (d) MnO_2^-; (e) ToF-SIMS 3D imaging profile for chloride ion, MnO and MnO_2 film for as-cast alloys: 1. Mg-4Zn-0.5Ca, 2. Mg-4Zn-0.5Ca-0.4Mn, 3. Mg-4Zn-0.5Ca-0.8Mn [279].

Table 4
Change in mechanical properties of Mg-based alloys after a certain period of implantation/ immersion.

Alloy composition	Processing history	Implantation period/ Immersion time	Loss in mechanical properties	Ref
Bare Mg	As-cast	Implantation period – 12 weeks (in rat)	Loss of tensile strength ∼ 47.5%	[284]
HAp coated Mg	As-cast	Implantation period– 12 weeks (in rat)	Loss of tensile strength ∼ 7.5%	[284]
Pure Mg scaffold (porous)	Additive manufacturing	Immersion time in SBF – 72 h	Loss of Young's modulus ∼ 70%	[285]
AZ31B screws	Extruded	Implantation period – 21 weeks (in rabbit model)	Strength loss ∼ 42.4% (from bending load test)	[286]
AZ31B silicon coated	Extruded	Implantation period – 21 weeks (in rabbit model)	Strength loss ∼ 29.9% (from bending load test)	[286]
Mg-0.8Ca	Cast and extruded	Implantation period – 6 months (in rabbit tibiae)	Volume loss ∼ 33.33%	[287]
LAE442 (Mg-4Li-4Al-2RE)	Cast and extruded	Implantation period – 6 months (in rabbit tibiae)	Volume loss ∼ 16.67%	[287]
WE43 (Mg-4Y-3RE)	Cast and extruded	Implantation period – 6 months (in rabbit tibiae)	Volume loss ∼ 30%	[287]

during degradation. It is reported that these impurity elements chemically react with other alloying elements, thus reducing their effective concentration in alloy as well form unwanted phases, leading to deterioration of corrosion resistance and overall mechanical integrity of the alloy [120]. Zone solidification has been identified as an effective technique to obtain high purity alloys. Also, additions of some alloying elements like Zn and Mn, which preferentially react with impurity elements (Fe and Ni), are proven to be helpful in reducing the level of impurities [292].

Apart from proper alloy designing and alloy purification processes, surface coatings also have a positive influence in enhancing the corrosion resistance of Mg-alloys. This important aspect has been discussed in details separately in Section 7 of the manuscript.

4.3. Cytotoxicity of Mg-based alloys

Cytotoxicity tests are essential to understand the potential of clinical translation of Mg-based alloys in terms of biosafety. Desirable biosafety is the first and foremost requirement for any material to be used for implants [120,293]. The ISO-10,993 standard (part 5 and part 12) are commonly accepted documents in accessing the cytotoxicity levels of medical devices [120,253], and the inflammation score ∼ 1–2% is regarded as an acceptable value [28]. In this context, it is important to mention that the microenvironments existing for *in-vitro* and *in-vivo* studies are not identical; therefore, the biocompatibility test results obtained in these two cases differ from each other [294,295]. It has been reported that most of the Mg-based alloys show less than 75% of cell viability in terms of ISO standards during *in-vitro* cytotoxicity test. However, under *in-vivo* condition, the ions that get released from the implant during degradation are capable to get diluted promptly by mixing with body fluid and readily diffuse through the circulating system of body prior to excretion. Therefore, for accurate assessment under *in-vitro* condition, extracts of Mg-based implants are diluted to mimic *in-vivo* findings [111,296]. The biocompatibility of any alloy depends on the amount of released ions, which is related to the degradation rate of the concerned alloy under the application environment. High rate of degradation of Mg-based alloys essentially leads to a rapid change in pH and ionic concentration, which adversely affects cell viability. Each and every metallic ion has a definite regular intake limit, beyond which it might exhibit some adverse effects in human body [120]. In addition to that, Al and some rare earth elements (viz. Ce, La, Pr, Ho etc.) show inherent elemental toxicity, which further restricts their tolerance limit in body [85-90]. The toxicity levels and pathophysiology of some relevant alloying elements are given in Table 5. Mg, though a well-known biocompatible element for human body, results in muscular paralysis or hypertension in case the Mg ion level in serum exceeds 1.05 mmol/l [297]. The ionic release of any elements should be within daily tolerance limit. However, this requires a tight control over the degradation rate of the alloy in human body. According to Feyerabend *et al.* [88], *in-vitro* cytotoxicity of various alloying elements like Y, Nd, Pr, Dy, Gd, Ce, La, Li, Zr is significantly influenced by their ionic radii. Drynda *et al.* [298] have developed trivalent chlorides of Ce, Nd, Y and Yb to assess their cytotoxicity levels in terms of metabolic activity of vascular muscle cells and concluded that the concentration of these rare earth elements interrupt in metabolism adversely. As the cytotoxic behaviour of most of the RE elements are still unknown to scientists, the use of these elements as the primary component in Mg based alloys is considered to be risky. On the other hand, Mg alloys containing nutrient elements are gaining considerable attention day by day due to their negligible cytotoxicity factor. Conduction of cytotoxicity test for both as-cast and as-extruded Mg-4.0Zn-2.0Ca alloy has been done on L-929 cells [86]. A combination of DMEM and 10% of FBS was used as cell culture medium. The cell morphology and cell spreading observed in the extracts after 7 days of incubation period were found to be in normal and healthy condition. The cytotoxicity level of these extracts was lying within Grade 0–1 of ISO 10,993–5:1999 [120], indicating suitable biosafety of Mg-4.0Zn-2.0Ca alloys for cellular applications. The cell lines cultured in extracts of Mg-1Ca, Mg-3Ca, Mg-6 Zn, Mg-1Zn-Mn, Mg-1Si, and Mg-2Sr have shown negligible cytotoxicity on both MG63 and L-929 type

Table 5
A summary highlighting the pathophysiology and toxicology of Mg and major alloying elements used for processing Mg-based alloys [106,120,293].

Elements		Blood serum level (mg/L)	Daily allowance (mg)	Pathophysiology	Toxicology	Solubility in Mg (wt%)	Effect on Mg-based alloys
Mg		17.7–25.8	400–700	Acts as activator for enzymes, co-regulator for protein synthesis and muscle contraction, helps generating DNA and RNA	Mg overdose leads to nausea, breathing problem, and kidney failure	_____	
Essential elements for body	Ca	36.8–39.7	1400	Ca is a primary element in forming teeth and bone; plays a crucial role in maintaining the structural as well as functional state of skeletal tissue and helps in cell signalling	Excessive Ca leads to kidney stone, heart problems, and Hypoparathyroidism	1.34	Improves mechanical properties by grain refinement; enhances corrosion resistance; deteriorates properties, specially ductility, over 1 wt%
	Fe	5000–17,600	10–18	Acts as a component of metalloproteins; crucial in oxygen sensing and transport through blood	Excess Fe causes liver damage and lesions in gastrointestinal track	_	Increases galvanic corrosion rapidly- not suitable as an alloying element; considered as an impurity element
Essential trace elements for body	Zn	0.8–1.14	15	Zn as a trace element appears in different enzyme classes; helps forming muscles	High Zn content leads to neurotoxicity, muscle crump, and hinders bone development	6.2	Enhances strength through solid solution strengthening and precipitation hardening; deteriorates overall properties over 5 wt%
	Mn	<0.0008	3.5	Serves as enzyme-activators; deficiency in Mn leads to osteoporosis, atherosclerosis	High Mn content causes psychiatric issues and neurotoxicity	2.2	Mn improves mechanical properties in presence of Zn as the primary alloying element by precipitate formation
	Cu	4.51–8.32	6	A vital element for immune system; shows antibacterial property; helps in cell proliferation	Excessive Cu leads to neurodegenerative diseases	_	Presence of Cu even in very small content results in galvanic corrosion; treated as an impurity element

(*continued on next page*)

Table 5 (*continued*)

Elements			Blood serum level (mg/L)	Daily allowance (mg)	Pathophysiology	Toxicology	Solubility in Mg (wt%)	Effect on Mg-based alloys
Other elements	RE	Y	_	∼ 4.2 (combined)	_	Highly toxic above tolerance limit; causes neurotoxicity, cardiovascular disease, affects blood pressure; toxicity level unknown for some rare-earths	12.4	Significant improvement in mechanical properties with increasing element content; good creep resistance; however, above 2 wt%, shows toxic effect
		Nd					3.6	
		Gd					23.49	
		Ce					0.74	
	Al		0.0021–0.0048	14	_	Al is toxic to neurons, causes Alzheimer disease, decreases osteoblast viability, and damages muscle fibre	12.7	Improves tensile strength by solid solution strengthening: provides sufficient elongation before failure
	Sr		0.17 mg (total)	5	99% of total Sr is located in bones; shows metabolic effects on bone; stimulate bone formation	Sr in high doses result in hypocalcemia and skeletal abnormalities	0.11	Improves strength and corrosion resistance upto 2 wt%
	Zr		<0.250 mg (total)	3.5	Shows low ionic toxicity and good biocompatibility	Accumulates in bone and nervous system	3.8	Acts as a powerful grain refiner
	Ti		_	2.4	Ti has high biocompatibility and considered as an ultimate choice for permanent implants	_	0.015	Very low solubility in Mg; in presence of Zn, solubility limit of Ti increases: improves mechanical properties by increasing precipitate fraction
	Si		_	24–33	_	High SiO_2 content leads to lung cancer gradually	∼ 0	Improves tensile properties by precipitate formation; impairs ductility
	Sn		_	3.5	_	Causes skin and eye irritation	14.5	_

cells [299–301]. Moreover, osteogenesis is an inherent property of Mg and its alloys, which makes the Mg-based alloys more effective in clinical applications. The osseous growth of Mg implants has been proven in many experimental trials over animals with the aid of computer tomography and fluorescent imaging. It is reported that the use of Mg implants can significantly enhance the formation of new bone around the implanted bone of mice [116]. The level of cytotoxicity of any medical device not only depends on the type of the material but also on the location of device application inside human body. For example, biomaterials which will be in close contact with blood (like cardiovascular stents) are of higher concern in terms of biocompatibility rather than the implants. Table 6 summarizes the effect of alloy designing and their processing history on *in-vivo* and *in-vitro* bio-corrosion properties as well as cytotoxic behaviour of the alloys.

In addition to assessing *in-vitro* cytotoxicity of these alloys, it is essential to investigate *in-vivo* biocompatibility to get the safety assurance prior to any clinical trial. In accordance to the ISO standards, numerous animal studies have been conducted to assess biological responses of Mg-based alloys. A series of Mg-based alloys have been tested so far on animal models mostly on Mg-RE and Mg-Al based alloys. The review published by Zhao *et al.* [109] discusses in details about cytotoxicity tests conducted on animals. However, one should be cautious about the discrepancy in results observed between animal tests and clinical trial as in most of the cases animal models are oversimplified in nature.

5. Current progress in clinical translation of Mg-based alloys as temporary devices

The discovery and production of elemental Mg by Sir Humphrey Davy dates back to more than two hundred years ago, in around 1808 [302]. Though elemental magnesium was produced around two centuries ago, the first clinical application of it has been reported in 1878 by Edward C. Huse [303] who used pure magnesium ligatures for stopping bleeding vessel. He reported about the *in-vivo* degradation of Mg and mentioned about the dependency of degradation rate on the size of Mg implant. Following that, many researchers and clinicians have put their best efforts in investigating the properties of Mg and its alloys to understand their usefulness as bio-implants and parallelly worked on enhancing their properties. The brief evolutional history and gradual progress in development of Mg-based alloys as biodegradable fixtures has been summarised in Fig. 7 [304]. The results of most of these early clinical trials were not so satisfying due to highly brittle nature of pure Mg, limited mechanical properties and high degradation rate. Consequently, the clinical applications of Mg implants were nearly ceased around 1950 [109,253,304]. There has not been any significant clinical study reported in between 1950 and 2000. However, with technological advancements in processing Mg alloys with better mechanical and bio-corrosion properties, researchers regained interest in Mg implants following the work of Heublein *et al.* [305] in around 2000–2003. They explored degradation characteristics of Mg to develop temporary biodegradable implants which radically change the aspects of Mg-implant research. After obtaining desired results in terms of efficacy and bio-safety of using Mg-based implants through conduction of a large number of studies on several animal models, more and more scientists and surgeons were inspired to reconsider the clinical application of some Mg-based alloys. Recently, appreciable advancement has been achieved for some of the Mg-based alloys for clinical applications. It must be mentioned here that apart from orthopaedic fixation devices like screws [306–311], microclips [312–314], and plates [315], some other Mg-based temporary devices like stents [316–318], scaffolds [319–322] etc. are quite popular. Fig. 8 shows some of the devices that have undergone clinical trial and some of the promising fixture devices which are at developmental stage.

Amongst these temporary devices, screws are considered as one of the most important temporary orthopaedic implant or fixation device for healing a fractured bone or tissue by providing temporary support. Several clinical trials of different Mg-based alloys have been conducted so far to understand their applicability. In a clinical trial conducted in China (ChiCTR-TRC-13,003,238), biodegradable screws made up of high purity Mg (99.99% pure) were used in 48 patients (of varying ages from 18 to 55 years) for treating osteonecrosis of femoral head [323]. With the help of computer-based tomography, it was observed that the mineral density around the screws was increased at the initial stage. The rate of degradation reported after 1, 3, 6 and 12 months are recorded as 3.7 ± 0.4%, 9.3 ± 0.8%, 13.7 ± 0.4%, and 25.2 ± 1.8%, respectively. Only 2 patients suffered from femoral head collapse after 6 months. Mg level in serum was reported to be under considerable limits. Recently, screws made of high purity Mg has been approved by Chinese authority for applications related to femoral head and femoral neck fractures [253,323].

MgYREZr alloys (commercially known as MAGNEZIX®) were studied for fixture applications for treating 26 patients suffering from mild hallux valgus [309]. The overall performance and bio-efficacy of MgYREZr alloy system was compared with conventional Ti screws using chevron osteotomy and the results obtained after 6 months of follow-up revealed their performance equivalence in terms of Range of Motion (ROM) and painscale assessment for first metatarsophalangeal joint (MTPJ) [309]. In the year 2013, MAGNEZIX® received CE mark due to its satisfactory clinical performance [91]. In 2015, the screws made of MgYREZr were in use for treating madelung deformity in Ireland [109].

The Mg-Ca-Zn system (commercial name RESOMET®) was first clinically tested in Korea for hand bone fracture treatment for 53 patients [324]. The screws were reported to be replaced completely by generation of new bone within 1 year of implantation (Fig. 9). Moreover, no sign of pain or allergic reactions or decrease in ROM was reported in this study, clearly revealing the clinical benefits of using essential nutritional elements like Zn and Ca in the alloy system. The improved contact between bone and implant indicated higher level of biocompatibility in cytotoxicity tests compared to LAE442 and WE43. In 2016, Korean Food and Drug admin-

Table 6
Effect of alloy designing and processing techniques on *in-vitro, in-vivo*, bio-corrosion properties and cytotoxicity of the alloys.

Mg and its alloys	Processing history	*In-vitro* corrosion rate			*In-vivo* corrosion		Cytotoxicity	Ref.
		Solution	Electrochemical	Immersion	Testing animal	Corrosion rate		
Pure Mg plate	As-cast	SBF	1.837 mm/yr	1.218 mm/yr (15 d)	Rabbit ulna	0.40 ± 0.02 mm/yr (8 weeks)	Non-toxic, increases serum Mg level in blood to some extent	[185]
AZ31 (2.5–3.5 Al)	As-cast	m-SBF	0.521 mm/yr	1.997 mm/yr (24 d)	Rabbit femora	40% volume loss in 12 weeks	_	[269]
AZ61 (5.8–7.2 Al)	As-cast	m-SBF	0.507 mm/yr	1.299 mm/yr (24 d)	_	_	Test on human osteosarcoma cells (MG63) showed high toxicity (grade II) according to ISO standard	[269]
AZ91 (8.5–9.5 Al)	Gravity cast	SBF	3.076 mm/yr	1.206 mm/yr (240 h)	Guinea pig femora	3.516 × 10–4 mm/yr (18 weeks)	_	[269]
LAE442 (Mg-4Li-3.6Al-2.4RE)	Gravity cast	SBF	6.9 mm/yr	5.5 mm/yr (240 h)	Guinea pig femora	Approximately 10% volume loss in 24 weeks	Minor cellular reactions	[266]
EW10 (Mg-1.2Nd-0.5Y-0.5Zr)	As-cast	SBF	0.3 mm/yr	1.02 mm/yr (5 d)	Wister male rat back	0.16 mm/yr (12 weeks)	_	[201]
Mg-1.2Nd-0.5Y-0.5Zr-1Ca	As-cast and rolled	SBF	0.18 mm/yr	0.8 mm/yr (5 d)	Wister male rat back	0.14 mm/yr (12 weeks)	80% cell viability after 5 days of culture in L929 cell line	[201]
Mg-2.5Zn-1Ca	As-cast	Hank's solution	_	0.15 mm/yr (7 d)	_	_	_	[275]
	Homogenised at 683 K for 24 h + Extruded at 633 K, extrusion ratio 36:1, speed 4 mm/s, rod diameter 12 mm	Hank's solution	_	0.18 mm/yr (7d)	_	_	_	[275]
ZX20 (Mg-1.5Zn-0.25Ca)	Homogenised at 623 K for 24 h and aged at 523 K for 105 h + extruded	SBF	0.12 mm/yr	_	9 male Sprague Dawley rats	225 ± 19 μm/yr (4 weeks)	Well tolerated by surrounding bone tissues - suitable for musculoskeletal condition	[270]
Mg-0.96Zn-0.75Mn	As-cast + extruded	Hank's solution	0.03 mm/yr	0.051 mm/yr (7d)	Rats	54% degradation of the alloy after 18 weeks	Haemolysis rate 59.3%,no inflammation was observed after 18 weeks	[319]
Mg-1Zn-0.2Ca-0.1Mn	As-cast	m-SBF	5.02 mm/yr	6.33 mm/yr (120 h)	Bone marrow cavity of rats	Completely degrades within 16 weeks after implantation	Highly compatible, helps in osteointegration	[301]
Mg-2Zr-2Sr	As-cast	SBF	_	6.33 mm/yr (120 h)	Male rabbit	Degrades completely after 4 months	Effectively induce bone formation, bone mineral content (BMC) and bone mineral density (BMD) values are significantly higher than those of control groups	[260]
Mg-1Zn-1Mn-0.5Sr	As-cast	Hank's solution	0.15 mm/yr	0.115 mm/yr (7 d)	_	_	Normal level of serum Mg in blood, signs of new bone formation	[283]

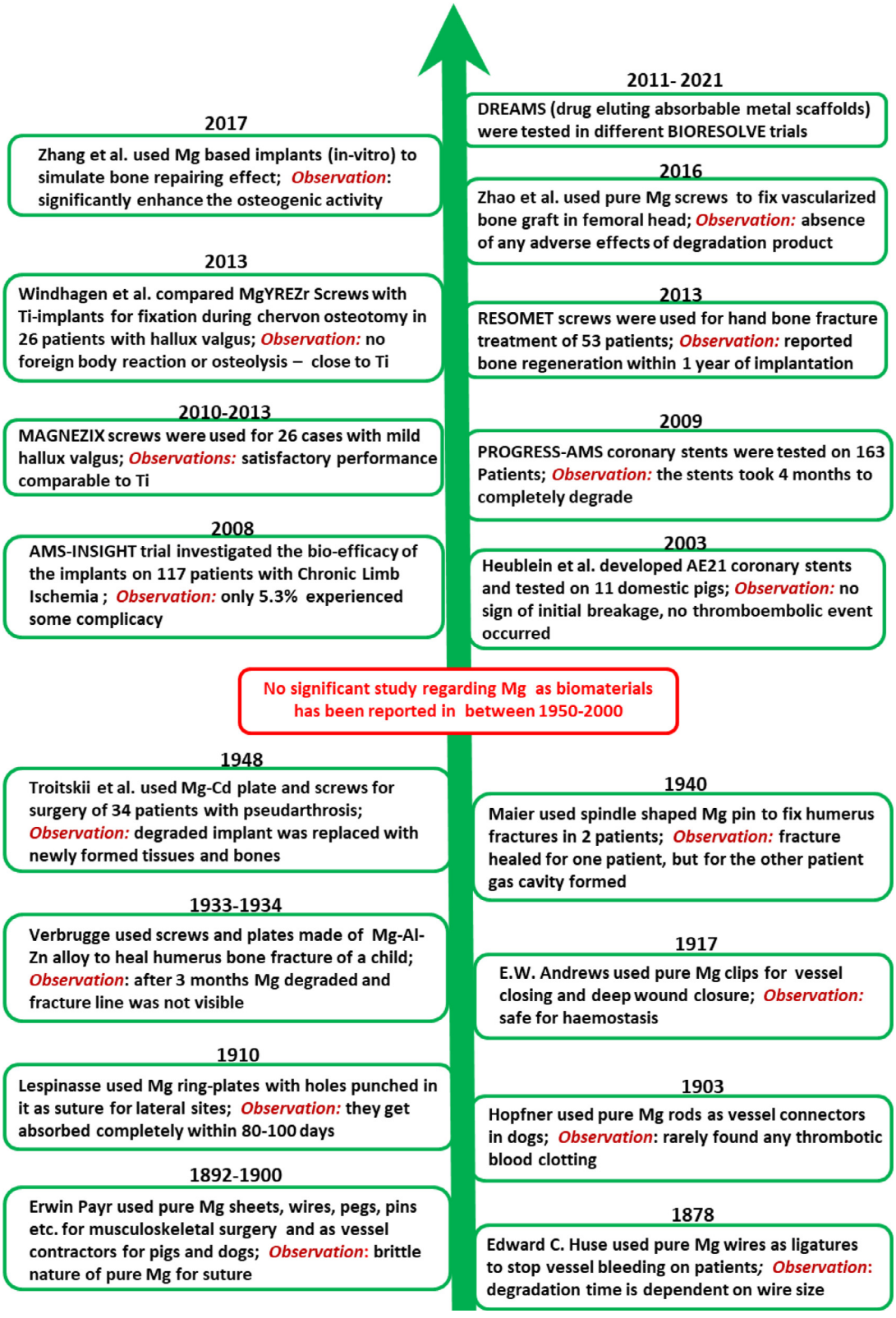

Fig. 7. Chronological evolution of Mg-based alloys as temporary fixture devices (adopted from references [109, 253, 304] and subsequently modified).

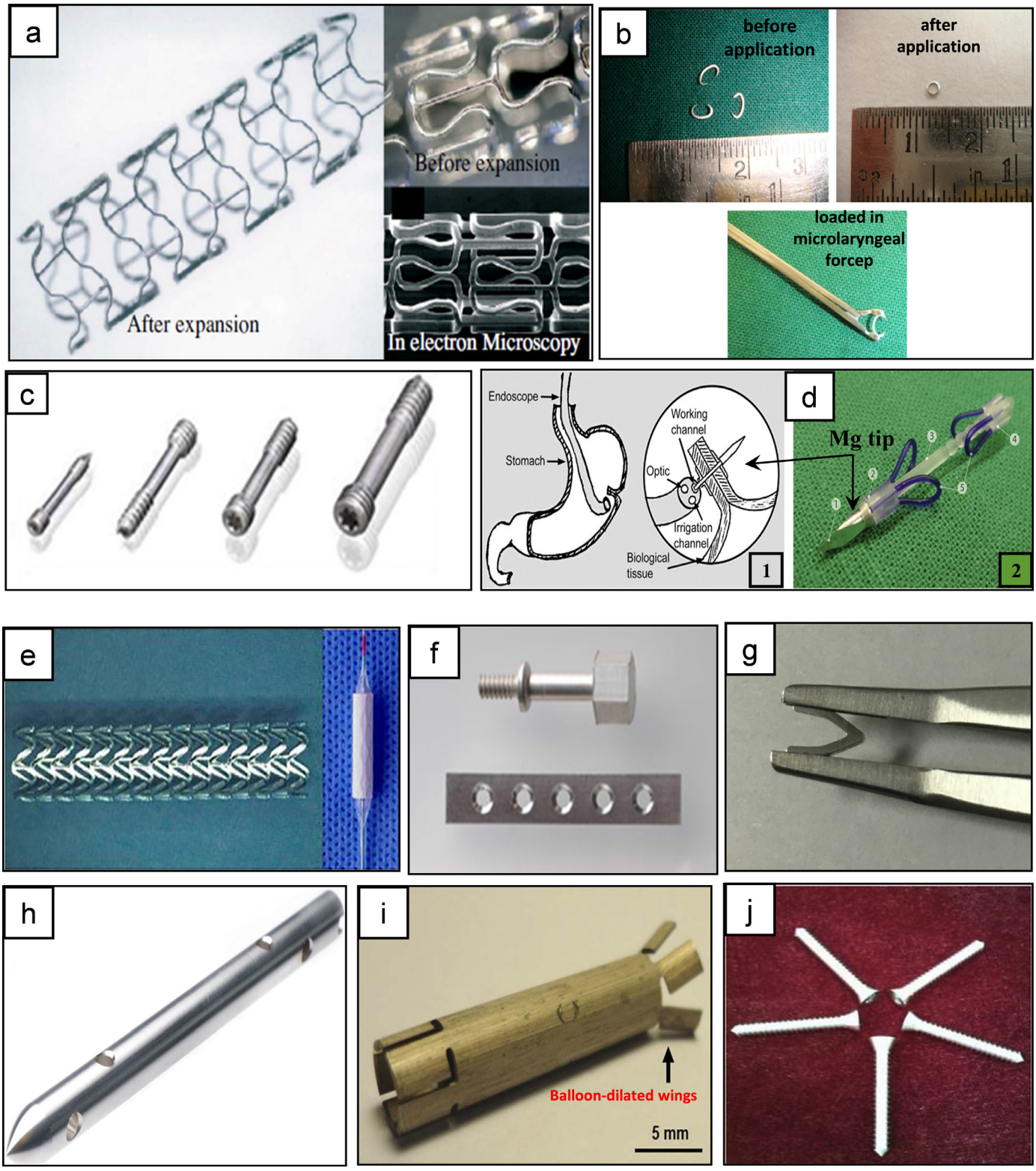

Fig. 8. Clinically trialled Mg-based temporary fixtures: (a) PROGRESS-AMS cardiovascular stents (BIOTRONIK, Germany) [321], (b) Mg-based microclips for surgical use [314], (c) MAGNEZIX® screws [306], (d) temporary device for wound closure application [320]: 1) schematic of joining tissues with the help of rivet, 2) model of a wound closing rivet with biodegradable Mg-tip (WZ21); Mg-based fixtures at developmental stage: (e) Mg-based stent for neurological application [316], (f) Mg-0.8 wt% Ca screw, ZEK-100 Plate [310], (g) biodegradable clip made of Mg-0.2 at% Zn-0.1 at% Ca [313], (h) bioabsorbable intramedullary nails of LAE442 alloy (length = 130 mm, shaft diameter = 9 mm) [312], (i) nasal stent made of Mg-2wt% Nd alloy and coated with MgF_2 (the arrow denoting the balloon-dilated wings) [318], (j) pure Mg screws (99% purity) for bone flap fixation (shaft diameter = 4.0 m, length = 40 mm) [323].

Fig. 9. Radiographs comparing the conventional stainless-steel screws and Mg-based RESOMET® screws for fixation of radius fracture. The Mg screw gets dissolved progressively within 12 months with appreciable bone regeneration and fracture healing [324].

istration (KFDA) granted approval of the screws for clinical applications [109,324]. Better biocompatibility and osseointegration property of this particular alloy system has inspired many researchers to formulate different variants of Mg-Zn-Ca alloy system in order to further improve the alloy properties.

6. Prime challenge in implementing biodegradable Mg-based alloys as temporary implants in extensive clinical practice

In spite of the remarkable advancement in the development of Mg-based alloys, the extensive clinical applications and commercialization of most of the Mg-based implants are still limited due to their uncontrollable degradation rate. The rapid degradation rate affects the mechanical integrity of the implants adversely and subsequently results in untimely failure of the implant. Several theories have been established by researchers to explain the mechanism of degradation for Mg-based alloys in different environments.

Mg is an active metal that degrades quickly in an aqueous environment forming magnesium hydroxide ($Mg(OH)_2$) layer and hydrogen gas bubbles. The representative reactions to describe the basic degradation phenomenon of Mg-based alloys in the physiological environment are given below [263,325–327],

$$Mg \rightarrow Mg^{2+} + 2e^- \quad (1)$$

$$2H_2O + 2e^- \rightarrow 2OH^- + H_2 \uparrow \quad (2)$$

$$Mg^{2+} + 2OH^- = Mg(OH)_2 \downarrow \quad (3)$$

$$Mg + 2H_2O \rightarrow Mg(OH)_2 + H_2 \uparrow \quad \text{(Overall reaction)} \quad (4)$$

After the formation of this partially protective hydroxide layer, it helps to protect the implant from further degradation. However, the degradation behaviour of Mg-implants is entirely different in the physiological environment due to the presence of several corrosive anions, especially chloride ions [328,329]. The protective hydroxide layer is unstable in the presence of chloride ions of concentration higher than 30 mM and gets converted to highly soluble magnesium chloride ($MgCl_2$), as shown below [263,325,327].

$$Mg(OH)_2 + Cl^- \rightarrow MgCl_2 + 2OH^- \quad (5)$$

The body fluid contains around 150 mM of chloride ions [330], which is much higher than the threshold limit and consequently results in rapid corrosion of implants. Some researchers have reported that the degradation process of Mg-based alloys in $NaCl/Na_2SO_4$ solutions takes place by formation of a combined MgO and $Mg(OH)_2$ films over the specimen surface [325,327,329,331]. The outer layer, composed of porous and partially protective $Mg(OH)_2$ layer (thickness 20–30 μm), allows easy penetration of aggressive anions present in the solution. The inner-protective film of MgO (thickness 1–10 nm) exist in equilibrium with $Mg(OH)_2$ as follows [325,326,329],

$$Mg(OH)_2 \leftrightarrow MgO + H_2O \quad (6)$$

The corrosion resistance of the alloy is dependant on the compactness and uniformity of the film formed over the specimen. A uniform film can significantly reduce the chances of localised attacks. Due to the presence of inherent defects in the surface film of the implanted material, the dissolution of the film can take place inhomogeneously in presence of body fluid and increases the tendency of undesirable localized corrosion [325,326]. Moreover, the presence of second phases, precipitates, impurities, and foreign elements on the implant surface profoundly influence the tendency of localized corrosion, mostly galvanic corrosion [332–335]. The different types of corrosion generally observed in case of Mg implants in body environment are schematically illustrated in **Fig. 10(a)** [336].

The local pH in the vicinity of the specimen surface has an important role over the continuous precipitation and dissolution of $Mg(OH)_2$ (brucite) film [337]. At the initial stage of immersion, the $Mg(OH)_2$ layer forms all over the specimen uniformly as governed by Eq. (3). The presence of higher number of OH^- ions (local pH $\sim$ 13) generated through Eq. (2) at the initial stage results in precipitation of this $Mg(OH)_2$ layer readily over the entire surface. In literatures, this stage has been associated with higher nucleation and slower growth rates of the brucite crystals, ensuring the formation of a compact and uniform $Mg(OH)_2$ film composed of similar sized brucite crystals [263,337]. Such film is reported to be able to restrict further diffusion of Mg^{2+} ions outward, thus limits the film growth. At this stage, the film is known as a passive film. This stage is illustrated in **Fig. 10(b-i)** [337]. The drop in local pH accompanied by decrease in OH^- ions post initial stage dissolves the brucite film partially due to higher solubility of the film at this pH range (pH $\sim$ 9–10). The crystals of $Mg(OH)_2$ dissolves at high energy regions, while the crystals at comparatively lower energy regions of the surface grow, creating an inhomogeneous film of $Mg(OH)_2$. Local thinning of $Mg(OH)_2$ creates local anode thus increasing the generation of Mg^{2+} ions, which again facilitates rapid nucleation of brucites in presence of OH^- ions. Whereas, at the adjacent cathodes, the local pH increases keeping the film intact (as illustrated in **Fig. 10(b-ii)**) [337]. Thus the precipitation-dissolution process of film continues over the specimen surface [325,337]. This precipitation-dissolution mechanism of film formation during degradation of Mg-based alloys has been reported by many researchers. Maltesa *et al.* [337] have recently investigated the kinetics of the corrosion product film formation in relation to change in local pH using in-situ Raman spectroscopy technique.

A significant part of the Mg^{2+} ions generated by the corrosion process (Eq. (1)) is stored in surrounding bone tissues, while some interact with different physiological reactions to maintain necessary activities within the body. The excess amount of these ions can be absorbed by macrophages and excreted through urine [338]. It can be observed that along with magnesium ions, hydrogen gas is also released by the reactions. Moreover, Mg-based alloys are reported to exhibit an anomalous behaviour, which significantly increases the hydrogen evolution rate during corrosion of these alloys. When a potential above the corrosion potential of the material is applied to the system, the volume of hydrogen evolution also increases along with an increase in the anodic reaction rate. This phenomenon is termed as negative difference effect (NDE) [325,329,339–342]. It has been shown schematically in **Fig. 10(c)** [342]. There are many hypotheses provided by the researchers to explain it, albeit this behaviour is not yet properly understood. An excessive amount of hydrogen gas generation may result in hydrogen embrittlement and thus leading to an uncertain failure of the implant. Moreover, it has been reported by Song *et al.* [343] that the tolerance limit of hydrogen is lesser than 0.01 mol/cm^2 per day and generation of hydrogen gas beyond the acceptable limit might form small hydrogen gas pockets surrounding the implants and in some worst cases can even lead to blood clotting and eventual death of the patient. Li *et al.* [344] have reported about an excessive evolution rate of H_2 gas at the initial stage of implantation. If the volume of generated hydrogen gas exceeds the saturation level of the body fluid, it leads to accumulation of gaseous hydrogen within the surrounding tissues and consequently forms gas pockets or gas cavities that adversely affects the formation of new bone due to localised gas pressure. The volume of hydrogen evolved (with respect to immersion time in SBF and Hank's solution) for some important binary alloy systems in as-cast and as-rolled conditions are graphically shown in **Fig. 11(a-d)** [300]. It depicts that for all the as-rolled material (**Fig. 11(c) & (d)**), the volume of evolved hydrogen is comparatively lesser compared to their as-cast counterpart (**Fig. 11(a) & (b)**). This has been attributed to the improved microstructural features obtained through the thermomechanical processing treatment. Moreover, the volume of evolved hydrogen also varies with the type of electrolytic solution

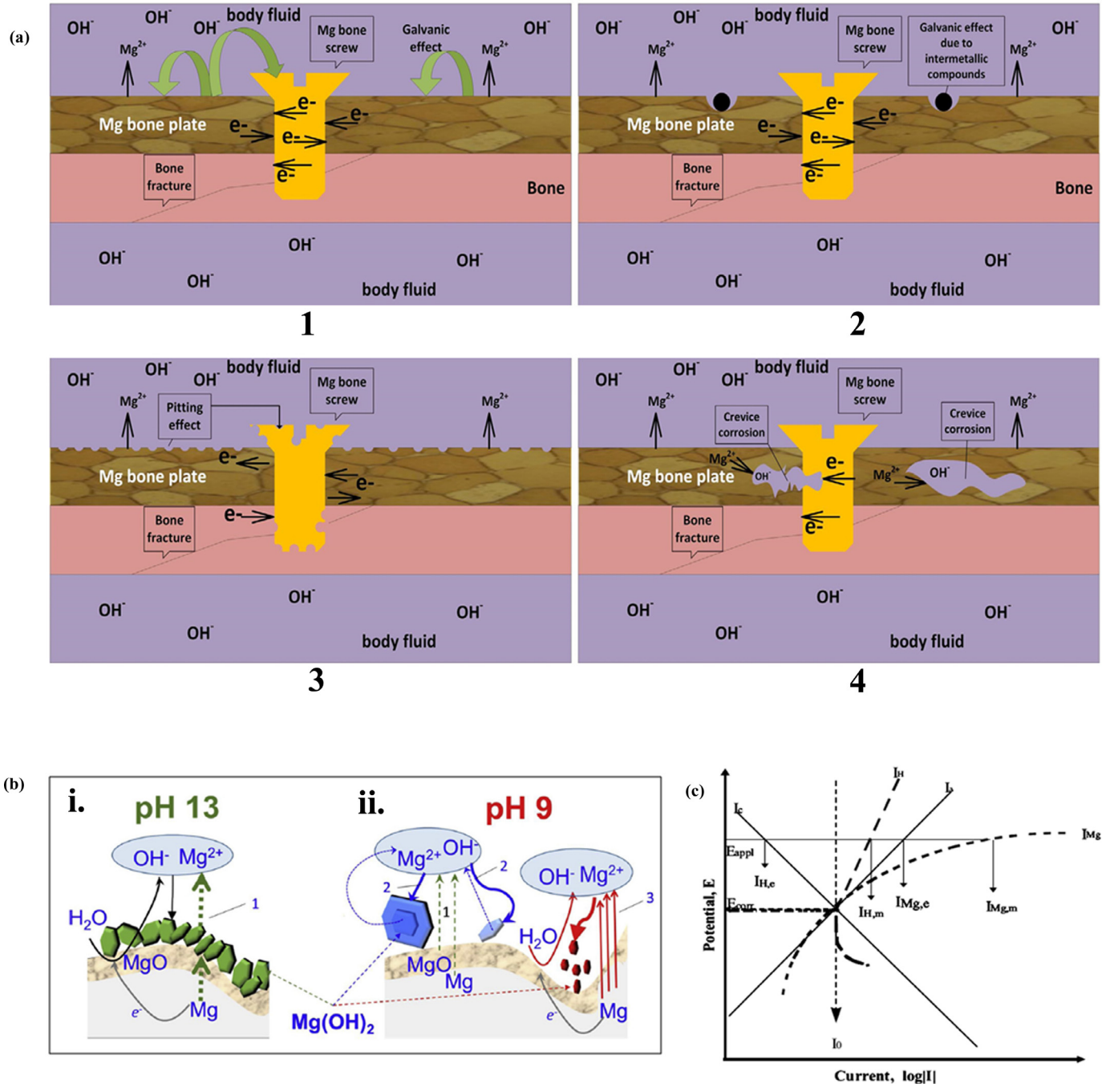

Fig. 10. (a) Schematic illustration of major types of corrosion processes observed for Mg implants under body fluid environment: 1. galvanic effect on implant, 2. galvanic corrosion due to intermetallic compounds, 3. pitting corrosion, and 4. crevice corrosion [336]; (b) The arrows shown in both (i) & (ii) signify different steps and the numbers associated with them denote the sequence of that step in the whole process. i. precipitation of $Mg(OH)_2$ layer by nucleation of brucite ($Mg(OH)_2$) crystals at around pH 13: 1) diffusion of Mg ions through the $Mg(OH)_2$ layer, ii. partial dissolution and reprecipitation of the film: 2) partial dissolution of $Mg(OH)_2$ film at high energy surface areas and growth of remaining brucite crystals at low energy surfaces when the pH is around 9, 3) rapid nucleation at local anodes where $Mg(OH)_2$ film thinning has happened [337]; (c) non-differential effect (NDE) observed in Mg-based alloys [342].

being used for immersion based on the concentration of aggressive anions present in it, as observed from Fig. 11.

Thus, the rapid degradation process in Mg-based alloys results in a significant loss in the load-bearing capability of the implants way earlier than intended. It is worth to mention here that the clinical translation of Mg-based temporary implants is still restricted due to its uncontrollable degradation rate in body environment. The bone remodelling process in human (refer Fig. 12 [32]) takes a minimum of 24–32 weeks and the temporary implant material should be designed in a way to survive that duration [120,123,345]. Unfortunately, most of the Mg based implants degrade completely within 6–12 weeks and consequently lose required mechanical integrity at a much early stage [123,346]. The schematic representation in Fig. 13

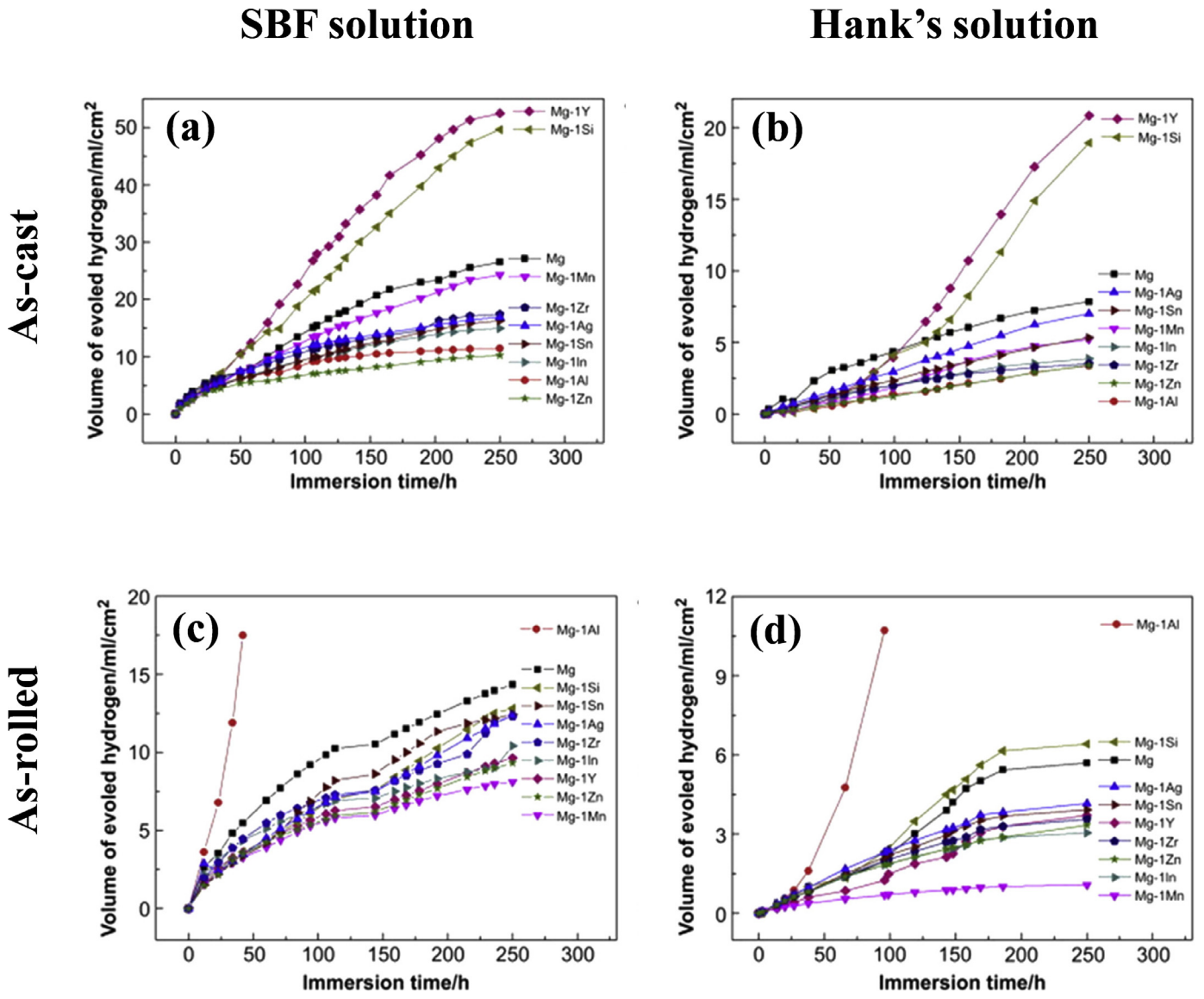

Fig. 11. Volume of hydrogen gas evolved for (a-b) as-cast, and (c-d) as-rolled binary alloys of Mg in (a, c) SBF solution and (b, d) Hank's solution [300].

gives a rough idea about the approximate difference between the desired and the actual degradation rate for most of the Mg based alloys [109]. Therefore, most of the research works are now orientated towards improving the *in-vivo* corrosion properties of the implants. Surface modification by incorporating appropriate surface coatings is explored as an efficient way to control the degradation rate of Mg-implants.

7. Surface modification: a strategy to improve degradation resistance of Mg-based alloys

It is apparent from the discussions in above sections that alloying has been considered as one of the efficient ways to improve the degradation behaviour of Mg-based alloys. Associated processing techniques, subsequent heat treatment and deformation procedures are accounted as the main key factors that can improve degradation property of the alloys to some extent. However, alloying alone is not sufficient to achieve a controlled degradation rate, especially when alloying of essential nutritional elements like Zn, Ca, Mn, Sr, Ti are considered. Moreover, it is indeed very difficult to predict the degradation behaviour of a multi-elemental alloy system due to formation of several new phases, intermetallic compounds or precipitates. Formation of numerous microgalvanic cells due to existing potential difference between second phase and matrix is a common problem anticipated in most of the newly formed alloys [120,291,347].

Recently, surface modification has emerged as the most promising means for elevating the performance characteristics of Mg based implants by considerable reduction in corrosion [348–351]. Suitable surface coatings act as a barrier between the metallic implant and the harsh body environment, thus protecting the implants from degradation. Surface of the biomaterial clearly acts as the most influencing factor

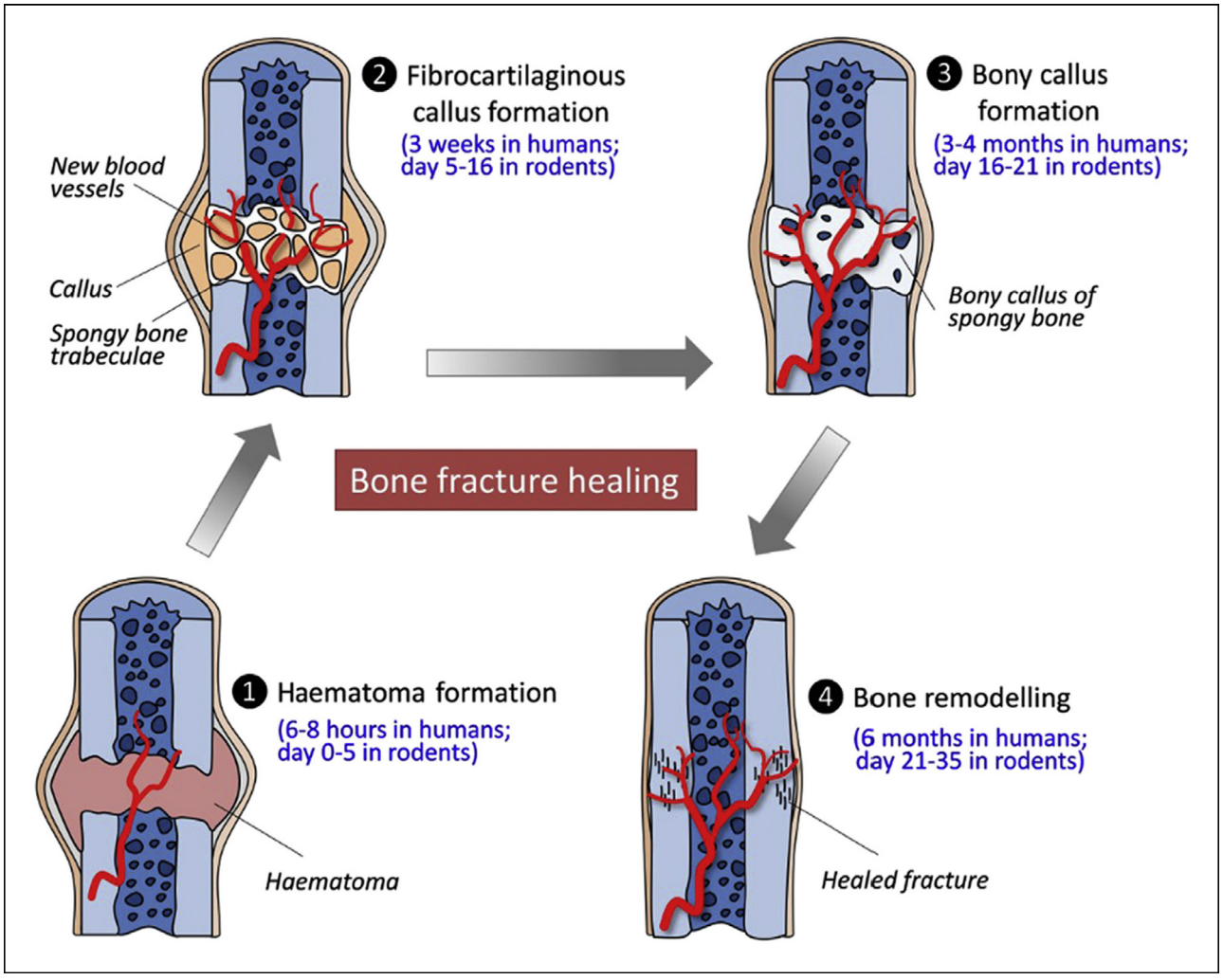

Fig. 12. Schematic representation of bone healing stages in human and rodents [32].

that regulates the type of interaction taking place between the foreign implant and bodily atmosphere since it is the implant surface that gets in contact with surrounding body tissues first [129,352]. The chemical composition of the implant surface as well as the surface topography are considered to be important factors in determining the specific interactions at interface including absorption of ions, minerals, proteins, body cells etc. [121,352–354]. In order to provide adequate corrosion protection to the substrate material, the coating should ideally be well adherent [355–359] and uniformly spread over the substrate surface without generation of pores and inhomogeneities [357-359]. However, when biodegradable implants are under consideration, the coatings must be designed to form a temporary surface over the implant which must possess some additional qualities like adequate biocompatibility and osseointegration. Adequate osseointegration demands suitable surface topography in terms of surface roughness and surface energy [360,361]. However, the highly chemically reactive nature of Mg makes it difficult to form a defect-free coating over the surface as pores and cracks form inevitably in the coatings during coating preparation. Mg is prone to form an oxide or hydroxide layer instantly in presence of air or water and this layer imposes detrimental effect on adhesion and uniformity of the coatings. Thus, pre-cleaning of the surface and appropriate surface engineering plays a vital role in cell adhesion and regeneration, impacting the overall quality of coating.

7.1. Bio-inert coatings

Numerous surface modification techniques for Mg-based biomaterials have come up over the years of extensive research, each having their own set of advantages and disadvantages. A review published by Devgan *et al.* [362] discusses the evolution trend of various surface modification techniques for Mg-based implants. Electrochemical deposition [363,364], plasma spray [365], micro-arc oxidation [366–370], physical vapour deposition [371,372], chemical vapour deposition [373], ion implantation [374,375], conversion coatings [376,377], laser treatments [378–381] are some of the extensively explored techniques in this regard. Bio-inert coatings like TiO_2, TiN, SS-based, Cr-based, ZrN, and DLC (diamond-like carbon) coatings were in research in the early phase due

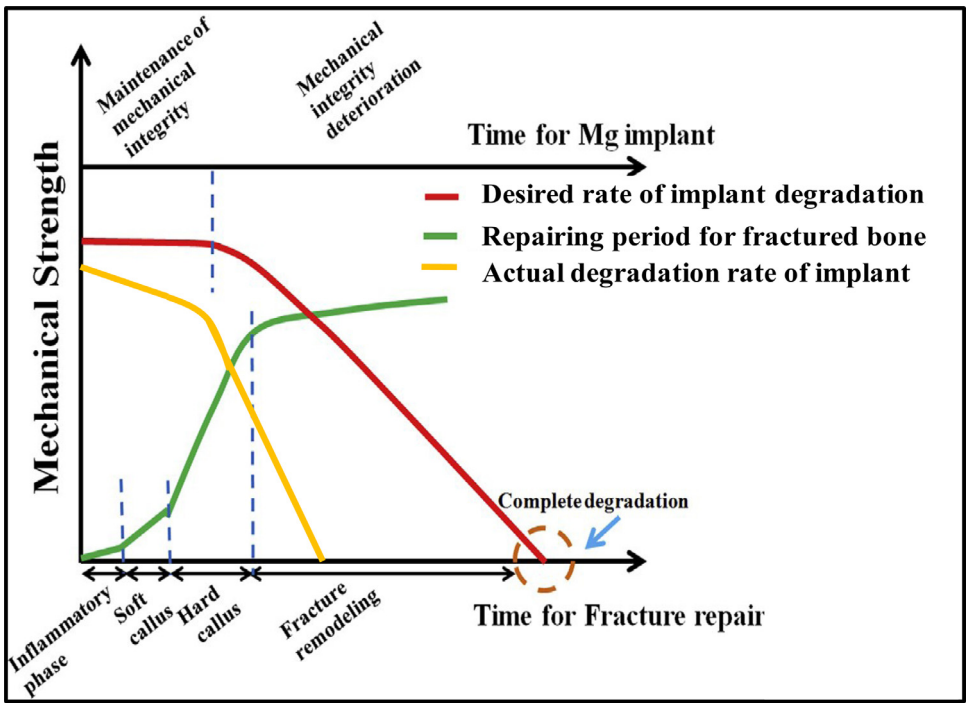

Fig. 13. The schematic showing the approximate difference existing between the desired rate and the actual rate of degradation of Mg-based implants in presence of body fluid (taken from [109] and subsequently modified).

to their superior corrosion properties [376]. However, these coatings are non-biodegradable in nature and they are prone to cause inflammation in human body during their stay in bodily environment over a prolonged period. The principles behind designing suitable surface coatings for biodegradable Mg-based implants have been thoroughly discussed by Wu *et al.* [382]. According to them, the coating should form a temporary barrier over the implant surface, possessing adequate mechanical properties, higher degradation resistance and good biocompatibility. Ideally, after completion of natural degradation, those temporary barriers must not produce any deleterious or toxic effect in human body. Thus, gradually the focus shifted towards investigating bio-active coatings due to their favourable bone regeneration and bone regrowth capability along with superior biocompatibility.

7.2. Bio-active coatings

Study by Furko *et al.* [383] describes thoroughly the preparation and characterization techniques for various bioactive coatings. Lin *et al.* [384] have thoroughly studied the degradation behaviour of forsterite containing micro-arc oxidation (MAO)-coated ZK60 alloy implants in physiological environment and commented on the influence of higher coating voltage in effectively reducing the corrosion rate. Witte *et al.* [80] have investigated the *in-vivo* corrosion behaviour of extruded LAE442 alloy coated with magnesium fluoride (MgF_2) to understand the behaviour of the coating. According to their observation, both the coated and uncoated Mg alloy underwent pitting corrosion. However, rate of corrosion is much lower in the coated sample (0.13 mm/y after 12 weeks) compared to the bare alloy sample (0.31 mm/y after 12 weeks). Li *et al.* [385] have reported that fluoridated hydroxyapatite (FHA) coated Mg-6wt% Zn alloy shows improved interfacial bioactivity of the implant providing enhanced cellular proliferation as well as cell differentiation under *in-vivo* condition. They concluded that FHA coatings are able to regulate the main osteogenic genes just within 21 days of culture and thus are favourable for more stable cell incubation. Wan *et al.* [353] have reported that electrodeposited coatings, bio-mimetic coatings, and chemical conversion coatings are capable to provide adequate anticorrosion properties, in addition to better biocompatibility. They have discussed on advantages of adding bioactive elements like Ca and P in the coating by micro-arc oxidation technique. The adhesion strength of these bioactive elements incorporated HAp coatings are reported to be sufficiently higher. Biomimetic coatings have gained attention over the years due to their ability to sense and response to internal and external stimuli of cell tissues like temperature, pH, and ionic concentration in body fluid etc. However, it is highly challenging to design biomaterials that can readily acquire the structural complexity required to mimic the extracellular matrix (ECM) of the natural bone. Bone is a natural composite made up of organic collagen fibrils and inorganic hydroxyapatite crystals [129]. Thus hydroxyapatite ($Ca_{10}(PO_4)_6(OH)_2$) coatings [352,386,387] and various calcium phosphate (CAp) based coatings [377] on Mg implants make them highly adaptable under *in-vivo* condition. Therefore, these coatings are considered to be the most suitable ones to form biomimetic

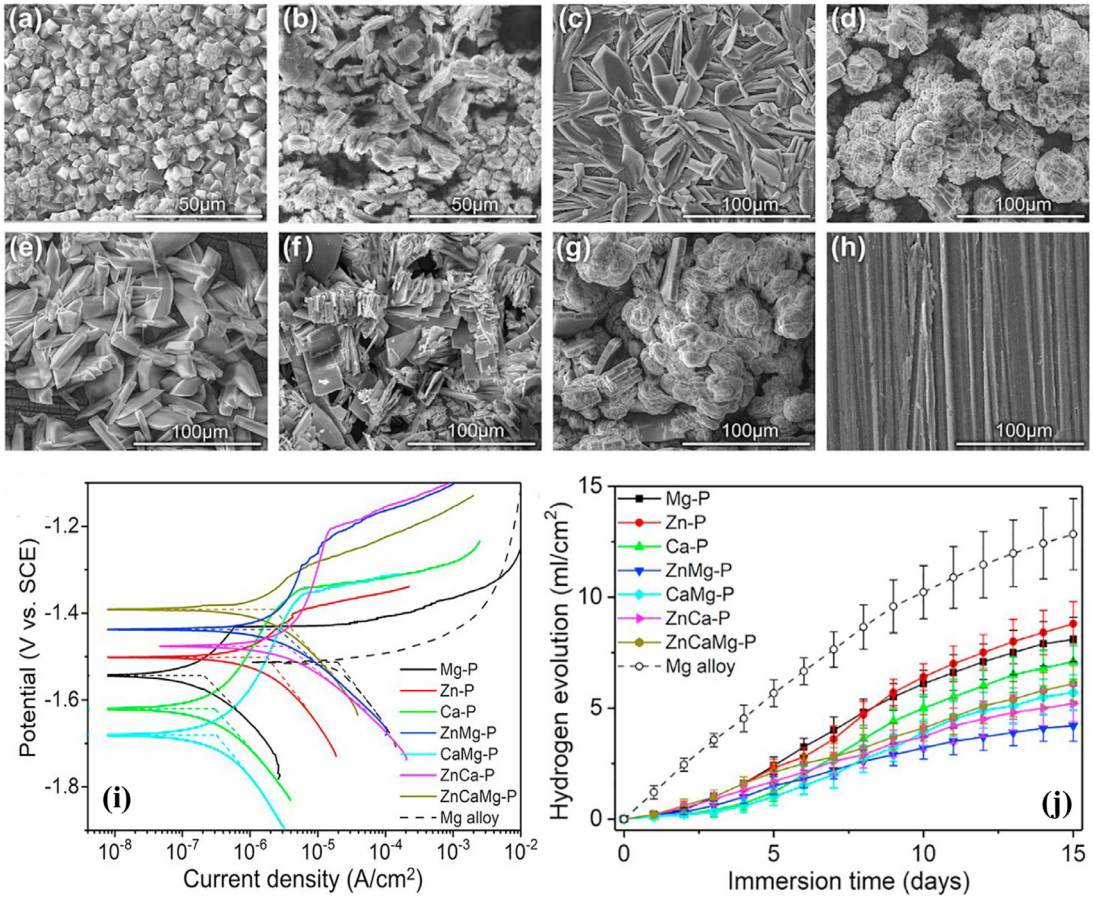

Fig. 14. Coating morphologies obtained through SEM for (a) Mg-P, (b) Zn-P, (c) Ca-P, (d) ZnMg-P, (e) CaMg-P, (f) ZnCa-P, (g) ZnCaMg-P, and (h) bare AZ31 alloy; (i) potentiodynamic polarization curves, and (j) volume of hydrogen evolved for different phosphate-based conversion coatings obtained in Hank's solution [377].

coatings. HAp and CAp based coatings are currently under thorough investigation to understand their suitability for *in-vivo* tissue engineering. The osteoconductive features of these ceramics come from close resemblance of their calcium to phosphate ratio with that of natural bone mineral phase [377]. Fig. 14(a)-(h) shows the morphology of some of the important phosphate-based conversion coatings [377]. The corrosion properties of these coatings are compared with the help of potentiodynamic polarization curves (Fig. 14(i)) and hydrogen evolution rates (Fig. 14(j)) in Hank's solution. It can be observed that the Ca-P coatings can provide a much-reduced corrosion rate along with lower hydrogen evolution rate. Shadanbaz and Dias [388] have reported in details about different types of calcium phosphate coatings explored by researchers. They discussed on diverse coating techniques and potential applications of calcium phosphate dihydrite (DCP), octacalcium phosphate (OCP), anhydrous calcium phosphate (ACP), tricalcium phosphate (TCP), and hydroxyapatite (HAp) on Mg-implants and concluded that electrophoretic and biomimetic coating techniques are two preferable routes in reducing degradation rate. Dorozhkin [389] has elaborately discussed on calcium orthophosphate coatings deposited on AZ91D alloy. His-publication lists down around 22 different deposition techniques along with mentioning the important pre and post-deposition treatments required for this bioactive coating. The coating crystallinity is highly influenced by post deposition annealing process which leads to formation of crystalline HAp or $Ca_2P_2O_7$ from amorphous calcium phosphate phase depending on the Ca to phosphate ratio present in the deposited coating. It has been reported that coating crystallinity improves corrosion resistance and reduces residual stress, thus enhancing overall coating characteristics [352]. Chemical treatments involving alkalis have also been reported to be an effective post-deposition treatment.

The surface roughness and number of porosities present on the coatings influence the surface topography as well as the surface energy and directly influence the osseogenesis or cell regeneration. Harun *et al.* [387] have recently written a comprehensive review from the perspective of adhesiveness of HAp based coatings formed using different deposition techniques. They have compared and listed the values of adhesion strength of HAp coated alloys based on deposition techniques and have concluded that introduction of an oxide inter-layer (with favourable topography in terms of surface energy, pore size and distribution, roughness etc.) between the substrate

and the final HAp coating significantly improves the adhesion strength of HAp layer. Ke *et al.* [390] have investigated the effect of strontium phosphate (SrP) as a biocompatible conversion coating on pure Mg implant under *in-vitro* condition. Their work also revealed that a complex bi-layer consisting of a magnesium oxide intermediate layer combined with an outer SrP layer improves the coating characteristics effectively in terms of electrochemical behaviour. Different laser-based surface modification techniques, especially pulsed laser deposition (PLD) and laser surface melting, are gaining significant attention now-a-days due to their ability to coat complex bio-implant structure in a partially or fully automated way along with providing desired surface composition [391–393]. Singh and Harimkar [394] have reviewed several laser surface modification techniques suitable for coating Mg-based bio-implants. Sankar *et al.* [395] have compared the characteristics of HAp layer over WE43 alloy coated using two different techniques namely electrophoretic coating technique and PLD. The electrochemical tests of the coated samples in Hank's Balanced Salt Solution (HBBS) at 37±2 °C temperature have revealed that PLD coated HAp layer provides much higher corrosion resistance (0.073 mm/y) compared to both electrophoretic deposition (EPD) coated sample (0.194 mm/y) and bare sample (0.97 mm/y). The significant improvement in adhesion strength as well as ability to form a protective layer with much lesser pores makes PLD as one of the potential techniques for coating Mg-implants. Santhanakrishnan *et al.* [391] have reported a significant improvement in corrosion behaviour of HAp coated AZ31B alloy (48% lesser corrosion rate compared to bare sample) in SBF solution. Selection of suitable laser processing parameters like energy density of laser beam, beam scanning speed, diameter of laser beam, laser power, and working distance are of utmost importance to obtain a desirable HAp coating using lasers [391,392]. Rau *et al.* [392] have recently reported a substantial improvement in corrosion behaviour of HAp coated Mg-Ca alloy deposited using PLD. Their work revealed that during laser coating the substrate temperature plays an important role in deciding the coating crystallinity and an optimum substrate temperature of 473–573 K has been suggested to obtain highest crystallinity of HAp coating. Fig. 15 provides a cumulative dataset showing the improved corrosion resistance of different Mg-based alloys obtained through incorporating bio-active surface coatings in recent times. It can be observed from the graph that the incorporation of coatings over the alloys have reduced the corrosion rate in each case. However, the extent of improvement in corrosion property varies with the type of coatings applied and also the process of incorporating those coatings over the material, as emphasized in Fig. 15. Moreover, it can be observed that the phosphate based biocompatible coatings are very effective in reducing the degradation rate significantly.

The above discussion provides a brief overview about the remarkable progress that has been made over the years of research involving suitable coating materials as well as coating technologies for Mg-based biodegradable implants. Many of the potential coating techniques are under investigation that can make biodegradable Mg-based implants useful in commercial clinical application.

8. Future prospects of Mg-based alloys

As evident from the above discussion, a large number of studies carried out on Mg-based bio-implants have already shown encouraging outcomes in terms of their applicability as temporary fixation devices. These studies have shown huge potential to utilize Mg-based implants in clinical practice. Despite all that, the widespread applications of Mg implants are still at halt due to high degradation rate of these implants, as pointed out in Section 6. Therefore, extensive research is still required in near future to overcome this hurdle. Alongside, diverse research directions can also be explored in future which can enhance the overall applicability of these implants and simultaneously impart a control over the degradation rate. Some of the future research prospects of Mg-based implants are discussed in this section.

8.1. Nanophased Mg-based alloys

Over the last few years, the use of nanotechnology in the field of medicine has begun to rise significantly. The idea of developing nanophased materials as bio-implants has been driven by the fact that the structure of natural bone is made up of organic collagen fibrils embedded with inorganic hydroxyapatite nano-crystals with length varying between 20 and 80 nm and diameter of 2–3 nm [129]. Therefore, nanomaterials are considered as highly promising candidates for future generation implant materials due to their ability to mimic or replicate the structure of natural bone effectively, thus serving as a smart material [336,396]. The key challenge is designing a smart implant lies in attaining the high degree of complexity that is required to replicate the cellular tissues. Nanophased materials with higher surface energy and desirable topography is capable of achieving similar level of surface roughness to that of natural bones, leading to improved bio-chemical interaction between the foreign implant and the host tissue (Fig. 16) [396]. Moreover, designing nanostructured materials and formation of functionalised nanocoatings over Mg-based implants will lead to desirable cellular response, stimuli responsive behaviour, better cell adhesion and higher osteointegration rate. Mg-based temporary implants are expected to serve as a fixture to join fractured bones and are expected to degrade after sufficient bone healing. Thus, improved cell adhesion and osteointegration are two most important factors to increase the effectiveness of temporary implants.

Nano-grained alloys made up of Ti-6Al-4 V, cobalt-chromium alloys, stainless steels etc. and some nanoceramic coatings of alumina, nano-hydroxyapatite etc. have exhibited increased cell adhesion and cell proliferation compared to conventional implant materials [2,396]. Moreover, a decrease in grain size from 167 nm to 24 nm has indicated 51% increase in osteoblast adhesion, resulting in faster rate of bone remodelling for the nano-grained Ti-alloys [2]. Apart from high degree of compatibility with natural tissue, nanophased

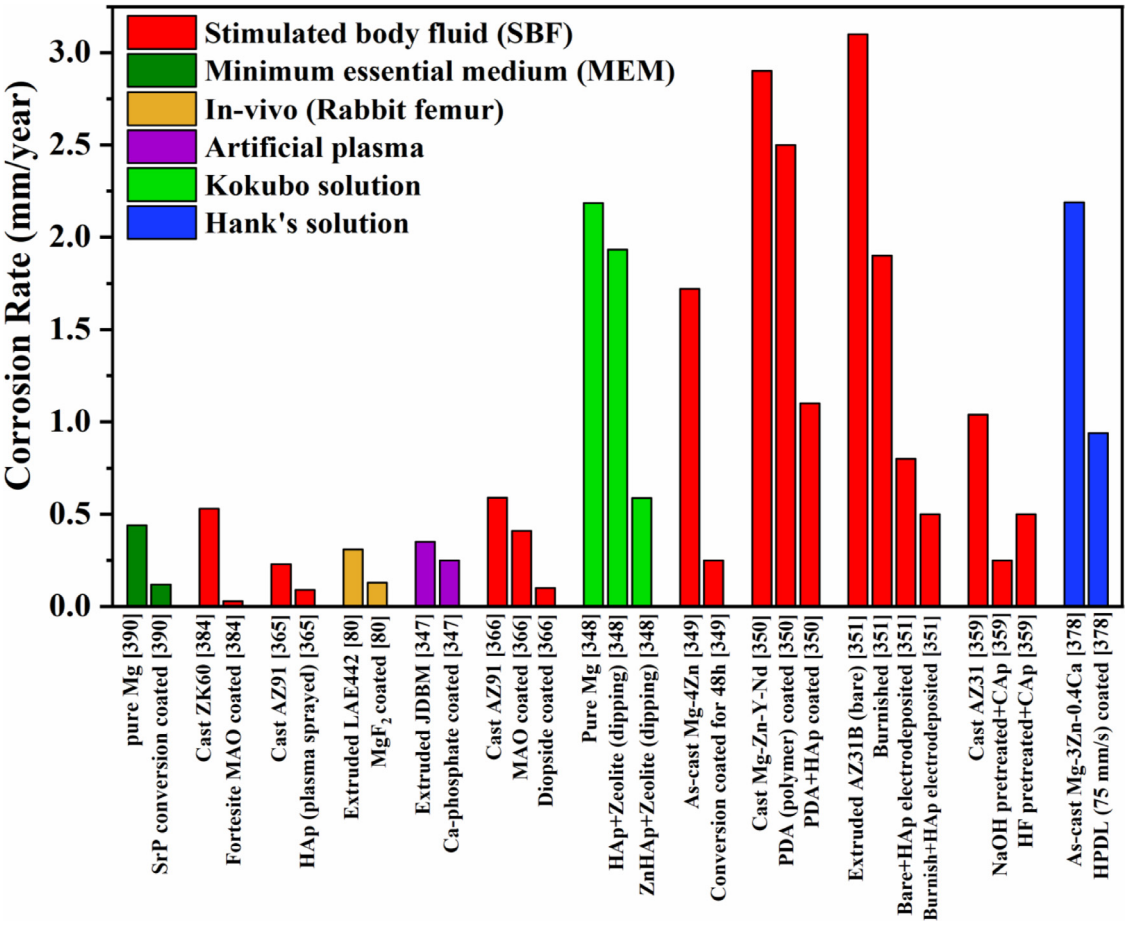

Fig. 15. Reduction in degradation rate of different Mg-based alloys by incorporation of bio-active surface coatings (see above mentioned references for further information).

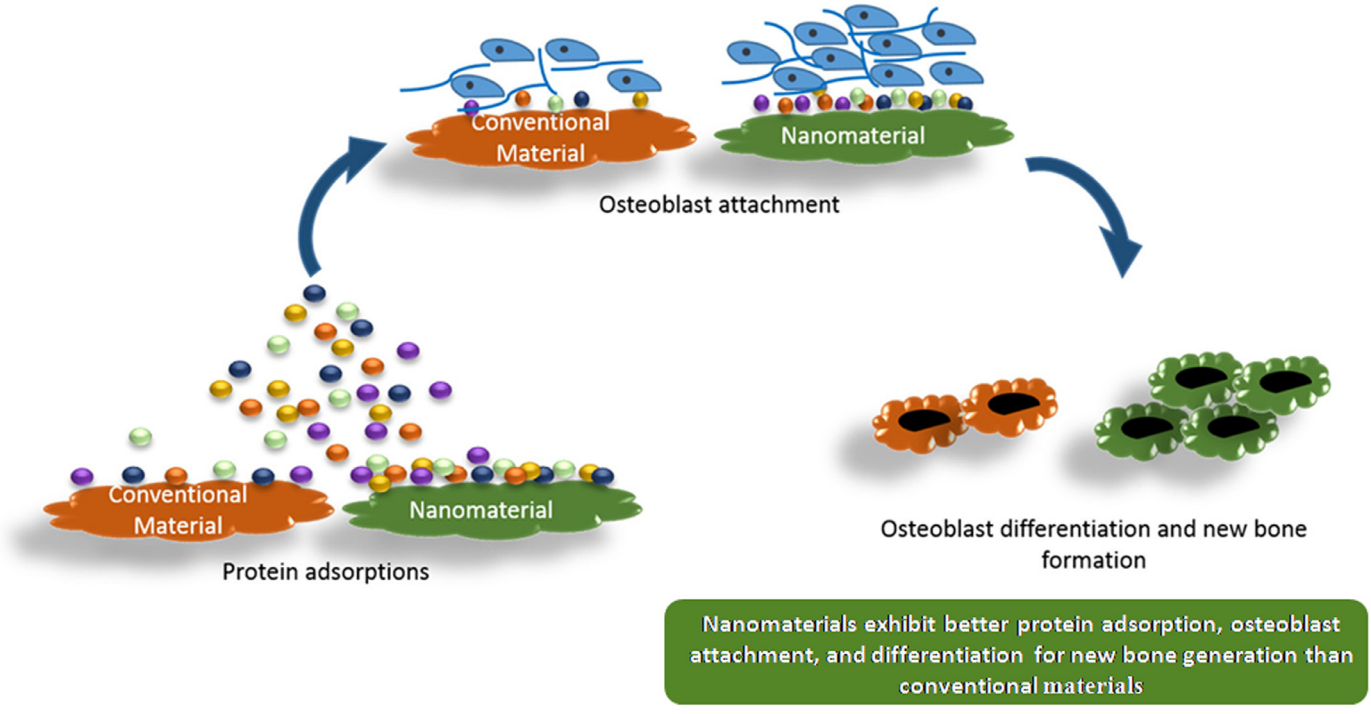

Fig. 16. Schematic representation showing the advantages of nano-phased biomaterials over conventional biomaterials in bone regeneration process [396].

implants are expected to possess improved mechanical properties due to presence of nano-sized grains. Nano-structured coatings formed on the surface of the implants are also expected to resolve the issue related to uncontrolled rate of corrosion of Mg implants. Kumar *et al.* [396] have recently published an article that comprehensively discusses recent advances on nanotechnology driven next generation bio-implants and their future prospects. Recently Mg-based nano-composites are gaining attention in the field of temporary implants. However, no research work has yet been reported regarding development of Mg-based nanophased alloys. The major challenge in formation of nanophased Mg alloys lies in designing advanced fabrication techniques. Moreover, extensive study is still needed to examine the cell-implant interaction to identify the health risks associated with it before coming up with new generation nano-phased Mg alloys.

8.2. Development of functionalized Mg-bone implants

The concept of designing functionalized Mg-based bone implants can be realized through incorporation of some specific alloying elements which bear certain bio-functionalities. For example, the elements like Cu and Ag are known to induce antibacterial effects [397]. Since bacterial infection is one of the reasons which cause an early implant failure, the development of such Mg-implants with antimicrobial feature can be highly beneficial. It is to be noted that the addition of Cu to stainless steel is known to promote in-stent restenosis (ISR), inhibit inflammation, and even induce new bone formation [398]. However, the precipitates that form due to incorporation of Cu or Ag into Mg matrix has shown to accelerate the microgalvanic corrosion of the alloy and hence result in much faster degradation of the alloy [399]. Regulating the shape, size, and distribution of the precipitates through designing a suitable thermomechanical processing might be helpful in reducing the adverse corrosion effects of Cu or Ag alloying to Mg. Significant effort is still required to study these aspects in future.

Sunai *et al.* [400] have recently reported to develop an Mg-La based implant with antitumor functionality which can effectively eliminate tumour spreading bone cells. They have mentioned that incorporation of 1.0 wt% La to ZK60 (Mg-6Zn-0.5Zr) alloy has exhibited around 61.9% of tumour cell inhibition rate while increasing cell viability to 91.9% for normal cells. However, the mechanism behind such characteristics have not been investigated in details by the authors. Mg-bone implants with in-built antitumor functionality is an interesting topic and requires further investigation in future.

Targeted drug delivery through medical devices is now a trending topic since it can facilitate controlled release of drug at a specific site of an organ. However, designing an implant for targeted drug delivery is quite a difficult task and very little progress is made in this aspect till now. Some authors have reported to load anti-inflammatory drug (dexamethasone) within polymeric coatings of pure Mg to achieve controlled drug delivery [364]. The pore structure can control the ability of the implant to carry the drug and release it sustainably [364]. However, thorough investigation is still required for in-depth understanding of the topic and to realize its applicability in near future.

8.3. Fabrication of Mg-based implants with tunable interfaces

Although surface coatings are known to remarkably improve the degradation resistance of the implant, the permeation of body fluid through the implant surface can swell the coating and initiate degradation of the substrate. Moreover, the presence of a small defect in the coating can accelerate the localized pitting corrosion, leading to a much faster degradation rate of the alloy. Hence, in such situation, the surface wettability can be regarded as a crucial factor that decides the extent of water attachment and permeation to the implant interface [401,402]. Therefore, development of a hydrophobic surface can help delaying the degradation of the implant to a large extent. Several studies have been carried out by the researchers which investigate the methods to tune the surface wettability as per application requirement in diverse frontiers of science and technology. Adjusting the surface roughness through chemical etching, application of laser, surface lithography etc. can significantly affect the surface wettability [403,404]. Also, adsorption or desorption of low energy polymeric monomer heptadecafluoro-1-decanethiol (HDFT) is reported to transform the hydrophilic CuO surface to superhydrophobic state [405]. Shin *et al.* [406] have discussed about the development of surfaces with extreme wettability (superhydrophobic or superhydrophilic) for biomedical applications. However, the development of such tunable surfaces for implants is still at its infancy. Therefore, the applicability of this aspect with regard to Mg-based implants can be explored in future since it can provide a new direction towards forming smart bio-implants with improved degradation resistance.

8.4. Mapping progressive degradation behaviour of implants

A large fraction of research works related to Mg-based implants has primarily focused on the effect of alloy designing strategy and associated fabrication techniques on the mechanical and corrosion properties of the alloy. Undoubtedly, these aspects are important for initial selection of a suitable alloy system and fabrication technique for the implant. However, in practice, the ultimate success of the implant highly depends on the progressive degradation behaviour of the implant under *in-vivo* condition and its impact on mechanical integrity. The morphological and structural integrity of the alloy is affected by progressive degradation of the implant, which in turn, will impact several other aspects like the adhesion of the implant to bone, its osteogenic properties, load bearing capability etc. Therefore, the correlation between the dynamic implant degradation and the above factors must be mapped throughout the whole degradation process for in-depth understanding of the degradation phenomenon [407]. Different in-situ characterization techniques might be helpful in understanding the localized changes that take place during progress in degradation

of the implant under *in-vivo* condition. However, these in-situ techniques are quite difficult to perform and a very limited number of works have been done till now on this aspect.

Sanz-Herrera *et al.* [408] have tried to simulate the Mg implant degradation with the help of a model that considers the important physio-chemical reactions during degradation process. Saad *et al.* [284] have adopted a computational approach to understand the impact of morphological changes on the structural properties of a porous implant made of pure Mg (purity 99.9%) through a dynamic immersion test. The specimens were initially subjected to dynamic immersion and then examined using micro-CT, followed by reconstruction of the degraded samples into a 3D model using finite element analysis. They have concluded that the dynamic degradation can significantly affect the morphological aspects of the porous implant and the mass loss data obtained through simulations is in agreement with the experimental results. However, the relevant research works in the field of Mg-based implants are still limited and demands more efforts in future to develop suitable computational models to understand the dynamic degradation behaviour of the implants and to validate them experimentally.

Also, designing the implant geometry is an important aspect since stress concentration at a particular point on the implant can locally induce accelerated stress corrosion cracking, which lead to an early implant failure [409]. A few literatures are available which tried to focus on modelling the implant geometry and mapping the distribution of stress throughout the structure [410,411]. This important aspect needs to be further explored for Mg-based implants.

8.5. Exploring potential hybrid coatings

The term 'hybrid coating' comes from the fact that the coatings are developed by combining both organic and inorganic components. Therefore, the advantages of both the type of components can be availed in a hybrid coating. Several research works have already been carried out to understand the efficiency of such hybrid coatings formed on Mg-based implants. Rahman *et al.* [412], in a review article, have elaborately discussed about several important studies carried out on different bioactive hybrid coating systems recently. Singh *et al.* [413] have recently reported about development of a TiO_2–HAp-PCL (polycaprolactone) based hybrid coating. Here TiO_2–HAp is the inorganic part while PCL is the organic part of the hybrid coating. PCL is known to show poor adhesion and cell proliferation characteristics, although it is reported to decrease the degradation rate of the Mg-alloy. On the other hand, HAp is known to improve osteointegration. Therefore, both the components can complement each other. The hybrid coating is reported to exhibit high adhesion strength as well as improved osteogenesis. It also showed significant improvement in corrosion resistance due to formation of a thick apatite layer over the substrate. Several other works on hybrid coatings have recently been published which have shown huge potential of such coatings in delaying the degradation of Mg alloys [413-415]. Further exploration in this field might be helpful in selecting suitable components for developing a hybrid coating which can deliver exceptional properties in terms of both degradation resistance and osteogenesis.

8.6. Advancement of additive manufacturing technology for Mg-based implant production

Laser based additive manufacturing has been identified as a highly promising technique since it can produce customized implants with excellent efficiency based on specific needs and provide extensive process flexibility. It can also precisely produce the intricate details associated with an implant design and form complex porous-interconnected scaffolds easily which is not possible by using traditional techniques [180]. Besides, additive manufacturing is the most appropriate technique to design innovative 'functionally graded structure' [416,417] which can ensure good corrosion resistance along with enhanced osteogenesis. Numerous other advantages are also associated with this technique as pointed out in Section 3.4. However, there are several constraints associated with this method in relation to fabrication of Mg-based implants, such as burn out and oxidation. Moreover, the formability of the Mg parts produced through this process is much poorer. Surface balling and presence of internal pores are some typical defects associated with the Mg-based products developed through additive manufacturing which deteriorate the properties of the alloy. To eliminate these constraints, one crucial step is to acquire an in-depth understanding about the correlation between different laser processing parameters and the alloy properties. The power density, interaction time of laser with substrate, size of laser beam, type of laser etc. can be suitably regulated to thoroughly investigate their effects on alloy characteristics. Moreover, the generation of residual stress associated with this process is an issue which needs to be minimized by exploring different post-processing heat treatments [184]. Suitably addressing these challenges can definitely make laser based additive manufacturing a major fabrication route for producing such implants in near future.

9. Conclusions

The capability of Mg-based alloys to degrade naturally in the physiological environment advocates their use as a suitable temporary implant material. Since the last two decades, the Mg-based alloys have been subjected to continuous and progressive modifications in terms of alloy composition and surface coatings to meet the target degradation rate in order to eliminate the existing mismatch between bone-healing and alloy degradation period. Development of the desired microstructure by tailoring the alloy design and processing metallurgy has been the key to achieve favourable bulk metallic properties whereas suitable surface coatings techniques have helped in restraining the bio-corrosion rate considerably. Recently, the field of attaining highly biocompatible and osteoconductive Mg-based alloys by incorporating essential body-

functional nutrient elements has gained immense attention due to the requisition of bio-safer elements in the field of temporary implants. Mg-Zn-Ca based alloys with addition of some micro-alloying elements have shown appreciable mechanical and corrosion properties, and delivered superior biocompatibility as compared to some Mg-Al or Mg-RE based alloys. Some of the stents and screws made of Mg alloys have already passed the clinical trials. These successful clinical applications have put forward the enormous potential and the obvious benefits of using biocompatible Mg-based alloys as temporary implants. Such progresses serve as an inspiration to encourage many researchers and clinicians for further exploring different aspects related to the limitations of their clinical translation, and overcome them eventually. Substantial research is still necessary in this field to attain a desirable degradation rate along with adequate osseointegration. Some of the future prospects in the field of temporary Mg-based implants have been discussed in this article. These investigations, in near-future, can meet the diverse requirements of temporary biodegradable implants to a large extent and might lead the researchers to a new dimension in the study of Mg-based temporary implants.

Declaration of Competing Interest

The authors declare that they have no known competing financial interests or personal relationships that could have appeared to influence the work reported in this paper.

References

[1] W. Greatbatch, C.F. Holmes, IEEE Eng. Med. Biol. Mag. 10 (2002) 38–41, doi:10.1109/51.84185.
[2] M. Geetha, A.K. Singh, R. Asokamani, A.K. Gogia, Prog. Mater. Sci. 54 (2009) 397–425, doi:10.1016/j.pmatsci.2008.06.004.
[3] E. Regar, G. Sianos, P.W. Serruys, Br. Med. Bull. 59 (2001) 227–248, doi:10.1093/bmb/59.1.227.
[4] S.K. Jaganathan, E. Supriyanto, S. Murugesan, A. Balaji, M.K. Asokan, Biomed Res. Int. 2014 (2014) 459465, doi:10.1155/2014/459465.
[5] S. Agarwal, J. Curtin, B. Duffy, S. Jaiswal, Mater. Sci. Eng. C. 68 (2016) 948–963, doi:10.1016/j.msec.2016.06.020.
[6] M. Peron, J. Torgersen, F. Berto, Metals (Basel) 7 (2017) 252, doi:10.3390/met7070252.
[7] H.M. Burt, W.L. Hunter, Adv. Drug Deliv. Rev. 58 (2006) 350–357, doi:10.1016/j.addr.2006.01.014.
[8] H. Hermawan, D. Dubé, D. Mantovani, Acta Biomater 6 (2010) 1693–1697, doi:10.1016/j.actbio.2009.10.006.
[9] D.T. Beiko, B.E. Knudsen, J.D. Watterson, P.A. Cadieux, G. Reid, J.D. Denstedt, J. Urol. 171 (2004) 2438–2444, doi:10.1097/01.ju.0000125001.56045.6c.
[10] P. Habibovic, J.E. Barralet, Acta Biomater 7 (2011) 3013–3026, doi:10.1016/j.actbio.2011.03.027.
[11] M.J. Yaszemski, D.J. Trantolo, K.-.U. Lewandrowski, V. Hasirci, D.E. Altobelli, D.L. Wise, Biomaterials in Orthopedics, CRC Press, New York, 2003.
[12] H. Qu, H. Fu, Z. Han, Y. Sun, RSC Adv 9 (2019) 26252–26262, doi:10.1039/c9ra05214c.
[13] Z. Sheikh, S. Najeeb, Z. Khurshid, V. Verma, H. Rashid, M. Glogauer, Materials (Basel) 8 (2015) 5744–5794, doi:10.3390/ma8095273.
[14] P.H. Long, Toxicol. Pathol. 36 (2008) 85–91, doi:10.1177/0192623307310951.
[15] E.H. Ledet, B. Liddle, K. Kradinova, S. Harper, Innov. Entrep. Heal. 5 (2018) 41–51, doi:10.2147/ieh.s133518.
[16] Y.P. Acklin, K. Stoffel, C. Sommer, Injury 44 (2013) 456–460, doi:10.1016/j.injury.2012.09.010.
[17] J.H. Beaty, J. Orthop. Sci. 14 (2009) 245–247, doi:10.1007/s00776-008-1320-9.
[18] M. Long, H. Rack, Biomaterials 19 (1998) 1621–1639, doi:10.1016/S0142-9612(97)00146-4.
[19] M.A. Minetto, A. Giannini, R. McConnell, C. Busso, G. Torre, G. Massazza, J. Clin. Med. 9 (2020) 1216, doi:10.3390/jcm9041216.
[20] J.H. Raphael, J.L. Southall, T.V. G.nanadurai, G.J. Treharne, G.D. Kitas, BMC Musculoskelet. Disord. 3 (2002) 1–8, doi:10.1186/1471-2474-3-17.
[21] O. Sumant, S. Shinde, Fortune Bus. Insights. (2019) https://www.alliedmarketresearch.com/orthopedic-implants-market. (accessed March 6, 2021).
[22] J.H. Lee, E. Do Kim, E.J. Jun, H.S. Yoo, J.W. Lee, Biomater. Res. 22 (2018) 1–10, doi:10.1186/s40824-018-0114-1.
[23] S. Garg, P.W. Serruys, J. Am. Coll. Cardiol. 56 (2010) 1–42, doi:10.1016/j.jacc.2010.06.007.
[24] S. Borhani, S. Hassanajili, S.H. Ahmadi Tafti, S. Rabbani, Prog. Biomater. 7 (2018) 175–205, doi:10.1007/s40204-018-0097-y.
[25] G. Rigatelli, U. Carraro, M. Barbiero, M. Zanchetta, L. Pedon, K. Dimopoulos, G. Rigatelli, P. Maiolino, F. Cobelli, R. Riccardi, S. Dalla Volta, ASAIO J 48 (2002) 119–123, doi:10.1097/00002480-200201000-00025.
[26] F.J. O'Brien, Mater. Today. 14 (2011) 88–95, doi:10.1016/S1369-7021(11)70058-X.
[27] T. Ghassemi, A. Shahroodi, M.H. Ebrahimzadeh, A. Mousavian, J. Movaffagh, A. Moradi, Arch. Bone Jt. Surg. 6 (2018) 90–99, doi:10.22038/abjs.2018.26340.1713.
[28] M. Razavi, Y. Huang, Biomater. Sci. 7 (2019) 2241–2263, doi:10.1039/c9bm00289h.
[29] N. Shayesteh Moghaddam, M. Taheri Andani, A. Amerinatanzi, C. Haberland, S. Huff, M. Miller, M. Elahinia, D. Dean, Biomanufacturing Rev 1 (2016) 1–16, doi:10.1007/s40898-016-0001-2.
[30] R.B. Minkowitz, S. Bhadsavle, M. Walsh, K.A. Egol, J. Bone Jt. Surg. - Ser. A. 89 (2007) 1906–1912, doi:10.2106/JBJS.F.01536.
[31] K.F. Farraro, K.E. Kim, S.L.Y. Woo, J.R. Flowers, M.B. McCullough, J. Biomech. 47 (2014) 1979–1986, doi:10.1016/j.jbiomech.2013.12.003.
[32] L. Tian, N. Tang, T. Ngai, C. Wu, Y. Ruan, L. Huang, L. Qin, J. Orthop. Transl. 16 (2019) 1–13, doi:10.1016/j.jot.2018.06.006.
[33] G. Chandra, A. Pandey, Biocybern. Biomed. Eng. 40 (2020) 596–610, doi:10.1016/j.bbe.2020.02.003.
[34] J.E.G. González, J.C. Mirza-Rosca, J. Electroanal. Chem. 471 (1999) 109–115, doi:10.1016/S0022-0728(99)00260-0.
[35] C.N. Elias, J.H.C. Lima, R. Valiev, M.A. Meyers, Biol. Mater. Sci. (2008) 46–49.
[36] L.K. Khoo, S. Kiattavorncharoen, V. Pairuchvej, N. Lakkhanachatpan, N. Wongsirichat, D. Seriwatanachai, Open Dent. J. 14 (2020) 52–58, doi:10.2174/1874210602014010052.
[37] M. Abdel-Hady Gepreel, M. Niinomi, J. Mech. Behav. Biomed. Mater. 20 (2013) 407–415, doi:10.1016/j.jmbbm.2012.11.014.
[38] D. Singh, R. Singh, K.S. Boparai, I. Farina, L. Feo, A.K. Verma, Compos. Part B Eng. 132 (2018) 107–114, doi:10.1016/j.compositesb.2017.08.019.
[39] R. Chen, H. Ni, H. Zhang, G. Yue, W. Zhan, P. Xiong, Vacuum 89 (2013) 249–253, doi:10.1016/j.vacuum.2012.05.025.
[40] S.V. Muley, A.N. Vidvans, G.P. Chaudhari, S. Udainiya, Acta Biomater 30 (2016) 408–419, doi:10.1016/j.actbio.2015.10.043.
[41] J.A. Hunt, J.T. Callaghan, C.J. Sutcliffe, R.H. Morgan, B. Halford, R.A. Black, Biomaterials 26 (2005) 5890–5897, doi:10.1016/j.biomaterials.2005.03.004.
[42] D.D. Xiang, P. Wang, X.P. Tan, S. Chandra, C. Wang, M.L.S. Nai, S.B. Tor, W.Q. Liu, E. Liu, Mater. Sci. Eng. A. 765 (2019) 138270, doi:10.1016/j.msea.2019.138270.

[43] C.K. Seal, K. Vince, M.A. Hodgson, IOP Conf. Ser. Mater. Sci. Eng. 4 (2009) 012011, doi:10.1088/1757-899X/4/1/012011.
[44] D.R. Sumner, J. Biomech. 48 (2015) 797–800, doi:10.1016/j.jbiomech.2014.12.021.
[45] G. Mani, M.D. Feldman, D. Patel, C.M. Agrawal, Biomaterials 28 (2007) 1689–1710, doi:10.1016/j.biomaterials.2006.11.042.
[46] H. Hermawan, D. Dubé, D. Mantovani, J. Biomed. Mater. Res. - Part A. 93 (2010) 1–11, doi:10.1002/jbm.a.32224.
[47] S.M. Zielinski, M.J. Heetveld, M. Bhandari, P. Patka, E.M.M. Van Lieshout, J Orthop. Trauma. 29 (2015) 285–292, doi:10.1097/BOT.0000000000000358.
[48] M. Backes, S.A. Dingemans, M.G.W. Dijkgraaf, H.R. van den Berg, B. van Dijkman, J.M. Hoogendoorn, P. Joosse, E.D. Ritchie, W.H. Roerdink, J.P.M. Schots, N.L. Sosef, I.J.B. Spijkerman, B.A. Twigt, A.H. van der Veen, R.N. van Veen, J. Vermeulen, D.I. Vos, J. Winkelhagen, J.C. Goslings, T. Schepers, JAMA 318 (2017) 2438, doi:10.1001/jama.2017.19343.
[49] Y.P. Acklin, C. Michelitsch, C. Sommer, BMC Musculoskelet. Disord. 17 (2016) 1–5, doi:10.1186/s12891-016-0977-z.
[50] B.D. Ulery, L.S. Nair, C.T. Laurencin, J. Polym. Sci. Part B Polym. Phys. 49 (2011) 832–864, doi:10.1002/polb.22259.
[51] S. Doppalapudi, A. Jain, W. Khan, A.J. Domb, Polym. Adv. Technol. 25 (2014) 427–435, doi:10.1002/pat.3305.
[52] C. Hassler, T. Boretius, T. Stieglitz, J. Polym. Sci. Part B Polym. Phys. 49 (2011) 18–33, doi:10.1002/polb.22169.
[53] N.A. Lynd, A.J. Meuler, M.A. Hillmyer, Prog. Polym. Sci. 33 (2008) 875–893, doi:10.1016/j.progpolymsci.2008.07.003.
[54] M.S. Mozumder, A. Mairpady, A.I. Mourad, Soc. Biomater. (2016) 1241–1259, doi:10.1002/jbm.b.33633.
[55] H.F. Li, X.H. Xie, Y.F. Zheng, Y. Cong, F.Y. Zhou, K.J. Qiu, X. Wang, S.H. Chen, L. Huang, L. Tian, L. Qin, Sci. Rep. 5 (2015) 1–14, doi:10.1038/srep10719.
[56] Y. Liu, B. Lu, Z. Cai, J. Nanomater. 2019 (2019) 1–16, doi:10.1155/2019/1310792.
[57] S. Lin, Q. Wang, X. Yan, X. Ran, L. Wang, J.G. Zhou, T. Hu, G. Wang, Mater. Lett. 234 (2019) 294–297, doi:10.1016/j.matlet.2018.09.092.
[58] A.G. Demir, L. Monguzzi, B. Previtali, Addit. Manuf. 15 (2017) 20–28, doi:10.1016/j.addma.2017.03.004.
[59] P. Trumbo, S. Schlicker, A.A. Yates, M. Poos, J Am Diet Assoc 102 (2002) 1621–1630, doi:10.1016/s0002-8223(02)90346-9.
[60] E.R. Shearier, P.K. Bowen, W. He, A. Drelich, J. Drelich, J. Goldman, F. Zhao, ACS Biomater. Sci. Eng. 2 (2016) 634–642, doi:10.1021/acsbiomaterials.6b00035.
[61] M.P. Staiger, A.M. Pietak, J. Huadmai, G. Dias, Biomaterials 27 (2006) 1728–1734, doi:10.1016/j.biomaterials.2005.10.003.
[62] P.K. Bowen, J. Drelich, J. Goldman, Adv. Mater. 25 (2013) 2577–2582, doi:10.1002/adma.201300226.
[63] A. Purnama, H. Hermawan, J. Couet, D. Mantovani, Acta Biomater 6 (2010) 1800–1807, doi:10.1016/j.actbio.2010.02.027.
[64] Zinc - Wikipedia, (n.d.). https://en.wikipedia.org/wiki/Zinc (accessed March 9, 2021).
[65] W.M. Haynes, J. Mol. Struct. 268 (1992) 5–80, doi:10.1016/0022-2860(92)85083-s.
[66] H. Han, I. Jun, H. Seok, K. Lee, K. Lee, F. Witte, D. Mantovani, Y. Kim, S. Glyn-Jones, J.R. Edwards, Adv. Sci. 7 (2020) 2000800, doi:10.1002/advs.202000800.
[67] M. Li, P. He, Y. Wu, Y. Zhang, H. Xia, Y. Zheng, Y. Han, Sci. Rep. 6 (2016) 1–13, doi:10.1038/srep32323.
[68] X. Guan, M. Xiong, F. Zeng, B. Xu, L. Yang, H. Guo, J. Niu, J. Zhang, C. Chen, J. Pei, H. Huang, G. Yuan, ACS Appl. Mater. Interfaces. 6 (2014) 21525–21533, doi:10.1021/am506543a.
[69] T.S. Lim, H.S. Ryu, S.H. Hong, Corros. Sci. 62 (2012) 104–111, doi:10.1016/j.corsci.2012.04.043.
[70] M. Mhaede, F. Pastorek, B. Hadzima, Mater. Sci. Eng. C. 39 (2014) 330–335, doi:10.1016/j.msec.2014.03.023.
[71] G.Ben Hamu, D. Eliezer, L. Wagner, J. Alloys Compd. 468 (2009) 222–229, doi:10.1016/j.jallcom.2008.01.084.
[72] S.M. Baek, H.J. Kim, H.Y. Jeong, S.D. Sohn, H.J. Shin, K.J. Choi, K.S. Lee, J.G. Lee, C.D. Yim, B.S. You, H.Y. Ha, S.S. Park, Corros. Sci. 112 (2016) 44–53, doi:10.1016/j.corsci.2016.07.011.
[73] H.S. Kim, W.J. Kim, Corros. Sci. 75 (2013) 228–238, doi:10.1016/j.corsci.2013.05.032.
[74] S. Feliu, A. Samaniego, V. Barranco, A.A. El-Hadad, I. Llorente, P. Adeva, Corros. Sci. 80 (2014) 461–472, doi:10.1016/j.corsci.2013.11.065.
[75] M.C. Zhao, M. Liu, G. Song, A. Atrens, Corros. Sci. 50 (2008) 1939–1953, doi:10.1016/j.corsci.2008.04.010.
[76] T.J. Luo, Y.S. Yang, Mater. Des. 32 (2011) 5043–5048, doi:10.1016/j.matdes.2011.05.038.
[77] W. Jin, G. Wu, H. Feng, W. Wang, X. Zhang, P.K. Chu, Corros. Sci. 94 (2015) 142–155, doi:10.1016/j.corsci.2015.01.049.
[78] B. Smola, L. Joska, V. Březina, I. Stulíková, F. Hnilica, Mater. Sci. Eng. C. 32 (2012) 659–664, doi:10.1016/j.msec.2012.01.003.
[79] P. Minárik, E. Jablonská, R. Král, J. Lipov, T. Ruml, C. Blawert, B. Hadzima, F. Chmelík, Mater. Sci. Eng. C. 73 (2017) 736–742, doi:10.1016/j.msec.2016.12.120.
[80] F. Witte, J. Fischer, J. Nellesen, C. Vogt, J. Vogt, T. Donath, F. Beckmann, Acta Biomater 6 (2010) 1792–1799, doi:10.1016/j.actbio.2009.10.012.
[81] L. Mao, G. Yuan, S. Wang, J. Niu, G. Wu, W. Ding, Mater. Lett. 88 (2012) 1–4, doi:10.1016/j.matlet.2012.08.012.
[82] H. Qin, Y. Zhao, Z. An, M. Cheng, Q. Wang, T. Cheng, Q. Wang, J. Wang, Y. Jiang, X. Zhang, G. Yuan, Biomaterials 53 (2015) 211–220, doi:10.1016/j.biomaterials.2015.02.096.
[83] J. Yang, J. Peng, M. Li, E.A. Nyberg, F.S. Pan, Acta Metall. Sin. (English Lett.). 30 (2017) 53–65, doi:10.1007/s40195-016-0492-0.
[84] M. Jamesh, S. Kumar, T.S.N. Sankara Narayanan, Corros. Sci. 53 (2011) 645–654, doi:10.1016/j.corsci.2010.10.011.
[85] S.S. Abd El-Rahman, Pharmacol. Res. 47 (2003) 189–194, doi:10.1016/S1043-6618(02)00336-5.
[86] S. Zhang, X. Zhang, C. Zhao, J. Li, Y. Song, C. Xie, H. Tao, Y. Zhang, Y. He, Y. Jiang, Y. Bian, Acta Biomater 6 (2010) 626–640, doi:10.1016/j.actbio.2009.06.028.
[87] Y. Nakamura, Y. Tsumura, Y. Tonogai, T. Shibata, Y. Ito, Fundam. Appl. Toxicol. 37 (1997) 106–116, doi:10.1006/faat.1997.2322.
[88] F. Feyerabend, J. Fischer, J. Holtz, F. Witte, R. Willumeit, H. Drücker, C. Vogt, N. Hort, Acta Biomater 6 (2010) 1834–1842, doi:10.1016/j.actbio.2009.09.024.
[89] K.T. Rim, K.H. Koo, J.S. Park, Saf. Health Work. 4 (2013) 12–26, doi:10.5491/SHAW.2013.4.1.12.
[90] S. Hirano, K.T. Suzuki, Environ. Health Perspect. 104 (1996) 85–95, doi:10.1289/ehp.96104s185.
[91] J. Bennett, Q. De Hemptinne, K. McCutcheon, Expert Rev. Med. Devices. 16 (2019) 757–769, doi:10.1080/17434440.2019.1649133.
[92] V. Roche, G.Y. Koga, T.B. Matias, C.S. Kiminami, C. Bolfarini, W.J. Botta, R.P. Nogueira, A.M. Jorge Junior, J. Alloys Compd. 774 (2019) 168–181, doi:10.1016/j.jallcom.2018.09.346.
[93] Y. Sun, B. Zhang, Y. Wang, L. Geng, X. Jiao, Mater. Des. 34 (2012) 58–64, doi:10.1016/j.matdes.2011.07.058.
[94] B. Zberg, P.J. Uggowitzer, J.F. Löffler, Nat. Mater. 8 (2009) 887–891, doi:10.1038/nmat2542.
[95] M. Ramya, S.G. Sarwat, V. Udhayabanu, S. Subramanian, B. Raj, K.R. Ravi, Mater. Des. 86 (2015) 829–835, doi:10.1016/j.matdes.2015.07.154.
[96] X. Liu, J. Sun, F. Zhou, Y. Yang, R. Chang, K. Qiu, Z. Pu, L. Li, Y. Zheng, Mater. Des. 94 (2016) 95–104, doi:10.1016/j.matdes.2015.12.128.
[97] D.H. Cho, J.H. Nam, B.W. Lee, K.M. Cho, I.M. Park, J. Alloys Compd. 676 (2016) 461–468, doi:10.1016/j.jallcom.2016.03.182.
[98] M. Kaviani, G.R. Ebrahimi, H.R. Ezatpour, Mater. Chem. Phys. 234 (2019) 245–258, doi:10.1016/j.matchemphys.2019.06.010.
[99] L.B. Tong, J.H. Chu, Z.H. Jiang, S. Kamado, M.Y. Zheng, J. Alloys Compd. 785 (2019) 410–421, doi:10.1016/j.jallcom.2019.01.181.
[100] Serum chloride - Wikipedia, (n.d.). https://en.wikipedia.org/wiki/Serum_chloride (accessed March 9, 2021).

[101] M.B. Kannan, R.K.S. Raman, Biomaterials 29 (2008) 2306–2314, doi:10.1016/j.biomaterials.2008.02.003.
[102] P.Chakraborty Banerjee, S. Al-Saadi, L. Choudhary, S.E. Harandi, R. Singh, Materials (Basel) 12 (2019) 136, doi:10.3390/ma12010136.
[103] Z. Shu-Rong, Z. Huai-Mei, Q. Shao-Zhen, S. Guo-Wei, R.F. Kaper, Eur. J. Contracept. Reprod. Heal. Care. 4 (1999) 85–93, doi:10.3109/13625189909064009.
[104] Y. Yang, C. He, E. Dianyu, W. Yang, F. Qi, D. Xie, L. Shen, S. Peng, C. Shuai, Mater. Des. 185 (2020) 108259, doi:10.1016/j.matdes.2019.108259.
[105] M.P. Staiger, A.M. Pietak, J. Huadmai, G. Dias, Biomaterials 27 (2006) 1728–1734, doi:10.1016/j.biomaterials.2005.10.003.
[106] F. Witte, N. Hort, C. Vogt, S. Cohen, K.U. Kainer, R. Willumeit, F. Feyerabend, Curr. Opin. Solid State Mater. Sci. 12 (2008) 63–72, doi:10.1016/j.cossms.2009.04.001.
[107] J. Vormann, Mol. Aspects Med. 24 (2003) 27–37, doi:10.1016/S0098-2997(02)00089-4.
[108] R. Touyz, Front. Bioscience 9 (2004) 1278–1293, doi:10.2741/1316.
[109] D. Zhao, F. Witte, F. Lu, J. Wang, J. Li, L. Qin, Biomaterials 112 (2017) 287–302, doi:10.1016/j.biomaterials.2016.10.017.
[110] N.E.L. Saris, E. Mervaala, H. Karppanen, J.A. Khawaja, A. Lewenstam, Clin. Chim. Acta. 294 (2000) 1–26, doi:10.1016/S0009-8981(99)00258-2.
[111] L. Jin, J. Wu, G. Yuan, T. Chen, PLoS ONE 13 (2018) 1–15, doi:10.1371/journal.pone.0193276.
[112] C. Gao, S. Peng, P. Feng, C. Shuai, Bone Res 5 (2017) 1–33, doi:10.1038/boneres.2017.59.
[113] S. Chen, Y. Guo, R. Liu, S. Wu, J. Fang, B. Huang, Z. Li, Z. Chen, Z. Chen, Colloids Surfaces B Biointerfaces 164 (2018) 58–69, doi:10.1016/j.colsurfb.2018.01.022.
[114] E. Abed, R. Moreau, Am. J. Physiol. - Cell Physiol. 297 (2009) 360–368, doi:10.1152/ajpcell.00614.2008.
[115] L.Y. He, X.M. Zhang, B. Liu, Y. Tian, W.H. Ma, Brazilian J. Med. Biol. Res. 49 (2016) 1–6, doi:10.1590/1414-431X20165257.
[116] Y. Zhang, J. Xu, Y.C. Ruan, M.K. Yu, M. O'Laughlin, H. Wise, D. Chen, L. Tian, D. Shi, J. Wang, S. Chen, J.Q. Feng, D.H.K. Chow, X. Xie, L. Zheng, L. Huang, S. Huang, K. Leung, N. Lu, L. Zhao, H. Li, D. Zhao, X. Guo, K. Chan, F. Witte, H.C. Chan, Y. Zheng, L. Qin, Nat. Med. 22 (2016) 1160–1169, doi:10.1038/nm.4162.
[117] X. Nie, X. Sun, C. Wang, J. Yang, Regen. Biomater. 7 (2019) 53–61, doi:10.1093/rb/rbz033.
[118] C. Yang, G. Yuan, J. Zhang, Z. Tang, X. Zhang, K. Dai, Biomed. Mater. 5 (2010) 045005, doi:10.1088/1748-6041/5/4/045005.
[119] D. Maradze, D. Musson, Y. Zheng, J. Cornish, M. Lewis, Y. Liu, Sci. Rep. 8 (2018) 1–15, doi:10.1038/s41598-018-28476-w.
[120] Y. Chen, Z. Xu, C. Smith, J. Sankar, Acta Biomater 10 (2014) 4561–4573, doi:10.1016/j.actbio.2014.07.005.
[121] J. Chen, L. Tan, X. Yu, I.P. Etim, M. Ibrahim, K. Yang, J. Mech. Behav. Biomed. Mater. 87 (2018) 68–79, doi:10.1016/j.jmbbm.2018.07.022.
[122] J. Zhang, C. Xu, Y. Jing, S. Lv, S. Liu, D. Fang, J. Zhuang, M. Zhang, R. Wu, Sci. Rep. 5 (2015) 1–16, doi:10.1038/srep13933.
[123] C.E. Baker, S.N. Moore-Lotridge, A.A. Hysong, S.L. Posey, J.P. Robinette, D.M. Blum, M.A. Benvenuti, H.A. Cole, S. Egawa, A. Okawa, M. Saito, J.R. McCarthy, J.S. Nyman, M. Yuasa, J.G. Schoenecker, Clin. Rev. Bone Miner. Metab. 16 (2018) 142–158, doi:10.1007/s12018-018-9256-x.
[124] S. Ghimire, S. Miramini, G. Edwards, R. Rotne, J. Xu, P. Ebeling, Bone Rep 14 (2021) 100740, doi:10.1016/j.bonr.2020.100740.
[125] M. Windolf, M. Ernst, R. Schwyn, D. Arens, S. Zeiter, Injury 52 (2021) 71–77, doi:10.1016/j.injury.2020.10.050.
[126] W.H. Cheung, S.K. ho Chow, M.H. Sun, L. Qin, K.S. Leung, Ultrasound Med. Biol. 37 (2011) 231–238, doi:10.1016/j.ultrasmedbio.2010.11.016.
[127] W. Chen, K. Xu, B. Tao, L. Dai, Y. Yu, C. Mu, X. Shen, Y. Hu, Y. He, K. Cai, Acta Biomater 74 (2018) 489–504, doi:10.1016/j.actbio.2018.04.043.
[128] S. Cheng, D. Zhang, M. Li, X. Liu, Y. Zhang, S. Qian, F. Peng, Bioact. Mater. 6 (2021) 91–105, doi:10.1016/j.bioactmat.2020.07.014.
[129] G.Eddy Jai Poinern, S. Brundavanam, D. Fawcett, Am. J. Biomed. Eng. 2 (2013) 218–240, doi:10.5923/j.ajbe.20120206.02.
[130] S.P. Massia, M.M. Holecko, G.R. Ehteshami, J. Biomed. Mater. Res. - Part A. 68 (2004) 177–186, doi:10.1002/jbm.a.20009.
[131] B.G.X. Zhang, D.E. Myers, G.G. Wallace, M. Brandt, P.F.M. Choong, Int. J. Mol. Sci. 15 (2014) 11878–11921, doi:10.3390/ijms150711878.
[132] H. Li, Y. Zheng, L. Qin, Prog. Nat. Sci. Mater. Int. 24 (2014) 414–422, doi:10.1016/j.pnsc.2014.08.014.
[133] S. Dutta, S.K.R. Narala, Mater. Today Proc 44 (2021) 86–91, doi:10.1016/j.matpr.2020.07.339.
[134] J. Trinidad, I. Marco, G. Arruebarrena, J. Wendt, D. Letzig, E. Sáenz De Argandoña, R. Goodall, Adv. Eng. Mater. 16 (2014) 241–247, doi:10.1002/adem.201300236.
[135] S. Lun Sin, A. Elsayed, C. Ravindran, Int. Mater. Rev. 58 (2013) 419–436, doi:10.1179/1743280413Y.0000000017.
[136] A. Kumar, S. Kumar, N.K. Mukhopadhyay, J. Magnes. Alloy. 6 (2018) 245–254, doi:10.1016/j.jma.2018.05.006.
[137] L. Xiao, G. Yang, R. Pei, Z. Zhen, W. Jie, Mater. Sci. Eng. A. 810 (2021) 141021, doi:10.1016/j.msea.2021.141021.
[138] L. Song, Y. Lu, Y. Zhang, X. Li, M. Cong, W. Xu, Vacuum 168 (2019) 108822, doi:10.1016/j.vacuum.2019.108822.
[139] H. Liao, J. Kim, T. Lee, J. Song, J. Peng, B. Jiang, F. Pan, J. Magnes. Alloy. 8 (2020) 1120–1127, doi:10.1016/j.jma.2020.06.009.
[140] R. Maurya, D. Mittal, K. Balani, J. Mater. Res. Technol. 9 (2020) 4749–4762, doi:10.1016/j.jmrt.2020.02.101.
[141] P. Duley, S. Sanyal, T.K. Bandyopadhyay, S. Mandal, Mater. Des. 164 (2019) 16–18, doi:10.1016/j.matdes.2018.107554.
[142] L. Wu, C. Cui, R. Wu, J. Li, H. Zhan, M. Zhang, Mater. Sci. Eng. A. 528 (2011) 2174–2179, doi:10.1016/j.msea.2010.11.063.
[143] G. Levi, S. Avraham, A. Zilberov, M. Bamberger, Acta Mater 54 (2006) 523–530, doi:10.1016/j.actamat.2005.09.023.
[144] R. Shi, J. Miao, A.A. Luo, Scr. Mater. 171 (2019) 92–97, doi:10.1016/j.scriptamat.2019.06.027.
[145] L. Balogh, R.B. Figueiredo, T. Ungár, T.G. Langdon, Mater. Sci. Eng. A. 528 (2010) 533–538, doi:10.1016/j.msea.2010.09.048.in-vitro.
[146] P. Duley, S. Sanyal, T.K. Bandyopadhyay, S. Mandal, Mater. Sci. Eng. A. 784 (2020) 139288, doi:10.1016/j.msea.2020.139288.
[147] J. Dai, M. Easton, S. Zhu, G. Wu, W. Ding, J. Mater. Res. 27 (2012) 2790–2797, doi:10.1557/jmr.2012.313.
[148] A. Rezaei, R. Mahmudi, C. Cayron, R. Loge, Mater. Sci. Eng. A. 806 (2021) 140803, doi:10.1016/j.msea.2021.140803.
[149] X. LUO, D. FANG, Q. LI, Y. CHAI, J. Rare Earths. 34 (2016) 1134–1138, doi:10.1016/S1002-0721(16)60145-X.
[150] D. Melt, D. Dmd, K.P. Rao, K. Suresh, Crystals 10 (2020) 647, doi:10.3390/cryst10080647.
[151] K.K. Alaneme, E.A. Okotete, J. Magnes. Alloy. 5 (2017) 460–475, doi:10.1016/j.jma.2017.11.001.
[152] J.S. Suh, D. Klaumünzer, H.S. Kim, Y.M. Kim, B.S. You, Procedia Eng 207 (2017) 908–913, doi:10.1016/j.proeng.2017.10.850.
[153] H.Da Zhao, G.W. Qin, Y.P. Ren, W.L. Pei, D. Chen, Y. Guo, Trans. Nonferrous Met. Soc. China 20 (2010) 493–497, doi:10.1016/S1003-6326(10)60525-0.
[154] K. Hagihara, Z. Li, M. Yamasaki, Y. Kawamura, T. Nakano, Acta Mater 163 (2019) 226–239, doi:10.1016/j.actamat.2018.10.016.
[155] C.Y. Ma, N. Xia, C. Wang, M.X. Li, Z.M. Hua, M.W. Ren, H.Y. Wang, J. Alloys Compd. 869 (2021) 159308, doi:10.1016/j.jallcom.2021.159308.
[156] T. DING, H. ge YAN, J. hua CHEN, W. jun XIA, B. SU, Z. lin YU, Trans. Nonferrous Met. Soc. China 29 (2019) 1631–1640, doi:10.1016/S1003-6326(19)65070-3.
[157] T. Mineta, H. Sato, Mater. Sci. Eng. A. 735 (2018) 418–422, doi:10.1016/j.msea.2018.08.077.
[158] Z. Yan, Z. Zhang, X. Li, J. Xu, Q. Wang, G. Zhang, J. Zheng, H. Fan, K. Xu, J. Zhu, Y. Xue, J. Alloys Compd. 822 (2020) 153698, doi:10.1016/j.jallcom.2020.153698.
[159] J. Čížek, I. Procházka, B. Smola, I. Stulíková, R. Kužel, Z. Matěj, V. Cherkaska, R.K. Islamgaliev, O. Kulyasova, Mater. Sci. Eng. A. 462 (2007) 121–126, doi:10.1016/j.msea.2006.01.177.

[160] Y. Li, J. Wang, R. Xu, Vacuum 178 (2020) 109396, doi:10.1016/j.vacuum.2020.109396.
[161] B. Sułkowski, M. Janoska, G. Boczkal, R. Chulist, M. Mroczkowski, P. Pałka, J. Magnes. Alloy. 8 (2020) 761–768, doi:10.1016/j.jma.2020.04.005.
[162] X. Zhang, G. Yuan, Z. Wang, Mater. Lett. 74 (2012) 128–131, doi:10.1016/j.matlet.2012.01.086.
[163] B. Dong, X. Che, Z. Zhang, J. Yu, M. Meng, J. Alloys Compd. 853 (2021) 157066, doi:10.1016/j.jallcom.2020.157066.
[164] L.B. Tong, J.H. Chu, W.T. Sun, C. Xu, D.N. Zou, K.S. Wang, S. Kamado, M.Y. Zheng, Mater. Charact. 171 (2021) 110804, doi:10.1016/j.matchar.2020.110804.
[165] A. Kumar, P.M. Pandey, J. Magnes. Alloy. 8 (2020) 883–898, doi:10.1016/j.jma.2020.02.011.
[166] Y. Yan, H. Cao, Y. Kang, K. Yu, T. Xiao, J. Luo, Y. Deng, H. Fang, H. Xiong, Y. Dai, J. Alloys Compd. 693 (2017) 1277–1289, doi:10.1016/j.jallcom.2016.10.017.
[167] S.Z. Khalajabadi, M.R. Abdul Kadir, S. Izman, M. Marvibaigi, J. Alloys Compd. 655 (2016) 266–280, doi:10.1016/j.jallcom.2015.09.107.
[168] H. Torabi, M. Hoseini, M. Sadrkhah, G. Faraji, A. Masoumi, Ceram. Int. 46 (2020) 2836–2844, doi:10.1016/j.ceramint.2019.09.276.
[169] A. Dubey, S. Jaiswal, D. Lahiri, J. Mater. Eng. Perform. 28 (2019) 800–809, doi:10.1007/s11665-018-3778-8.
[170] Kundan Kumar, Ashish Das, Shashi Bhushan Prasad, Materials Today: Proceedings 44 (2021) 2038–2042, doi:10.1016/j.matpr.2020.12.133.
[171] M. Karasoglu, S. Karaoglu, G. Arslan, Proc. Inst. Mech. Eng. Part L J. Mater. Des. Appl. 233 (2019) 1972–1984, doi:10.1177/1464420718805119.
[172] K. Narita, Q. Tian, I. Johnson, C. Zhang, E. Kobayashi, H. Liu, J. Biomed. Mater. Res. - Part B Appl. Biomater. 107 (2019) 2238–2253, doi:10.1002/jbm.b.34316.
[173] M. Knapek, M. Zemková, A. Greš, E. Jablonská, F. Lukáč, R. Král, J. Bohlen, P. Minárik, J. Magnes. Alloy. 9 (2021) 853–865, doi:10.1016/j.jma.2020.12.017.
[174] S. Dutta, K.B. Devi, S. Gupta, B. Kundu, V.K. Balla, M. Roy, J. Biomed. Mater. Res. - Part B Appl. Biomater. 107 (2019) 352–365, doi:10.1002/jbm.b.34127.
[175] R. Allavikutty, P. Gupta, T.S. Santra, J. Rengaswamy, Curr. Opin. Biomed. Eng. 18 (2021) 100276, doi:10.1016/j.cobme.2021.100276.
[176] D. Gu, Y.C. Hagedorn, W. Meiners, G. Meng, R.J.S. Batista, K. Wissenbach, R. Poprawe, Acta Mater 60 (2012) 3849–3860, doi:10.1016/j.actamat.2012.04.006.
[177] J. Deckers, J. Vleugels, J.P. Kruth, J. Ceram. Sci. Technol. 5 (2014) 245–260, doi:10.4416/JCST2014-00032.
[178] K. Zhang, Q.V. Le, J. Composites Compounds 2 (2020) 10–17, doi:10.29252/jcc.2.1.2.
[179] M. Schmid, A. Amado, K. Wegener, J. Mater. Res. 29 (2014) 1824–1832, doi:10.1557/jmr.2014.138.
[180] Y. Li, J. Zhou, P. Pavanram, M.A. Leeflang, L.I. Fockaert, B. Pouran, N. Tümer, K.U. Schröder, J.M.C. Mol, H. Weinans, H. Jahr, A.A. Zadpoor, Acta Biomater 67 (2018) 378–392, doi:10.1016/j.actbio.2017.12.008.
[181] Y. Yang, C. Lu, L. Shen, Z. Zhao, S. Peng, C. Shuai, J. Magnes. Alloy. (2021) in presshttps://doi.org/, doi:10.1016/j.jma.2021.04.009.
[182] Y. Yang, C. Lu, S. Peng, L. Shen, D. Wang, F. Qi, C. Shuai, Virtual Phys. Prototyp. 15 (2020) 278–293, doi:10.1080/17452759.2020.1748381.
[183] C. Shuai, Y. Cheng, Y. Yang, S. Peng, W. Yang, F. Qi, J. Alloys Compd. 798 (2019) 606–615, doi:10.1016/j.jallcom.2019.05.278.
[184] V.S. Telang, R. Pemmada, V. Thomas, S. Ramakrishna, P. Tandon, H.S. Nanda, Curr. Opin. Biomed. Eng. 17 (2021) 100264, doi:10.1016/j.cobme.2021.100264.
[185] A. Chaya, S. Yoshizawa, K. Verdelis, N. Myers, B.J. Costello, D.T. Chou, S. Pal, S. Maiti, P.N. Kumta, C. Sfeir, Acta Biomater 18 (2015) 262–269, doi:10.1016/j.actbio.2015.02.010.
[186] W.M. Gan, Y.D. Huang, R. Wang, G.F. Wang, A. Srinivasan, H.G. Brokmeier, N. Schell, K.U. Kainer, N. Hort, Mater. Des. 63 (2014) 83–88, doi:10.1016/j.matdes.2014.05.057.
[187] W. Lei, D. Zhu, H. Wang, W. Liang, J. Wuhan Univ. Technol. Sci. Ed. 34 (2019) 1193–1196, doi:10.1007/s11595-019-2177-9.
[188] D. Ahmadkhaniha, Y. Huang, M. Jaskari, A. Järvenpää, M.H. Sohi, C. Zanella, L.P. Karjalainen, T.G. Langdon, J. Mater. Sci. 53 (2018) 16585–16597, doi:10.1007/s10853-018-2779-1.
[189] K. Matsubara, Y. Miyahara, Z. Horita, T.G. Langdon, Metall. Mater. Trans. A Phys. Metall. Mater. Sci. 35 A (2004) 1735–1744, doi:10.1007/s11661-004-0082-z.
[190] W. Wang, K. Wang, Q. Guo, N. Wu, Xiyou Jinshu Cailiao Yu Gongcheng/Rare Met. Mater. Eng. 41 (2012) 1522–1526, doi:10.1016/s1875-5372(13)60004-1.
[191] Y. Xu, L.X. Hu, Y. Sun, J.B. Jia, J.F. Jiang, Q.G. Ma, Trans. Nonferrous Met. Soc. China (English Ed. 25 (2015) 381–388, doi:10.1016/S1003-6326(15)63614-7.
[192] V. Vignesh, R. Padmanaban, R. Mohan, D. Kovukkal, G. Myilsamy, Met. Mater. Int. 26 (2020) 409–430, doi:10.1007/s12540-019-00346-8.
[193] M. Bamberger, G. Dehm, Annu. Rev. Mater. Res. 38 (2008) 505–533, doi:10.1146/annurev.matsci.020408.133717.
[194] S. Sanyal, M. Paliwal, T.K. Bandyopadhyay, S. Mandal, Mater. Sci. Eng. A. 800 (2021) 140322, doi:10.1016/j.msea.2020.140322.
[195] S. Sanyal, S. Kanodia, R. Saha, T.K. Bandyopadhyay, S. Mandal, J. Alloys Compd. 800 (2019) 343–354, doi:10.1016/j.jallcom.2019.06.026.
[196] T. Ying, M.Y. Zheng, Z.T. Li, X.G. Qiao, J. Alloys Compd. 608 (2014) 19–24, doi:10.1016/j.jallcom.2014.04.107.
[197] N.B. Tork, H. Saghafian, S.H. Razavi, R. Ebrahimi, R. Mahmudi, Integr. Med. Res. 8 (2019) 1288–1299, doi:10.1016/j.jmrt.2018.06.023.
[198] S. Sanyal, O.G. Gabhale, T.K. Bandyopadhyay, S. Mandal, J. Alloys Compd. 861 (2021) 158540, doi:10.1016/j.jallcom.2020.158540.
[199] B. Chen, D.L. Lin, L. Jin, X.Q. Zeng, C. Lu, Mater. Sci. Eng. A. 483–484 (2008) 113–116, doi:10.1016/j.msea.2006.10.199.
[200] D. Liu, D. Yang, X. Li, S. Hu, J. Mater. Res. Technol. 8 (2019) 1538–1549, doi:10.1016/j.jmrt.2018.08.003.
[201] E. Aghion, G. Levy, J. Mater. Sci. 45 (2010) 3096–3101, doi:10.1007/s10853-010-4317-7.
[202] H. Chen, S.B. Kang, H. Yu, J. Cho, H.W. Kim, G. Min, J. Alloys Compd. 476 (2009) 324–328, doi:10.1016/j.jallcom.2008.08.077.
[203] Y. Zhang, Z. Liu, S. Pang, T. Meng, Y. Zhi, Y. Xu, L. Xiao, R. Li, Mater. Sci. Eng. A. 805 (2020) 140567, doi:10.1016/j.msea.2020.140567.
[204] C. Wang, Y. Zhang, Q. Huo, Z. Zhang, J. Tang, A. Hashimoto, X. Yang, Mater. Sci. Eng. A. 800 (2021) 140309, doi:10.1016/j.msea.2020.140309.
[205] S.V. Dobatkin, L.L. Rokhlin, E.A. Lukyanova, M.Y. Murashkin, T.V. Dobatkina, N.Y. Tabachkova, Mater. Sci. Eng. A. 667 (2016) 217–223, doi:10.1016/j.msea.2016.05.003.
[206] P. Minárik, R. Král, J. Pešička, F. Chmelík, J. Mater. Res. Technol. 4 (2015) 75–78, doi:10.1016/j.jmrt.2014.10.012.
[207] Y.H. Kang, Z.H. Huang, S.C. Wang, H. Yan, R.S. Chen, J.C. Huang, J. Magnes. Alloy. 8 (2020) 103–110, doi:10.1016/j.jma.2019.11.012.
[208] X. Zhang, G. Yuan, L. Mao, J. Niu, P. Fu, W. Ding, J. Mech. Behav. Biomed. Mater. 7 (2012) 77–86, doi:10.1016/j.jmbbm.2011.05.026.
[209] J. Chen, L. Tan, X. Yu, I.P. Etim, M. Ibrahim, K. Yang, J. Mech. Behav. Biomed. Mater. 87 (2018) 68–79, doi:10.1016/j.jmbbm.2018.07.022.
[210] S. Zhang, X. Zhang, C. Zhao, J. Li, Y. Song, C. Xie, H. Tao, Y. Zhang, Y. He, Y. Jiang, Y. Bian, Acta Biomater 6 (2010) 626–640, doi:10.1016/j.actbio.2009.06.028.
[211] H. Ha, J. Kang, J. Yang, C. Dong, B. Sun, Corros. Sci. 75 (2013) 426–433, doi:10.1016/j.corsci.2013.06.027.
[212] M. Paliwal, I. Jung, J. Cryst. Growth. 394 (2014) 28–38, doi:10.1016/j.jcrysgro.2014.02.010.
[213] B.P. Zhang, Y. Wang, L. Geng, Biomater. - Phys. Chem. 9 (2011) 183–204, doi:10.5772/23929.
[214] A.F. Lotfabadi, H.R. Bakhsheshi-Rad, M.H. Idris, E. Hamzah, M. Kasiri-Asgarani, Can. Metall. Q. 55 (2016) 53–64, doi:10.1179/1879139515Y.0000000031.
[215] H.R. Bakhsheshi-Rad, E. Hamzah, M. Medraj, M.H. Idris, A.F. Lotfabadi, M. Daroonparvar, M.A.M. Yajid, Mater. Corros. 65 (2014) 999–1006, doi:10.1002/maco.201307492.

[216] Y.Z. Du, X.G. Qiao, M.Y. Zheng, D.B. Wang, K. Wu, I.S. Golovin, Mater. Des. 98 (2016) 285–293, doi:10.1016/j.matdes.2016.03.025.
[217] S.A. Abdel-Gawad, M.A. Shoeib, Surfaces and Interfaces 14 (2019) 108–116, doi:10.1016/j.surfin.2018.11.011.
[218] E. Zhang, D. Yin, L. Xu, L. Yang, K. Yang, Mater. Sci. Eng. C. 29 (2009) 987–993, doi:10.1016/j.msec.2008.08.024.
[219] Y. Yandong, K. Shuzhen, P. Teng, L. Jie, L. Caixia, Metallogr. Microstruct. Anal. 4 (2015) 381–391, doi:10.1007/s13632-015-0224-2.
[220] Y. Zhang, J. Li, J. Li, J. Mech. Behav. Biomed. Mater. 80 (2018) 246–257, doi:10.1016/j.jmbbm.2018.01.028.
[221] L.B. Tong, M.Y. Zheng, S.W. Xu, S. Kamado, Y.Z. Du, X.S. Hu, K. Wu, W.M. Gan, H.G. Brokmeier, G.J. Wang, X.Y. Lv, Mater. Sci. Eng. A. 528 (2011) 3741–3747, doi:10.1016/j.msea.2011.01.037.
[222] J. Buha, J. Alloys Compd. 472 (2009) 171–177, doi:10.1016/j.jallcom.2008.05.019.
[223] M. Yang, H. Li, C. Duan, J. Zhang, J. Alloys Compd. 579 (2013) 92–99, doi:10.1016/j.jallcom.2013.05.064.
[224] Q. Li, Q. Wang, Y. Wang, X. Zeng, W. Ding, J. Alloys Compd. 427 (2007) 115–123, doi:10.1016/j.jallcom.2006.02.054.
[225] M.Y. Zheng, X.G. Qiao, S.W. Xu, K. Wu, S. Kamado, Y. Kojima, J. Mater. Sci. 40 (2005) 2587–2590, doi:10.1007/s10853-005-2081-x.
[226] J.Y. Lee, D.H. Kim, H.K. Lim, D.H. Kim, Mater. Lett. 59 (2005) 3801–3805, doi:10.1016/j.matlet.2005.06.052.
[227] X. Gao, S.M. Zhu, B.C. Muddle, J.F. Nie, Scr. Mater. 53 (2005) 1321–1326, doi:10.1016/j.scriptamat.2005.08.035.
[228] M. Kavyani, G.R. Ebrahimi, H.R. Ezatpour, M. Jahazi, J. Magnes. Alloy. (2020) in presshttps://doi.org/, doi:10.1016/j.jma.2020.11.013.
[229] Y. Sun, B. Zhang, Y. Wang, L. Geng, X. Jiao, Mater. Des. 34 (2012) 58–64, doi:10.1016/j.matdes.2011.07.058.
[230] O. Sivakesavam, Y.V.R.K. Prasad, Mater. Sci. Eng. A. 362 (2003) 118–124, doi:10.1016/S0921-5093(03)00296-X.
[231] P. Duley, S. Sanyal, T.K. Bandyopadhyay, S. Mandal, Mater. Charact. 172 (2021) 110885, doi:10.1016/j.matchar.2021.110885.
[232] J. Liu, W. Wang, Y. Huang, J. Xie, W. Huang, S. Shi, Jinshu Rechuli/Heat Treat. Met. 42 (2017) 89–92, doi:10.13251/j.issn.0254-6051.2017.08.020.
[233] T.L. Chia, M.A. Easton, S.M. Zhu, M.A. Gibson, N. Birbilis, J.F. Nie, Intermetallics 17 (2009) 481–490, doi:10.1016/j.intermet.2008.12.009.
[234] L. Gao, S. Xue, L. Zhang, Z. Sheng, G. Zeng, F. Ji, J. Mater. Sci. Mater. Electron. 21 (2010) 643–648, doi:10.1007/s10854-009-9970-8.
[235] D. Wenwen, S. Yangshan, M. Xuegang, X. Feng, Z. Min, W. Dengyun, Mater. Sci. Eng. A. 356 (2003) 1–7, doi:10.1016/S0921-5093(02)00551-8.
[236] Y. Kawamura, K. Yahashi, A. Inoue, T. Masumoto, Met. Trans. 42 (2002) 1172–1176, doi:10.2320/matertrans.42.1172.
[237] M. Qian, A. Das, Scr. Mater. 54 (2006) 881–886, doi:10.1016/j.scriptamat.2005.11.002.
[238] D.H. Stjohn, M.A. Qian, M.A. Easton, P. Cao, Z.O.Ë. Hildebrand, Metall. Mater. Trans. A. 36 (2005) 1669–1679, doi:10.1007/s11661-005-0030-6.
[239] Z.G. Huan, M.A. Leeflang, J. Zhou, L.E. Fratila-Apachitei, J. Duszczyk, J. Mater. Sci. Mater. Med. 21 (2010) 2623–2635, doi:10.1007/s10856-010-4111-8.
[240] R.P. Verma, Mater. Today Proc. 26 (2020) 3148–3151, doi:10.1016/j.matpr.2020.02.649.
[241] J. Murray, Bull. Alloy Phase Diagrams. 7 (1986) 245–246, doi:10.1007/BF02868999.
[242] G. Liang, R. Schulz, J. Mater. Sci. 8 (2003) 1179–1184, doi:10.1023/A:1022889100360.
[243] J. Chen, Y. Sun, J. Zhang, W. Cheng, X. Niu, C. Xu, J. Magnes. Alloy. 3 (2015) 121–126, doi:10.1016/j.jma.2015.05.001.
[244] Calcium - Health Professional Fact Sheet, (n.d.). https://ods.od.nih.gov/factsheets/Calcium-HealthProfessional/ (accessed March 11, 2021).
[245] V. Tai, W. Leung, A. Grey, I.R. Reid, M.J. Bolland, BMJ 351 (2015) 4183, doi:10.1136/bmj.h4183.
[246] H. Reza, B. Rad, M. Hasbullah, M. Rafiq, A. Kadir, S. Farahany, Mater. Des. 33 (2012) 88–97, doi:10.1016/j.matdes.2011.06.057.
[247] J.W. Seong, W.J. Kim, Acta Biomater 11 (2015) 531–542, doi:10.1016/j.actbio.2014.09.029.
[248] S.E. Harandi, M. Mirshahi, S. Koleini, M.H. Idris, H. Jafari, M.R.A. Kadir, Mater. Res. 16 (2012) 11–18, doi:10.1590/S1516-14392012005000151.
[249] Z. Li, X. Gu, S. Lou, Y. Zheng, Biomaterials 29 (2008) 1329–1344, doi:10.1016/j.biomaterials.2007.12.021.
[250] S. Koleini, M. Hasbullah, H. Jafari, J. Mater. 33 (2012) 20–25, doi:10.1016/j.matdes.2011.06.063.
[251] H. Du, Z. Wei, X. Liu, E. Zhang, Mater. Chem. Phys. 125 (2011) 568–575, doi:10.1016/j.matchemphys.2010.10.015.
[252] G. Levi, S. Avraham, A. Zilberov, M. Bamberger, Acta Mater 54 (2006) 523–530, doi:10.1016/j.actamat.2005.09.023.
[253] H. Han, S. Loffredo, I. Jun, J. Edwards, Y. Kim, H. Seok, F. Witte, D. Mantovani, S. Glyn-jones, Mater. Today. 23 (2019) 57–71, doi:10.1016/j.mattod.2018.05.018.
[254] I.S. Berglund, H.S. Brar, N. Dolgova, A.P. Acharya, B.G. Keselowsky, M. Sarntinoranont, M.V. Manuel, J. Biomed. Mater. Res. Part B Appl. Biomater. 100B (2012) 1524–1534, doi:10.1002/jbm.b.32721.
[255] F.S. Mirza, J. Nutr. Heal. Food Sci. 4 (2016) 1–3, doi:10.15226/jnhfs.2016.00167.
[256] C. Zhao, F. Pan, L. Zhang, H. Pan, K. Song, A. Tang, Mater. Sci. Eng. C. 70 (2017) 1081–1088, doi:10.1016/j.msec.2016.04.012.
[257] H.S. Brar, J. Wong, M.V. Manuel, J. Mech. Behav. Biomed. Mater. 7 (2012) 87–95, doi:10.1016/j.jmbbm.2011.07.018.
[258] A.A. Alfarraj, A. Sukumaran, M.D. Al, Odontology 106 (2018) 37–44, doi:10.1007/s10266-017-0296-3.
[259] L. Rogal, A. Kania, K. Berent, K. Janus, L. Lityńska-Dobrzyńska, J. Mater. Res. Technol. 8 (2019) 1121–1131, doi:10.1016/j.jmrt.2018.09.002.
[260] Y. Li, C. Wen, D. Mushahary, R. Sravanthi, N. Harishankar, G. Pande, P. Hodgson, Acta Biomater 8 (2012) 3177–3188, doi:10.1016/j.actbio.2012.04.028.
[261] Y. Ding, J. Lin, C. Wen, D. Zhang, Y. Li, Nat. Publ. Gr. 6 (2016) 1–10, doi:10.1038/srep31990.
[262] Y.-L. Zhou, J. An, D.-M. Luo, W.-Y. Hu, Y.C. Li, P. Hodgson, C.E. Wen, Mater. Technol. 27 (2012) 52–54, doi:10.1179/175355511-13240279340200.
[263] A.D. Südholz, N.T. Kirkland, R.G. Buchheit, N. Birbilis, Electrochem. Solid-State Lett. 14 (2011) 2010–2012, doi:10.1149/1.3523229.
[264] M. Esmaily, J.E. Svensson, S. Fajardo, N. Birbilis, G.S. Frankel, S. Virtanen, R. Arrabal, S. Thomas, L.G. Johansson, Prog. Mater. Sci. 89 (2017) 92–193, doi:10.1016/j.pmatsci.2017.04.011.
[265] X. Zhang, G. Yuan, J. Niu, P. Fu, W. Ding, J. Mech. Behav. Biomed. Mater. 9 (2012) 153–162, doi:10.1016/j.jmbbm.2012.02.002.
[266] F. Witte, J. Fischer, J. Nellesen, H.A. Crostack, V. Kaese, A. Pisch, F. Beckmann, H. Windhagen, Biomaterials 27 (2006) 1013–1018, doi:10.1016/j.biomaterials.2005.07.037.
[267] M. Ascencio, M. Pekguleryuz, S. Omanovic, Corros. Sci. 87 (2014) 489–503, doi:10.1016/j.corsci.2014.07.015.
[268] H. Wang, Y. Estrin, H. Fu, G. Song, Z. Zúberová, Adv. Eng. Mater. 9 (2007) 967–972, doi:10.1002/adem.200700200.
[269] Z. Wen, C. Wu, C. Dai, F. Yang, J. Alloys Compd. 488 (2009) 392–399, doi:10.1016/j.jallcom.2009.08.147.
[270] M. Cihova, E. Martinelli, P. Schmutz, A. Myrissa, R. Schäublin, A.M. Weinberg, P.J. Uggowitzer, J.F. Löffler, Acta Biomater 100 (2019) 398–414, doi:10.1016/j.actbio.2019.09.021.
[271] P. Yin, N.F. Li, T. Lei, L. Liu, C. Ouyang, J. Mater. Sci. Mater. Med. 24 (2013) 1365–1373, doi:10.1007/s10856-013-4856-y.
[272] J. Wang, S. Huang, S. Guo, Y. Wei, F. Pan, Trans. Nonferrous Met. Soc. China. 23 (2013) 1930–1935, doi:10.1016/S1003-6326(13)62679-5.
[273] E. Zhang, L. Yang, Mater. Sci. Eng. A. 497 (2008) 111–118, doi:10.1016/j.msea.2008.06.019.
[274] D. Zander, N.A. Zumdick, Corros. Sci. 93 (2015) 222–233, doi:10.1016/j.corsci.2015.01.027.
[275] D. Liu, C. Guo, L. Chai, V.R. Sherman, X. Qin, Y. Ding, M.A. Meyers,

Mater. Sci. Eng. B Solid-State Mater. Adv. Technol. 195 (2015) 50–58, doi:10.1016/j.mseb.2015.02.001.
[276] Y. Xia, B. Zhang, Y. Wang, M. Qian, L. Geng, Mater. Sci. Eng. C. 32 (2012) 665–669, doi:10.1016/j.msec.2012.01.004.
[277] Y.H. Xia, B.P. Zhang, C.X. Lu, L. Geng, Mater. Sci. Eng. C. 33 (2013) 5044–5050, doi:10.1016/j.msec.2013.08.033.
[278] S.U.N. Yu, K. Min-xiu, J. Xiao-hui, Trans. Nonferrous Met. Soc. China. 21 (2011) 252–257, doi:10.1016/S1003-6326(11)61587-2.
[279] D.H. Cho, B.W. Lee, J.Y. Park, K.M. Cho, I.M. Park, J. Alloys Compd. 695 (2017) 1166–1174, doi:10.1016/j.jallcom.2016.10.244.
[280] X.N. Gu, N. Li, Y.F. Zheng, L. Ruan, Mater. Sci. Eng. B. 176 (2011) 1778–1784, doi:10.1016/j.mseb.2011.05.032.
[281] D. Jiang, Y. Dai, Y. Zhang, C. Liu, K. Yu, Mater. Res. Express. 6 (2019) 056556, doi:10.1088/2053-1591/ab0803.
[282] W. Zhang, M. Li, Q. Chen, W. Hu, W. Zhang, W. Xin, Mater. Des. 39 (2012) 379–383, doi:10.1016/j.matdes.2012.03.006.
[283] J. Wang, Y. Ma, S. Guo, W. Jiang, Q. Liu, Mater. Des. 153 (2018) 308–316, doi:10.1016/j.matdes.2018.04.062.
[284] S.M. Kim, J.H. Jo, S.M. Lee, M.H. Kang, H.E. Kim, Y. Estrin, J.H. Lee, J.W. Lee, Y.H. Koh, J. Biomed. Mater. Res. - Part A. 102 (2014) 429–441, doi:10.1002/jbm.a.34718.
[285] A.P. Md Saad, A.T. Prakoso, M.A. Sulong, H. Basri, D.A. Wahjuningrum, A. Syahrom, Biomech. Model. Mechanobiol. 18 (2019) 797–811, doi:10.1007/s10237-018-01115-z.
[286] L. Tan, Q. Wang, X. Lin, P. Wan, G. Zhang, Q. Zhang, K. Yang, Acta Biomater 10 (2014) 2333–2340, doi:10.1016/j.actbio.2013.12.020.
[287] A. Krause, N. Von Der Höh, D. Bormann, C. Krause, F.W. Bach, H. Windhagen, A. Meyer-Lindenberg, J. Mater. Sci. 45 (2010) 624–632, doi:10.1007/s10853-009-3936-3.
[288] N. Hort, Y. Huang, D. Fechner, M. Störmer, C. Blawert, F. Witte, C. Vogt, H. Drücker, R. Willumeit, K.U. Kainer, F. Feyerabend, Acta Biomater 6 (2010) 1714–1725, doi:10.1016/j.actbio.2009.09.010.
[289] N. Sezer, Z. Evis, S.M. Kayhan, A. Tahmasebifar, M. Koç, J. Magnes. Alloy. 6 (2018) 23–43, doi:10.1016/j.jma.2018.02.003.
[290] H. Cao, M. Huang, C. Wang, S. Long, J. Zha, G. You, J. Magnes. Alloy. 7 (2019) 370–380, doi:10.1016/j.jma.2019.07.002.
[291] Q. Peng, Y. Huang, L. Zhou, N. Hort, K.U. Kainer, Biomaterials 31 (2010) 398–403, doi:10.1016/j.biomaterials.2009.09.065.
[292] F. Pan, X. Chen, T. Yan, T. Liu, J. Mao, W. Luo, Q. Wang, J. Peng, A. Tang, B. Jiang, J. Magnes. Alloy. 4 (2016) 8–14, doi:10.1016/j.jma.2016.02.003.
[293] X.N. Gu, Y.F. Zheng, Front. Mater. Sci. China. 4 (2010) 111–115, doi:10.1007/s11706-010-0024-1.
[294] A. Helvia, M. Sanchez, B.J.C. Luthringer, F. Feyerabend, R. Willumeit, Acta Biomater 13 (2014) 16–31, doi:10.1016/j.actbio.2014.11.048.
[295] P.Yin Yee Chin, Q. Cheok, A. Glowacz, W. Caesarendra, Appl. Sci. 10 (2020) 3141, doi:10.3390/app10093141.
[296] X. Gai, C. Liu, G. Wang, Y. Qin, C. Fan, J. Liu, Y. Shi, Regen. Biomater. 7 (2020) 321–329, doi:10.1093/rb/rbaa017.
[297] W. Jahnen-Dechent, M. Ketteler, Clin. Kidney J. 5 (2012) 3–14, doi:10.1093/ndtplus/sfr163.
[298] A. Drynda, N. Deinet, N. Braun, M. Peuster, J. Biomed. Mater. Res. - Part A. 91 (2009) 360–369, doi:10.1002/jbm.a.32235.
[299] N. Li, Y. Zheng, J. Mater. Sci. Technol. 29 (2013) 489–502, doi:10.1016/j.jmst.2013.02.005.
[300] X. Gu, Y. Zheng, Y. Cheng, S. Zhong, T. Xi, Biomaterials 30 (2009) 484–498, doi:10.1016/j.biomaterials.2008.10.021.
[301] L. Wei, J. Li, Y. Zhang, H. Lai, Mater. Chem. Phys. 241 (2020) 122441, doi:10.1016/j.matchemphys.2019.122441.
[302] C. Kammer, Magnesium Taschenbuch, Aluminium-Verlag, Düsseldorf, 2000.
[303] E.C. Huse, Chicago Med J Exam (1878) 172 2.
[304] F. Witte, Acta Biomater 23 (2015) 28–40, doi:10.1016/j.actbio.2015.07.017.
[305] B. Heublein, R. Rohde, M. Niemeyer, V. Kaese, W. Hartung, C. Röcken, J. Am. Coll. Cardiol. 35 (2000) 14–15.
[306] J.M. Seitz, A. Lucas, M. Kirschner, Jom 68 (2016) 1177–1182, doi:10.1007/s11837-015-1773-1.
[307] J.L. Wang, J.K. Xu, C. Hopkins, D.H.K. Chow, L. Qin, Adv. Sci. 7 (2020) 1902443, doi:10.1002/advs.201902443.
[308] R. Biber, J. Pauser, M. Geßlein, H.J. Bail, Case Rep. Orthop 2016 (2016) 1–4, doi:10.1155/2016/9673174.
[309] H. Windhagen, K. Radtke, A. Weizbauer, J. Diekmann, Y. Noll, U. Kreimeyer, R. Schavan, C. Stukenborg-Colsman, H. Waizy, Biomed Eng 19 (2020) 1–10, doi:10.1186/s12938-020-00818-8.
[310] H. Waizy, J.M. Seitz, J. Reifenrath, A. Weizbauer, F.W. Bach, A. Meyer-Lindenberg, B. Denkena, H. Windhagen, J. Mater. Sci. 48 (2013) 39–50, doi:10.1007/s10853-012-6572-2.
[311] T. Deguchi, T. Takano-Yamamoto, R. Kanomi, J.K. Hartsfield, W.E. Roberts, L.P. Garetto, J. Dent. Res. 82 (2003) 377–381, doi:10.1177/154405910308200510.
[312] M. Krämer, M. Schilling, R. Eifler, B. Hering, J. Reifenrath, S. Besdo, H. Windhagen, E. Willbold, A. Weizbauer, Mater. Sci. Eng. C. 59 (2016) 129–135, doi:10.1016/j.msec.2015.10.006.
[313] T. Yoshida, T. Fukumoto, T. Urade, M. Kido, H. Toyama, S. Asari, T. Ajiki, N. Ikeo, T. Mukai, Y. Ku, Surg. (United States) 161 (2017) 1553–1560, doi:10.1016/j.surg.2016.12.023.
[314] C.B. Chng, D.P. Lau, J.Q. Choo, C.K. Chui, Acta Biomater 8 (2012) 2835–2844, doi:10.1016/j.actbio.2012.03.051.
[315] O. Wetterlövcharyeva, JSM Dent. Surg. 2 (2017) 2–4.
[316] W. Wang, Y.L. Wang, M. Chen, L. Chen, J. Zhang, Y.D. Li, M.H. Li, G.Y. Yuan, Sci. Rep. 6 (2016) 1–9, doi:10.1038/srep37401.
[317] J. Liu, B. Zheng, P. Wang, X. Wang, B. Zhang, Q. Shi, T. Xi, M. Chen, S. Guan, ACS Appl. Mater. Interfaces. 8 (2016) 17842–17858, doi:10.1021/acsami.6b05038.
[318] M. Durisin, J. Reifenrath, C.M. Weber, R. Eifler, H.J. Maier, T. Lenarz, J.M. Seitz, J. Biomed. Mater. Res. - Part B Appl. Biomater. 105 (2017) 350–365, doi:10.1002/jbm.b.33559.
[319] M. Li, M.J. Mondrinos, X. Chen, M.R. Gandhi, F.K. Ko, P.I. Lelkes, J. Biomed. Mater. Res. Part A. 79 (2006) 63–73, doi:10.1002/jbm.a.
[320] A.C. Hänzi, A. Metlar, M. Schinhammer, H. Aguib, T.C. Lüth, J.F. Löffler, P.J. Uggowitzer, Mater. Sci. Eng. C. 31 (2011) 1098–1103, doi:10.1016/j.msec.2011.03.012.
[321] R. Erbel, C. Di Mario, J. Bartunek, J. Bonnier, B. de Bruyne, F.R. Eberli, P. Erne, M. Haude, B. Heublein, M. Horrigan, C. Ilsley, D. Böse, J. Koolen, T.F. Lüscher, N. Weissman, R. Waksman, Lancet 369 (2007) 1869–1875, doi:10.1016/S0140-6736(07)60853-8.
[322] H. Kitabata, R. Waksman, B. Warnack, Cardiovasc. Revascularization Med. 15 (2014) 109–116, doi:10.1016/j.carrev.2014.01.011.
[323] D. Zhao, S. Huang, F. Lu, B. Wang, L. Yang, L. Qin, K. Yang, Y. Li, W. Li, W. Wang, S. Tian, X. Zhang, W. Gao, Z. Wang, Y. Zhang, X. Xie, J. Wang, J. Li, Biomaterials 81 (2016) 84–92, doi:10.1016/j.biomaterials.2015.11.038.
[324] J.W. Lee, H.S. Han, K.J. Han, J. Park, H. Jeon, M.R. Ok, H.K. Seok, J.P. Ahn, K.E. Lee, D.H. Lee, S.J. Yang, S.Y. Cho, P.R. Cha, H. Kwon, T.H. Nam, J.H. Lo Han, H.J. Rho, K.S. Lee, Y.C. Kim, D. Mantovani, Proc. Natl. Acad. Sci. 113 (2016) 716–721, doi:10.1073/pnas.1518238113.
[325] G. Baril, G. Galicia, C. Deslouis, N. Pébère, B. Tribollet, V. Vivier, J. Electrochem. Soc. 154 (2007) C108, doi:10.1149/1.2401056.
[326] H. Torbati-Sarraf, S.A. Torbati-Sarraf, A. Poursaee, T.G. Langdon, Corros. Sci. 154 (2019) 90–100, doi:10.1016/j.corsci.2019.04.006.
[327] H. Medhashree, A.N. Shetty, J. Mater. Res. Technol. 6 (2017) 40–49, doi:10.1016/j.jmrt.2016.04.003.
[328] G. Song, A. Atrens, D. St. John, X. Wu, J. Nairn, Corros. Sci. 39 (1997) 1981–2004, doi:10.1016/S0010-938X(97)00090-5.
[329] M.P. Gomes, I. Costa, N. Pébère, J.L. Rossi, B. Tribollet, V. Vivier, Electrochim. Acta. 306 (2019) 61–70, doi:10.1016/j.electacta.2019.03.080.
[330] N. Eliaz, Materials (Basel). 12 (2019) 407, doi:10.3390/ma12030407.
[331] H. Pan, K. Pang, F. Cui, F. Ge, C. Man, X. Wang, Z. Cui, Corros. Sci. 157 (2019) 420–437, doi:10.1016/j.corsci.2019.06.022.
[332] S. Yin, W. Duan, W. Liu, L. Wu, J. Yu, Z. Zhao, M. Liu, P. Wang, J. Cui, Z. Zhang, Corros. Sci. 166 (2020) 108419, doi:10.1016/j.corsci.2019.108419.

[333] Z. Yin, R. He, Y. Chen, Z. Yin, K. Yan, K. Wang, H. Yan, H. Song, C. Yin, H. Guan, C. Luo, Z. Hu, C. Luc, Appl. Surf. Sci. 536 (2021) 147761, doi:10.1016/j.apsusc.2020.147761.
[334] B. Feng, G. Liu, P. Yang, S. Huang, D. Qi, P. Chen, C. Wang, J. Du, S. Zhang, J. Liu, J. Magnes. Alloy. (2021) in presshttps://doi.org/, doi:10.1016/j.jma.2020.12.013.
[335] C. Cai, R. Song, L. Wang, J. Li, Appl. Surf. Sci. 462 (2018) 243–254, doi:10.1016/j.apsusc.2018.08.107.
[336] M. Shahin, K. Munir, C. Wen, Y. Li, Acta Biomater 96 (2019) 1–19, doi:10.1016/j.actbio.2019.06.007.
[337] A. Maltseva, V. Shkirskiy, G. Lefèvre, P. Volovitch, Corros. Sci. 153 (2019) 272–282, doi:10.1016/j.corsci.2019.03.024.
[338] M. Pogorielov, E. Husak, A. Solodivnik, S. Zhdanov, Interv. Med. Appl. Sci. 9 (2017) 27–38, doi:10.1556/1646.9.2017.1.04.
[339] S. Thomas, N.V. M.edhekar, G.S. Frankel, N. Birbilis, Curr. Opin. Solid State Mater. Sci. 19 (2015) 85–94, doi:10.1016/j.cossms.2014.09.005.
[340] S. Bender, J. Goellner, A. Heyn, S. Schmigalla, Mater. Corros. 63 (2012) 707–712, doi:10.1002/maco.201106225.
[341] A. Maltseva, V. Shkirskiy, G. Lefèvre, P. Volovitch, Corros. Sci. 153 (2019) 272–282, doi:10.1016/j.corsci.2019.03.024.
[342] G. Song, A. Atrens, D. Stjohn, J. Nairn, Y. Lit, Corros. Sci. 39 (1997) 855–875, doi:10.1016/S0010-938X(96)00172-2.
[343] G. Song, Corros. Sci. 49 (2007) 1696–1701, doi:10.1016/j.corsci.2007.01.001.
[344] Y. Li, C. Wen, D. Mushahary, R. Sravanthi, N. Harishankar, G. Pande, P. Hodgson, Acta Biomater 8 (2012) 3177–3188, doi:10.1016/j.actbio.2012.04.028.
[345] M.R. Norton, G.W. Kay, M.C. Brown, D.L. Cochran, Int. J. Adhes. Adhes. 102 (2020) 102647, doi:10.1016/j.ijadhadh.2020.102647.
[346] M.S. Song, R.C. Zeng, Y.F. Ding, R.W. Li, M. Easton, I. Cole, N. Birbilis, X.B. Chen, J. Mater. Sci. Technol. 35 (2019) 535–544, doi:10.1016/j.jmst.2018.10.008.
[347] L. Mao, H. Zhu, L. Chen, H. Zhou, G. Yuan, C. Song, J. Mater. Res. Technol. 9 (2020) 6409–6419, doi:10.1016/j.jmrt.2020.04.024.
[348] N. IQBAL, S. IQBAL, T. IQBAL, H.R. BAKHSHESHI-RAD, A. ALSAKKAF, A. KAMIL, M.R. ABDUL KADIR, M.H. IDRIS, H.B. RAGHAV, Trans. Nonferrous Met. Soc. China (English Ed. 30 (2020) 123–133, doi:10.1016/S1003-6326(19)65185-X.
[349] D.B. Prabhu, P. Gopalakrishnan, K.R. Ravi, J. Alloys Compd. 812 (2020) 152146, doi:10.1016/j.jallcom.2019.152146.
[350] J. an Li, L. Chen, X. qi Zhang, S. kang Guan, Mater. Sci. Eng. C. 109 (2020) 110607, doi:10.1016/j.msec.2019.110607.
[351] M. Uddin, C. Hall, V. Santos, R. Visalakshan, G. Qian, K. Vasilev, Mater. Sci. Eng. C. 118 (2021) 111459, doi:10.1016/j.msec.2020.111459.
[352] S. Devgan, S.S. Sidhu, Mater. Chem. Phys. 233 (2019) 68–78, doi:10.1016/j.matchemphys.2019.05.039.
[353] P. Wan, L. Tan, K. Yang, J. Mater. Sci. Technol. 32 (2016) 827–834, doi:10.1016/j.jmst.2016.05.003.
[354] V. Huynh, N.K. Ngo, T.D. Golden, Int. J. Biomater. 2019 (2019) 3806504, doi:10.1155/2019/3806504.
[355] A. Abdal-Hay, M. Dewidar, J.K. Lim, Appl. Surf. Sci. 261 (2012) 536–546, doi:10.1016/j.apsusc.2012.08.051.
[356] A.I. Bita, G.E. Stan, M. Niculescu, I. Ciuca, E. Vasile, I. Antoniac, J. Adhes. Sci. Technol. 30 (2016) 1968–1983, doi:10.1080/01694243.2016.1171569.
[357] H. Hornberger, S. Virtanen, A.R. Boccaccini, Acta Biomater 8 (2012) 2442–2455, doi:10.1016/j.actbio.2012.04.012.
[358] M. Hatami, M. Saremi, R. Naderi, Prog. Nat. Sci. Mater. Int. 25 (2015) 478–485, doi:10.1016/j.pnsc.2015.10.001.
[359] H. Zhao, S. Cai, S. Niu, R. Zhang, X. Wu, G. Xu, Z. Ding, Ceram. Int. 41 (2015) 4590–4600, doi:10.1016/j.ceramint.2014.12.002.
[360] I. Antoniac, F. Miculescu, C. Cotrut, A. Ficai, J.V. R.au, E. Grosu, A. Antoniac, C. Tecu, I. Cristescu, Materials (Basel) 13 (2020) 263, doi:10.3390/ma13020263.
[361] S. Agarwal, J. Curtin, B. Duffy, S. Jaiswal, Mater. Sci. Eng. C. 68 (2016) 948–963, doi:10.1016/j.msec.2016.06.020.
[362] S. Devgan, S. Singh, Mater. Chem. Phys. 233 (2019) 68–78.
[363] F. Wu, J. Liang, W. Li, J. Magnes. Alloy. 3 (2015) 231–236, doi:10.1016/j.jma.2015.08.004.
[364] X. Luo, X.T. Cui, Acta Biomater 7 (2011) 441–446, doi:10.1016/j.actbio.2010.09.006.
[365] Y.L. Gao, Y. Liu, X.Y. Song, J. Therm. Spray Technol. 27 (2018) 1381–1387, doi:10.1007/s11666-018-0760-9.
[366] M. Razavi, M. Fathi, O. Savabi, D. Vashaee, L. Tayebi, Mater. Sci. Eng. C. 41 (2014) 168–177, doi:10.1016/j.msec.2014.04.039.
[367] X. Ly, S. Yang, T. Nguyen, Surf. Coatings Technol. 395 (2020) 125923, doi:10.1016/j.surfcoat.2020.125923.
[368] L.R. Krishna, G. Poshal, A. Jyothirmayi, G. Sundararajan, Mater. Des. 77 (2015) 6–14, doi:10.1016/j.matdes.2015.04.006.
[369] Z.Q. Zhang, L. Wang, M.Q. Zeng, R.C. Zeng, M.B. Kannan, C.G. Lin, Y.F. Zheng, Bioact. Mater. 5 (2020) 398–409, doi:10.1016/j.bioactmat.2020.03.005.
[370] H. Tang, Y. Han, T. Wu, W. Tao, X. Jian, Y. Wu, F. Xu, Appl. Surf. Sci. 400 (2017) 391–404, doi:10.1016/j.apsusc.2016.12.216.
[371] M. Zarka, B. Dikici, M. Niinomi, K.V. E.zirmik, M. Nakai, H. Yilmazer, Vacuum 183 (2021) 109850, doi:10.1016/j.vacuum.2020.109850.
[372] F. Hollstein, R. Wiedemann, J. Scholz, Surf. Coatings Technol. 162 (2003) 261–268, doi:10.1016/S0257-8972(02)00671-0.
[373] N. Zhao, D. Zhu, Int. J. Biomed. Eng. Technol. 12 (2013) 382–398, doi:10.1504/IJBET.2013.057677.
[374] Y. Zheng, L. Zang, Y. Bi, Y. Li, Y. Chen, Coatings 8 (2018) 1–12, doi:10.3390/coatings8080261.
[375] M. Jamesh, G. Wu, Y. Zhao, P.K. Chu, Corros. Sci. 69 (2013) 158–163, doi:10.1016/j.corsci.2012.11.037.
[376] M.S. Uddin, C. Hall, P. Murphy, Sci. Technol. Adv. Mater. 16 (2015) 53501, doi:10.1088/1468-6996/16/5/053501.
[377] W. Zai, X. Zhang, Y. Su, H.C. Man, G. Li, J. Lian, Surf. Coatings Technol. 397 (2020) 125919, doi:10.1016/j.surfcoat.2020.125919.
[378] N. Pulido-González, B. Torres, M.L. Zheludkevich, J. Rams, Surf. Coatings Technol. 402 (2020) 126314, doi:10.1016/j.surfcoat.2020.126314.
[379] E. Chen, K. Zhang, J. Zou, Appl. Surf. Sci. 367 (2016) 11–18, doi:10.1016/j.apsusc.2016.01.124.
[380] J. Park, H.S. Han, J. Park, H. Seo, J. Edwards, Y.C. Kim, M.R. Ok, H.K. Seok, H. Jeon, Appl. Surf. Sci. 448 (2018) 424–434, doi:10.1016/j.apsusc.2018.04.088.
[381] B.H. Kear, E.M. Breinan, L.E. Greenwald, Met. Technol. 6 (1979) 121–129, doi:10.1179/030716979803276796.
[382] G. Wu, J.M. Ibrahim, P.K. Chu, Surf. Coatings Technol. 233 (2013) 2–12, doi:10.1016/j.surfcoat.2012.10.009.
[383] M. Furkó, K. Balázsi, C. Balázsi, Rev. Adv. Mater. Sci. 48 (2017) 25–51.
[384] X. Lin, L. Tan, Q. Zhang, K. Yang, Z. Hu, J. Qiu, Y. Cai, Acta Biomater 9 (2013) 8631–8642, doi:10.1016/j.actbio.2012.12.016.
[385] C.G. Li, M.F. Chen, S.Z. Sun, J. Zhang, Mater. Sci. Forum. 849 (2016) 647–653, doi:10.4028/www.scientific.net/MSF.849.647.
[386] R.I.M. Asri, W.S.W. Harun, M.A. Hassan, S.A.C. Ghani, Z. Buyong, J. Mech. Behav. Biomed. Mater. 57 (2016) 95–108, doi:10.1016/j.jmbbm.2015.11.031.
[387] W.S.W. Harun, R.I.M. Asri, J. Alias, F.H. Zulkifli, K. Kadirgama, S.A.C. Ghani, J.H.M. Shariffuddin, Ceram. Int. 44 (2018) 1250–1268, doi:10.1016/j.ceramint.2017.10.162.
[388] S. Shadanbaz, G.J. Dias, Acta Biomater 8 (2012) 20–30, doi:10.1016/j.actbio.2011.10.016.
[389] S.V. D.orozhkin, Acta Biomater 10 (2014) 2919–2934, doi:10.1016/j.actbio.2014.02.026.
[390] C. Ke, K. Pohl, N. Birbilis, X.B. Chen, Mater. Sci. Technol. 30 (2014) 521–526, doi:10.1179/1743284714Y.0000000508.
[391] S. Santhanakrishnan, Y.H. Ho, N.B. Dahotre, Mater. Technol. 27 (2012) 273–277, doi:10.1179/1753555712Y.0000000022.
[392] J.V. R.au, I. Antoniac, M. Filipescu, C. Cotrut, M. Fosca, L.C. Nistor, R. Birjega, M. Dinescu, Ceram. Int. 44 (2018) 16678–16687, doi:10.1016/j.ceramint.2018.06.095.

[393] C. Prakash, S. Singh, B.S. Pabla, M.S. Uddin, Surf. Coatings Technol. 346 (2018) 9–18, doi:10.1016/j.surfcoat.2018.04.035.
[394] A. Singh, S.P. Harimkar, JOM 64 (2012) 716–733, doi:10.1007/s11837-012-0340-2.
[395] M. Sankar, S. Suwas, S. Balasubramanian, G. Manivasagam, Surf. Coatings Technol. 309 (2017) 840–848, doi:10.1016/j.surfcoat.2016.10.077.
[396] S. Kumar, M. Nehra, D. Kedia, N. Dilbaghi, K. Tankeshwar, K.H. Kim, Mater. Sci. Eng. C. 106 (2020) 110154, doi:10.1016/j.msec.2019.110154.
[397] S. Rtimi, D.D. Dionysiou, S.C. Pillai, J. Kiwi, Appl. Catal. B Environ. 240 (2019) 291–318, doi:10.1016/j.apcatb.2018.07.025.
[398] L. Ren, K. Yang, J. Mater. Sci. Technol. 29 (2013) 1005–1010, doi:10.1016/j.jmst.2013.09.008.
[399] C. Shuai, L. Liu, M. Zhao, P. Feng, Y. Yang, W. Guo, C. Gao, F. Yuan, J. Mater. Sci. Technol. 34 (2018) 1944–1952, doi:10.1016/j.jmst.2018.02.006.
[400] C. Shuai, L. Liu, Y. Yang, C. Gao, M. Zhao, L. Yi, S. Peng, Appl. Sci. 8 (2018) 2109, doi:10.3390/app8112109.
[401] B. Zahiri, P.K. Sow, C.H. Kung, W. Mérida, Adv. Mater. Interfaces. 4 (2017) 1–12, doi:10.1002/admi.201700121.
[402] M. Rahman, N.K. Dutta, N.Roy Choudhury, Front. Bioeng. Biotechnol. 8 (2020) 564, doi:10.3389/fbioe.2020.00564.
[403] A. Riveiro, P. Pou, J. del Val, R. Comesaña, F. Arias-González, F. Lusquiños, M. Boutinguiza, F. Quintero, A. Badaoui, J. Pou, Procedia CIRP 94 (2020) 879–884, doi:10.1016/j.procir.2020.09.065.
[404] F. Xia, L. Jiang, Adv. Mater. 20 (2008) 2842–2858, doi:10.1002/adma.200800836.
[405] I.A. Larmour, S.E.J. Bell, G.C. Saunders, Angew. Chemie - Int. Ed. 46 (2007) 1710–1712, doi:10.1002/anie.200604596.
[406] S. Shin, J. Seo, H. Han, S. Kang, H. Kim, T. Lee, Materials (Basel) 9 (2016) 116, doi:10.3390/ma9020116.
[407] M. Abdalla, A. Joplin, M. Elahinia, H. Ibrahim, Corros. Mater. Degrad. 1 (2020) 219–248, doi:10.3390/cmd1020011.
[408] J.A. Sanz-Herrera, E. Reina-Romo, A.R. Boccaccini, J. Mech. Behav. Biomed. Mater. 79 (2018) 181–188, doi:10.1016/j.jmbbm.2017.12.016.
[409] S. Prasadh, S. Suresh, K.L. Hong, A. Bhargav, V. Rosa, R.C.W. Wong, J. Mech. Behav. Biomed. Mater. 103 (2020) 103548, doi:10.1016/j.jmbbm.2019.103548.
[410] C. I-Chiang, L. Shyh-Yuan, W. Ming-Chang, C.W. Sun, C.P. Jiang, Comput. Methods Biomech. Biomed. Engin. 17 (2014) 516–526, doi:10.1080/10255842.2012.697556.
[411] A. Büchter, D. Wiechmann, C. Gaertner, M. Hendrik, M. Vogeler, H.P. Wiesmann, J. Piffko, U. Meyer, Clin. Oral Implants Res. 17 (2006) 714–722, doi:10.1111/j.1600-0501.2006.01233.x.
[412] M.M. Rahman, R. Balu, A. Abraham, N.K. Dutta, N.R. Choudhury, ACS Appl. Bio Mater. 4 (2021) 5542–5555, doi:10.1021/acsabm.1c00366.
[413] N. Singh, U. Batra, K. Kumar, A. Mahapatro, J. Magnes. Alloy. 9 (2021) 627–646, doi:10.1016/j.jma.2020.08.003.
[414] L. Liu, B. Huang, X. Liu, W. Yuan, Y. Zheng, Z. Li, K.W.K. Yeung, S. Zhu, Y. Liang, Z. Cui, S. Wu, Bioact. Mater. 6 (2021) 568–578, doi:10.1016/j.bioactmat.2020.08.013.
[415] M. Zhang, S. Cai, S. Shen, G. Xu, Y. Li, R. Ling, X. Wu, J. Alloys Compd. 658 (2016) 649–656, doi:10.1016/j.jallcom.2015.10.282.
[416] A. Dubey, S. Jaiswal, S. Haldar, P. Roy, D. Lahiri, Biomed. Mater. 16 (2021) 015017, doi:10.1088/1748-605X/abb721.
[417] H. Shi, P. Zhou, J. Li, C. Liu, L. Wang, Front. Bioeng. Biotechnol. 8 (2021) 616845, doi:10.3389/fbioe.2020.616845.